

AD-A037 182

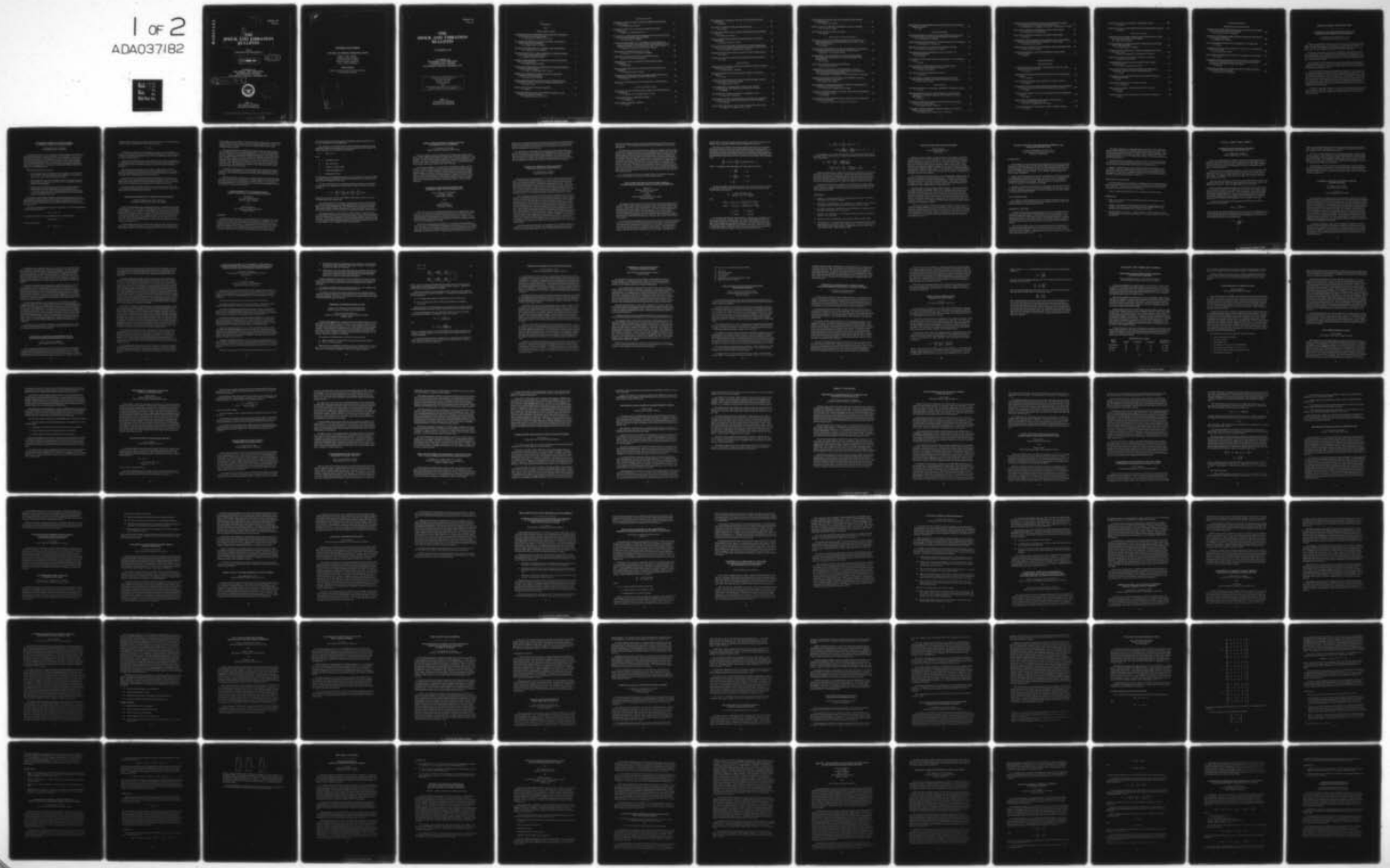
NAVAL RESEARCH LAB WASHINGTON D C SHOCK AND VIBRATION--ETC F/G 20/11  
THE SHOCK AND VIBRATION BULLETIN. PART 1. SUMMARIES OF PRESENT--ETC(U)  
OCT 75

UNCLASSIFIED

BULL-46-PT-1

NL

1 of 2  
ADA037182



ADA037182

70  
J  
Bullettin 46  
(Part 1)

⑥  
**THE  
SHOCK AND VIBRATION  
BULLETIN.**

Part 1•  
Summaries of Presented Papers •

① OCTOBER 1975

⑫ 138p.

A Publication of  
THE SHOCK AND VIBRATION  
INFORMATION CENTER  
Naval Research Laboratory, Washington, D.C.

⑭ Bull-46-pt-1



DDC  
REFUGED  
MAR 22 1977  
REFUGED  
JY A

Office of  
The Director of Defense  
Research and Engineering

This document has been approved for public release and sale; its distribution is unlimited.

389 004

BB

P.95-134  
Approved for  
public release by  
the NSA  
Ref. 917673306  
20 3-25-77

## **SYMPPOSIUM MANAGEMENT**

### **THE SHOCK AND VIBRATION INFORMATION CENTER**

Henry C. Pusey, Director  
Rudolph H. Volin, Coordinator  
J. Gordan Showalter, Coordinator  
Barbara Szymanski, Registration  
Carol A. Healey, Registration

#### **Bulletin Production**

Graphic Arts Branch, Technical Information Division,  
Naval Research Laboratory



Bulletin 46  
(Part 1)

# THE SHOCK AND VIBRATION BULLETIN

OCTOBER 1975

A Publication of  
**THE SHOCK AND VIBRATION  
INFORMATION CENTER**  
Naval Research Laboratory, Washington, D.C.

46th Shock and Vibration Symposium  
Royal Inn at the Wharf  
San Diego, California  
21-23 October 1975  
Hosts  
Naval Electronics Laboratory Center, San Diego, CA  
and Naval Undersea Center, San Diego, CA

Office of  
The Director of Defense  
Research and Engineering

↓  
CONTENTS

Part I

Shock Testing and Analysis

EARTHQUAKE TEST ENVIRONMENT—SIMULATION AND PROCEDURE FOR COMMUNICATIONS EQUIPMENT .....	1
N. J. DeCapua, M. G. Hetman and S. C. Liu	
AN ALTERNATE APPROACH TO MODAL DAMPING AS APPLIED TO SEISMIC SENSITIVE EQUIPMENT .....	2
L. A. Bergman and A. J. Hannibal	
THE SHOCK ENVIRONMENT OF A FREIGHT TRAIN DERAILMENT .....	3
W. W. Wassman and J. H. Armstrong	
THE DEVELOPMENT OF A GENERALIZED IMPACT RESPONSE MODEL FOR A BULK CUSHIONING MATERIAL .....	4
D. McDaniel and R. M. Wyskida	
BARREL TAMPED EXPLOSIVELY PROPELLED PLATES FOR OBLIQUE IMPACT EXPERIMENTS .....	6
F. H. Mathews and B. W. Duggin	
ESTIMATION OF SHIP SHOCK PARAMETERS FOR CONSISTENT DESIGN AND TEST SPECIFICATION .....	6
G. C. Hart, T. K. Hasselman and W. N. Jones	
STRESS WAVE APPROACH TO THE ANALYSIS OF SUBMARINE COMPONENT SHOCK RESPONSE .....	7
J. D. Colton and J. E. Malinak	
POWER SERIES EXPANSION OF THE DYNAMIC STIFFNESS MATRIX INCLUDING ROTARY INERTIA AND SHEAR DEFORMATION .....	8
M. Paz and L. Dung	
EFFECT OF PHASE SHIFT ON SHOCK RESPONSE .....	11
C. T. Morrow	
DYNAMIC BUCKLING OF SHALLOW IMPERFECT SPHERICAL CAPS UNDER STEP PRESSURE LOADS .....	12
C. Lakshmikantham and Tien-Yu Tsui	

Fluid-Structure Topics

DETERMINATION OF DYNAMIC LOADS FROM MISSILE MODEL WIND TUNNEL DATA .....	15
P. G. Bolds and D. K. Barrett	
FEASIBILITY STUDY OF AN ACOUSTIC COVER FOR SHUTTLE PAYLOADS .....	16
M. Ferrante, C. V. Stahle and F. J. On	
LONGITUDINAL VIBRATION CHARACTERISTICS OF THE SPACE SHUTTLE SOLID ROCKET BOOSTER TEST SEGMENT.....	17
D. L. Linton and J. C. Bartlett	
A STUDY OF THE DAMPING OF A CYLINDRICAL TANK PARTIALLY FILLED WITH LIQUID, AND APPLICATION TO THE FRENCH LAUNCH VEHICLE DIAMANT B P4 TO COUNTERACT THE "POGO" EFFECT .....	19
M. Poizat, P. Cochery, M. Vedrenne and P. Vialatoux	
VIBRATIONS OF PERFORATED PIPES IN FLUID .....	20
D. Krajcinovic, S. S. Chen and G. S. Rosenberg	
VIBRATION AND STABILITY OF FLUID-CONVEYING PIPES .....	22
Hsuan-Chi Lin and Shoei-Sheng Chen	
EXPERIMENTAL LIQUID FUEL/POSITIVE EXPULSION BLADDER DYNAMICS .....	23
M. Wohltmann	
FINITE ELEMENT SOLUTION OF FLUID-STRUCTURE INTERACTION PROBLEMS .....	24
E. A. Schroeder and M. S. Marcus	
EXPERIMENTAL DETERMINATION OF ROCKET MOTOR STRUCTURAL RESPONSE TO INTERNAL ACOUSTIC EXCITATION .....	25
F. R. Jensen	
EFFECT OF FLUID MEDIUM ON THE VIBRATION OF AN OPEN SHELL .....	26
J. L. Lai	
Acoustic and Vibration Testing	
SIMULATING TACTICAL MISSILE FLIGHT VIBRATION WITH PNEUMATIC VIBRATORS .....	29
J. G. Maloney, D. G. Vandegriff and W. D. Ayers	
A THREE DIRECTIONAL VIBRATION SYSTEM .....	30
F. M. Edgington	
DUAL SHAKER VIBRATION FACILITY .....	31
C. V. Ryden	

HIGH FREQUENCY VIBRATION ANALYSIS FOR INCIPIENT FAILURE DETECTION .....	33
D. B. Board	
ANALYSIS OF FATIGUE UNDER RANDOM VIBRATION.....	33
R. G. Lambert	
RANDOM VIBRATION FATIGUE TESTS OF WELDBONDED AND BONDED JOINTS .....	34
F. Sandow and O. Mauder	
FATIGUE PREDICTION FOR STRUCTURES SUBJECTED TO RANDOM VIBRATION .....	35
W. J. Kacena, III, and P. J. Jones	
MEAN LIFE EVALUATION FOR A STOCHASTIC LOADING PROGRAMME WITH A FINITE NUMBER OF STRAIN LEVELS USING MINER'S RULE ...	36
H. H. E. Leipholz, G. Philippin and T. H. Topper	
THERMO-ACOUSTIC SIMULATION OF CAPTIVE FLIGHT ENVIRONMENT.....	37
W. D. Everett	
THE EFFECT OF SIGNAL CLIPPING IN RANDOM VIBRATION TESTING .....	38
A. G. Ratz	
Impact and Blast	
PREDICTION OF STANDOFF DISTANCES TO PREVENT LOSS OF HEARING FROM MUZZLE BLAST .....	41
P. S. Westine and J. C. Hokanson	
DYNAMIC RESPONSE OF THE HUMAN BODY THORAX TO FRONTAL IMPACT .....	42
P. H. Chen	
A STUDY OF THE SPACE SHUTTLE SOLID ROCKET BOOSTER NOZZLE WATER IMPACT RECOVERY LOADS .....	43
E. A. Rawls and D. A. Kross	
AN EXPERIMENTAL INVESTIGATION OF THE AXIAL FORCES GENERATED BY THE OBLIQUE WATER ENTRY OF CONES .....	44
J. L. Baldwin	
DELAMINATION STUDIES OF IMPACTED COMPOSITE PLATES.....	46
C. A. Ross and R. Sierakowski	
SIMULATION OF X-RAY BLOWOFF IMPULSE LOADING ON A REENTRY VEHICLE AFT END USING LIGHT-INITIATED HIGH EXPLOSIVES .....	47
R. A. Benham	
BLAST PRESSURES INSIDE AND OUTSIDE SUPPRESSIVE STRUCTURES .....	47
E. D. Esparza, G. A. Oldham and W. E. Baker	

DEVELOPMENT OF STRUCTURES FOR INTENSE GROUND MOTION ENVIRONMENTS .....	48
T. O. Hunter and G. W. Barr	
DESIGN STUDY OF A NEW BRL EXPERIMENTAL BLAST CHAMBER .....	49
P. A. Cox and W. E. Baker	
ANALYSIS OF CONCRETE ARCH MAGAZINE.....	50
J. M. Ferritto	
Measurements and Criteria Development	
BOUNDARY LAYER FLUCTUATING PRESSURE DATA OBTAINED IN A HIGH BACKGROUND NOISE ENVIRONMENT ON A SMALL SCALE WIND TUNNEL MODEL.....	53
G. L. Getline	
THE DYNAMIC MEASUREMENT OF THE LOW FREQUENCY COMPONENTS OF TRACK INDUCED RAILCAR WHEEL ACCELERATIONS .....	54
S. MacIntyre, T. Jones and B. Scofield	
DEVELOPMENT AND APPLICATION OF A MINATURE RECORDER/ ANALYZER FOR MEASUREMENT OF THE TRANSPORTATION ENVIRONMENT .....	55
M. A. Venetos	
ADVANCES IN SHIPPING DAMAGES PREVENTION .....	57
H. Caruso and W. Silver, II	
EXPERIMENTAL VERIFICATION OF DETERMINING IN-FLIGHT VIBRATION LOADS ON HELICOPTERS USING ACCELEROMETER DATA AND IMPEDANCE MEASUREMENTS .....	58
J. H. McGarvey, F. D. Bartlett, Jr., T. W. Forsberg and W. G. Flannelly	
COHERENCE METHODS USED TO DEFINE TRANSMISSION PATHS OF AIRBORNE ANTENNA VIBRATION .....	59
R. E. Thaller and J. Pearson	
DEVELOPMENT OF COMPONENT RANDOM VIBRATION REQUIREMENTS CONSIDERING RESPONSE SPECTRA .....	60
C. V. Stahle, H. R. Gongloff and W. B. Keegan	
STATISTICAL DETERMINATION OF RANDOM VIBRATION REQUIREMENTS FOR SUBASSEMBLY TESTS .....	62
J. M. Medaglia	
EVALUATION OF THE HARPOON MISSILE AIRCRAFT LAUNCH EJECTION SHOCK ENVIRONMENT .....	64
J. A. Zara, J. L. Gubser, W. N. Jones and A. G. Piersol	

DEVELOPMENT OF SHIP SHOCK LOADS TEST ON THE AGM 84A/RGM84A MISSILE (HARPOON) .....	65
T. L. Eby	
Isolation and Damping	
THE MEASUREMENT OF DAMPING AND THE DETECTION OF DAMAGES IN STRUCTURES BY THE RANDOM DECREMENT TECHNIQUE .....	67
J. C. S. Yang and D. W. Caldwell	
SURFACE VIBRATION REDUCTION OF MARINE PROPULSION GEARBOXES ..	68
E. V. Thomas and A. J. Roscoe, III	
RESPONSE ANALYSIS OF A SYSTEM WITH DISCREET DAMPERS .....	69
G. K. Hobbs, D. J. Kuyper and J. J. Brooks	
THE APPLICATION OF ELASTOMERIC LEAD-LAG DAMPERS TO HELICOPTER ROTORS .....	70
D. P. McGuire	
EVALUATION OF ISOLATION MOUNTS IN REDUCING STRUCTUREBORNE NOISE .....	71
T. F. Derby	
THE ANALYSIS OF SHOCK ISOLATION OF A FLEXIBLE BODY PROTECTED BY ELASTOMERIC MATERIALS .....	72
C. W. Gilson and R. Bolton	
FOCALIZATION OF SEMI-SYMMETRIC SYSTEMS .....	74
A. J. Hannibal	
USE OF GENERAL PURPOSE COMPUTER PROGRAMS TO DERIVE EQUATIONS OF MOTION FOR OPTIMAL ISOLATION STUDIES .....	77
W' Pilkey and Y. H. Chen	
Dynamic Analysis	
DYNAMIC RESPONSE OF LAMINATED COMPOSITE CYLINDRICAL SHELLS...	81
C. T. Sun	
SPECTRUM AND RMS LEVELS FOR STRESSES IN CLOSELY SPACED STIFFENED CYLINDRICAL SHELLS, SUBJECTED TO ACOUSTIC EXCITATION .....	82
G. Maymon	
THE USE OF COMPUTER GRAPHICS IN EVALUATING THE DYNAMIC RESPONSE OF STRUCTURES .....	83
G. H. Workman and W. C. Bruce, Jr.	
A GENERAL PURPOSE COMPUTER GRAPHICS DISPLAY SYSTEM FOR FINITE ELEMENT MODELS .....	84
H. M. Christiansen, B. E. Brown and L. E. McCleary	

VIBRATION CHARACTERISTICS OF THE 1/8 SCALE DYNAMIC MODELS OF THE SPACE SHUTTLE SOLID ROCKET BOOSTERS .....	86
W. B. Stephens, S. A. Leadbetter, J. R. Barrett, J. W. Majka and J. L. Sewall	
MECHANICAL IMPEDANCE TECHNIQUES IN SMALL BOAT DESIGN .....	87
B. E. Douglas and H. S. Kenchington	
DYNAMIC BALANCING OF ROTORS—AN ORDERLY PROCEDURE .....	88
D. M. Janssen	
FREQUENCIES AND MODE SHAPES OF GEOMETRICALLY AXISYMMETRIC ROTATING STRUCTURES, APPLICATION TO A JET ENGINE.....	90
P. Trompette and M. LaLanne	
EIGENSOLUTION SENSITIVITY TO PARAMETRIC MODEL PERTURBATIONS..	91
C. W. White and B. D. Maytum	
DYNAMIC RESPONSE OF LAMINATED COMPOSITE PLATES UNDER INITIAL STRESS .....	92
C. T. Sun	

#### CLASSIFIED SESSION I

Minuteman Dynamics

AN INTRODUCTION TO THE DESIGN AND QUALIFICATION OF LARGE SHOCK ISOLATION SYSTEMS .....	95
L. L. Luschei	
POLYURETHANE FOAM ISOLATORS FOR SHOCK ISOLATED EQUIPMENT FLOORS .....	96
W. C. Gustafson	
ACTUATOR DEVELOPMENT FOR SYSTEM-LEVEL SHOCK TESTING .....	98
G. R. Burwell	
COMPONENT TESTING OF LIQUID SHOCK ISOLATORS AND ELASTOMERS IN SUPPORT OF RECENT SHOCK ISOLATION SYSTEM DESIGNS .....	100
J. P. Ashley	
ANALYSIS AND TESTING OF FULL SCALE SHOCK ISOLATED EQUIPMENT FLOORS .....	102
W. R. Milne	
EQUIVALENT AXISYMMETRIC STRUCTURAL LOADING FOR A TRAVELING OVERPRESSURE PULSE .....	104
D. J. Ness, J. J. Farrell and G. M. Teraoka	
DYNAMIC RESPONSE OF ELECTRICAL CABLES TO SHOCK MOTION .....	105
R. W. Doll	

FAILURE ANALYSIS BY STATISTICAL TECHNIQUES (FAST) .....	106
W. H. Rowan	
DESIGN OF A BLAST LOAD GENERATOR FOR OVERPRESSURE TESTING ...	108
P. Lieberman	
Modal Test and Analysis	
PREDICTING THE DYNAMICAL BEHAVIOR OF COMPLEX STRUCTURES, USING PART EXPERIMENT, PART THEORY .....	111
J.C. Cromer and M. LaLanne	
THE EXPERIMENTAL DETERMINATION OF VIBRATION PARAMETERS FROM TIME RESPONSES .....	112
S. R. Ibrahim and E. C. Mikulcik	
IDENTIFICATION OF STRUCTURAL MODAL PARAMETERS BY MODAL DYNAMIC TESTS .....	113
F. LeLeux, N. Miramand, J. F. Billaud and J. P. Kernevez	
VISCOUS VS. STRUCTURAL DAMPING IN MODAL ANALYSIS .....	114
M. Richardson and R. Potter	
EXPERIENCES IN USING MODAL SYNTHESIS WITHIN PROJECT REQUIREMENTS .....	115
J. A. Garba, B. K. Wada and J. C. Chen	
VIBRATION ANALYSIS OF THE BSE SPACECRAFT USING MODAL SYNTHESIS AND THE DYNAMIC TRANSFORMATION .....	116
E. J. Kuhar	
VIBRATION ANALYSIS OF STRUCTURES USING FIXED-INTERFACE COMPONENT MODES .....	117
C. Szu	
SYMMETRIC COMPONENTS IN SYSTEM ANALYSIS.....	118
W. A. McClelland	
APPLICATION OF MODAL ANALYSIS SURVEYS IN THE TEST LABORATORY .....	120
H. Caruso	
MATRIX FORMULATION OF MULTIPLE AND PARTIAL COHERENCE .....	122
R. Potter	

CLASSIFIED SESSION II

Shipboard Problems and Blast Effects

TRANSIENT WAVEFORM VIBROACOUSTIC DATA ANALYSIS FOR TURBINE VANE AND RAM PUMP LAUNCH SYSTEMS .....	125
R. C. Leibowitz and J. L. Clatterbuck	
PROTECTION OF SUBMARINE DECK MOUNTED ELECTRONIC EQUIPMENT FROM SHIPBOARD SHOCK .....	126
R. Bolton and N. M. Nilsen	
A FINITE ELEMENT ANALYSIS OF LOW FREQUENCY TRANSDUCERS .....	127
C. S. Nichols	
FRAGMENT VELOCITIES FROM BURSTING CYLINDRICAL AND SPHERICAL PRESSURE VESSELS .....	128
R. L. Bessey and J. J. Kulesz	
STRUCTURES TO SUPPRESS THE EFFECTS OF ACCIDENTAL EXPLOSIONS ..	130
D. F. Haskell	
EXPERIMENTAL DETERMINATION OF THE EFFECTS OF VARIATIONS IN THE EXCITATION PARAMETERS OF BLAST WAVES ON THE HIGH FREQUENCY RESPONSE OF CIRCULAR RINGS .....	130
P. J. Mirabella	
MATHEMATICAL MODEL OF A SUBMARINE TEST SECTION SUBJECTED TO UNDERWATER EXPLOSIONS .....	133
R. P. Brooks and B. C. McNaught	

## SHOCK TESTING AND ANALYSIS

---

### EARTHQUAKE TEST ENVIRONMENT-SIMULATION AND PROCEDURE FOR COMMUNICATIONS EQUIPMENT

N. J. DeCapua, M. G. Hetman and S. C. Liu  
Bell Laboratories, Whippny, New Jersey

Telephone communications facilities are located across the entire contiguous United States, and a significant portion of these facilities are in seismically active regions. In order to maintain a high reliability at a reasonable earthquake protection cost, it is imperative that a realistic equipment seismic test environment be developed.

In this paper a procedure is described for determining an earthquake test environment which includes, i) the in-building response characteristics of a broad range of telephone buildings subjected to earthquake excitations of Modified Mercalli Intensity VI to IX, ii) the variation of earthquake hazard across the country, and iii) building amplification of free-field ground motions.

The earthquake hazard is related to the test environment through regional intensity or acceleration contours that resulted from a separate microzonation study. Building amplification is determined by examination of a large collection of data recorded during the San Fernando earthquake of 1971.

Two test simulation techniques are described and compared, i.e., the "sweep-sine" and "synthesized earthquake" methods. Ideally earthquake motion employed for equipment testing on shakers should satisfy all or most of the following requirements in order to achieve a good simulation, that is, the maintenance of the resemblance of the appearance of wave forms, and the matching of response spectra, peak acceleration, peak velocities, and durations. The synthesized waveform, which generates test table motion via a d-a converter and a hydro-control system according to a digitally generated artificial earthquake accelerogram, is chosen because of its definite advantages over the sweep-sine in almost every item considered.

A shaker-table application of the test procedure for communications switching equipment is described. The seismic reliability of the equipment in terms of the test results and its relation to equipment earthquake survivability and protection requirements are discussed in detail.

## AN ALTERNATE APPROACH TO MODAL DAMPING AS APPLIED TO SEISMIC SENSITIVE EQUIPMENT

L. A. Bergman and A. J. Hannibal  
Lord Kinematics, Erie, Pennsylvania

Damping has been shown to be an extremely important parameter in the response of dynamic systems subjected to random vibrations, such as earthquakes. Therefore, its mathematical representation and treatment become critical elements in the analysis of such systems, especially if the Spectral Method is utilized. Unfortunately, damping models commonly used today either do not adequately represent system damping or are mathematically cumbersome. The method described in this paper is both simple and accurate, obviating much of the experience and judgment normally required in the definition of modal damping factors.

Damping models presently in vogue are:

1. Viscous Damping—Here the dissipative element is assumed to be a linear function of velocity. The damping coefficients are difficult, if not impossible, to define and the system cannot normally be decoupled.
2. Modal Damping—In this case, the undamped system is decoupled and viscous damping factors are defined for each mode. To do so accurately requires experience and good judgment.
3. Proportional Damping (Rayleigh Form)—Proportional damping implies the damping matrix is a linear combination of the mass stiffness matrices:  
 $C = \alpha M + \beta K$ . Since both  $M$  and  $K$  diagonalize simultaneously, so also does  $C$ . The unfortunate drawback is that the Rayleigh form does not realistically represent the damping in the system.

The approach, recommended in this paper, involves decoupling the system in the complex domain utilizing a complex stiffness approach (structural damping). By accurate determination of the damping in each system component, represented in the form  $E = E'(1 + j\eta)$ , the modal damping factors can be readily calculated using a standard complex eigenvalue routine.

Essentially, the stiffness matrix is derived in the form  $K^* = K' + jK''$  yielding damped equations of motion given by

$$M\ddot{\mathbf{x}} + K^*\mathbf{x} = \mathbf{F}.$$

The eigenvalue problem can, then, be formulated in the complex domain as

$$\det |Ms^2 + K^*| = 0;$$

where the  $i$ th eigenvalue,

$$S_i^2 = \omega_i^2(1 + j\eta_i),$$

contains both the natural frequency and loss factor for each mode. An equivalent damping factor can be computed for each mode from the equation

$$\xi_i = \frac{1}{2}\eta_i .$$

Consequently, much like the modal damping technique, the viscous equivalent,  $\xi_i$ , is added to the  $i$ th mode. Since the conversion yields equal damping at a resonant frequency for which a single degree-of-freedom acts like a filter, it is reasonably accurate through the region of greatest interest.

This method is both simple and accurate, limited by the loss factor representation of the dissipative elements in the system, the size of the matrix which can be decoupled in the complex domain, and the broad-band accuracy of the viscous-complex equivalence assumption.

The above procedure is applied to a scale model of a high voltage circuit breaker mounted on elastomeric suspension systems of various damping characteristics. Natural frequencies, modal damping, participation factors, and transmissibilities are computed for each mode, and the results are subjected to spectral analysis.

Fabrication of the scale model is described, including application of damping compounds to the model to simulate actual circuit breaker component loss factors. Transmissibilities of the various modes of the model are obtained in shaker test and are compared with the previous analytical results to demonstrate the viability of the analysis.

Finally, the analytical method is applied to a full scale circuit breaker and the advantages and disadvantages of auxiliary elastomeric suspension systems for seismic protection as applied to circuit breakers are discussed.

#### THE SHOCK ENVIRONMENT OF A FREIGHT TRAIN DERAILMENT

William W. Wassmann and John H. Armstrong  
Naval Surface Weapons Center, White Oak, Maryland

Direct, reportable damage costs to railroad property due to equipment-caused freight train derailments in the U. S. amount to \$30 million per year; total costs including damage to lading, delays, etc., are estimated to be from \$90 to 150 million per year. The largest single contributor to these accident costs is axle failure from overheated journal bearings ("hot boxes") not detected in time. In addition, some derailments caused by wheel, rail or other defects initially involve only a single axle, truck or car, but go undetected for many miles until a general pile-up results when a grade crossing, or turnout is encountered. The severity of such derailments may be reduced by a local derailment detector or "wheel-on-the-ground sensor."

The Naval Surface Weapons Center/White Oak Laboratory, after conducting a feasibility study in 1972/73, has embarked on a two-year program for the Federal Railroad Administration's Office of Research and Development to develop an on-train System for

**Train-Accident Reduction (STAR).** This system includes self-powered hot journal sensors and local derailment detectors which actuate the existing air brake system. It will be installed for test on a 124-car unit ore train of the Duluth, Missabe and Iron Range (DM&IR) Railway Company.

This paper will describe the establishment of design criteria for a seismic local derailment detector based on the measured environment. In November 1974, derailment tests were conducted on an instrumented DM&IR 70-ton ore car. The purpose of the tests was to determine acceleration and velocity thresholds which could be used to identify a derailment condition. A total of 12 tests were conducted to measure the shock effects of a wheel impacting the roadbed, in an empty car vs a loaded car and at the "field-side" wheel location (where the flange side of the wheel drops from the outside of the rail) vs the "gauge-side" location (where the tread of the wheel drops from the inside of the rail). Also investigated were effects of train velocity and of the wheel's impact point with respect to cross ties.

Acceleration measurements were also made during normal, over-the-road operations on both the empty and loaded cars, as well as during loading, unloading and coupling operations. All acceleration measurements were made on the unsprung-mass portion of the trucks.

It was determined that a combination of acceleration and velocity-change thresholds exists which can be used to uniquely define a derailment signature. The analysis of data from these tests has led to the development of a seismic detector with an acceleration threshold determined by a preloaded spring and a velocity threshold established by means of the distance of travel prior to actuation.

#### **THE DEVELOPMENT OF A GENERALIZED IMPACT RESPONSE MODEL FOR A BULK CUSHIONING MATERIAL**

Don McDaniel  
U. S. Army Missile Command  
Redstone Arsenal, Alabama

and

Richard M. Wyskida  
The University of Alabama in Huntsville  
Huntsville, Alabama

#### **SUMMARY**

This paper discusses the results of a research effort that was conducted to formulate a valid model of impact response for bulk cushioning materials. Temperature was of particular concern in the model in that temperature effects have been shown to possess a significant effect on impact response. It was postulated that viscoelastic theory could be utilized to formulate a model of impact response that incorporates temperature effects. The current design practice for predicting impact response is predicated on dynamic cushioning curves which do not account for temperature effects on impact response.

A model of impact response that accounts for temperature effects was expected to improve the predictability of cushioning systems.

The construction of the impact response model for cushioning materials at varying temperatures required the development of a functional relationship of the variables. The required relationship can be expressed mathematically as:

$$G = F(\sigma_s, T, \theta, h)$$

where

$G$  = acceleration G-level

$\sigma_s$  = static stress in psi

$T$  = thickness of cushion inches

$\theta$  = cushion temperature in °F

$h$  = drop height in inches.

The relationship of each independent variable ( $\sigma_s, T, \theta, h$ ) and its effect upon the dependent variable (G-level) was studied and the finalized relationship for each independent variable was then incorporated into the model.

The model development process proceeded through many iterations of development and verification and culminated in the General Model of impact response stated mathematically as

$$G = C_0 + \sum_{\ell=0}^S h^{\ell/2} \sum_{k=0}^R \frac{1}{T^{(1/2+k)}} \sum_{j=1}^N \theta^j \sum_{i=0}^M C_{ijk\ell} \sigma_s^i .$$

Statistical results indicate that the model reliably predicts impact response in terms of  $G$ 's experienced by the protected item.

Once a valid model of impact response was developed, it could be used as the basis of a procedure that performs a constrained sequential search for the preferred material thickness for a specified fragility level. The technique searches for limits of acceptable  $G$ -level values along the dynamic cushioning curves. The search routine has been automated and the output is in the form of plots of superimposed dynamic cushioning curves.

The developed model has been found to be a better predictor of impact response than the dynamic cushioning curves currently being utilized. The inclusion of the temperature effect appears to be the primary cause for the increased precision in impact response prediction. An automated optimization is being provisioned with these models for several of the frequently used bulk cushioning materials and the automated design procedure will be made available for use to designers of bulk cushioning systems.

## **BARREL TAMPED EXPLOSIVELY PROPELLED PLATES FOR OBLIQUE IMPACT EXPERIMENTS**

F. H. Mathews, B. W. Duggin  
Sandia Laboratories, Albuquerque, New Mexico

The use of explosively driven rotating flyer plates for high velocity impact experiments at shallow angles was described in the 45th Shock and Vibration Symposium. The detonation of a solid explosive is used to accelerate massive, slowly rotating plates to high velocities. The device to be impacted is positioned at a distance along the flight path sufficient to allow rotation of the flyer plate before impact. Thus, any angle between the plate's surfaces and the plate velocity vector can be obtained.

In this paper, the addition of a massive barrel surrounding the explosive with the detonation normally incident on the plate improves energy transfer between explosive and plate. Data from small experiments in combination with one-dimensional analysis allows prediction of velocity as a function of plate thickness for geometrically similar systems. Methods are described for fireball suppression, fragment control, and experiment protection which are essential for oblique impact experiments on full size fusing hardware. Results are presented from several large experiments including a 190 kg explosive system which propels a rotating 11 kg aluminum plate at a velocity of 3700 meters/sec.

## **ESTIMATION OF SHIP SHOCK PARAMETERS FOR CONSISTENT DESIGN AND TEST SPECIFICATION**

Gary C. Hart and T. K. Hasselman  
J. H. Wiggins Company  
Redondo Beach, California

and

W. N. Jones  
Naval Weapons Center  
China Lake, California

The need to characterize recorded ship shock data for use in design and test constitutes one of the reasons for conducting full scale shock tests. The characteristic parameters which one specifies and proceeds to numerically quantify are functions of the underlying approach or philosophy used in design and test practice. Therefore, a fundamental, and most important decision must be made on which characterization procedure is to be used for analyzing the shock data.

This technical paper presents the application of a procedure which analytically represents the shock as a time-modulated nonstationary stochastic process with a time varying mean. The parameters which must be quantified for such a representation are the shock's mean value function, time-modulating function and power spectral density function. These parameters are defined in the paper. Utilizing actual measured ship shock data the

parameters are estimated by statistical methods of analysis. Results from different digital data processing techniques are presented to show their influence on the final parameter estimates. The results from this part of the analysis enable digitally simulated test functions to be generated for use in stock tests.

The paper goes on to demonstrate how the previously defined characterization parameters can be utilized in the development of probabilistic shock spectra. Probabilistic spectra are developed using the parameter values estimated from the ship shock data. These spectra are then compared with standard deterministic shock spectra obtained using the original shock records, and with peak component response data from the same test. The application of all three types of spectra to ship shock design is discussed.

### STRESS WAVE APPROACH TO THE ANALYSIS OF SUBMARINE COMPONENT SHOCK RESPONSE

J. D. Colton and J. E. Malinak  
Stanford Research Institute

Survival of internal submarine equipment is critical for mission success under nuclear attack. Although several investigations have been made of internal equipment response, little is known about the response of equipment to the initial stress waves propagated through the submarine when it is subjected to an underwater shock wave. A previous study at Stanford Research Institute showed that high strength steel bolts used to hard mount mock components to a simple structure can fail under the sudden displacement of the structure associated with the initial stress waves propagated through it. The objective of the present study is to determine if similar component damage is inflicted on a submerged submarine. A combined experimental and theoretical approach was taken.

In the experimental part of the study, 6-inch-diameter, 0.040-inch-thick, 3-foot-long, stainless steel cylinders were sealed at the ends and tested underwater. Simple cylinders as well as cylinders with 0.038-inch-thick horizontal decks spanning the cylinder diameter were used. In some tests both edges of the deck were rigidly attached to the cylinder walls (fixed deck); in other tests there was a gap of about 0.015 inch between the deck and the cylinder (free deck; the deck was then supported by styrofoam blocks). This free deck configuration more accurately simulates the slip-joint configuration in submarines. These structures were loaded by underwater shock waves generated by bundles of from 8 to 16 strands of 80 grain/ft primacord. Strand lengths ranging from 10 to 15 inches were placed from 1.5 to 5 feet from the structures. These charges produced underwater shock waves with a step rise followed by a constant amplitude of up to 1000 psi, not great enough to cause significant structural damage to a submarine. Instrumentation in these tests consisted of piezoelectric gage probes to measure the free field pressure, strain gages to measure the wave propagation in the cylinder and deck, and, in one test, an ytterbium piezoresistive gage to measure the interaction pressure on the surface of the simple cylinder.

In the theoretical part of the study, wave propagation in the cylinder and deck was predicted for the plane strain condition. The curved-wave approximation was used to model the early-time fluid-structure interaction, the Herrmann-Mirsky shell equations

were used to model the cylinder, and simple one-dimensional plate theory was used to model the deck. The associated governing equations were integrated by the method of characteristics.

Good agreement was obtained between the measured and predicted response of these structures up to at least the time the shock wave engulfed the cylinder. The overall time history of the compressive strains at the leading edge of the deck, on which some of the internal equipment would be mounted, were approximately constant in amplitude for several transit times of a stress wave across the deck. For the fixed deck the wave front was rounded. For the free deck a sharp wave front was created by the impact between the cylinder and the deck; disturbances from waves reflected from the unloaded side of the deck were also apparent, but the effect was only to reduce the amplitude of the strain for a short time. Although the strain amplitude generated in the decks was always less than the yield strain of the material (about 0.1 per cent), the corresponding displacement for twice the wave transit time across a full scale deck was as large as 0.5 inch; even larger displacements are produced at later times. Such displacements can shear large bolts that penetrate the deck.

It is concluded that stress waves can damage hard mounted submarine equipment and that a wave approach to the analysis of this response is needed.

#### **POWER SERIES EXPANSION OF THE DYNAMIC STIFFNESS MATRIX INCLUDING ROTARY INERTIA AND SHEAR DEFORMATION**

Mario Paz  
Professor, University of Louisville  
Louisville, Kentucky  
and  
Lam Dung  
Graduate Student, University of Louisville  
Louisville, Kentucky

The dynamic analysis of frame-type structures whose members have distributed mass is usually sought by transforming the continuous structure into an approximate discrete system (1). The derivation of the required stiffness, mass, and geometric matrices is generally obtained from static displacement functions. The process of discretizing based on the classical Bernoulli-Euler theory of flexural vibration or on the more accurate Timoshenko beam theory results in transcendental trigonometric and hyperbolic functions (2). Mathematical singularities and the complexity of these functions (3) make the Bernoulli-Euler or Timoshenko beam theory less attractive than the approximate method of discretizing.

It is noteworthy that the stiffness and mass matrices derived from the static displacement functions have also been obtained through a power series expansion of the dynamic stiffness matrix based on Bernoulli-Euler beam theory (3). The stiffness and mass matrices are in fact the first-order terms of the resulting series expansion. Second-order terms have also been obtained simply by extending the series expansion. This mathematical approach delineates the range of convergence of the series. Hence, it provides the

analytical basis to ascertain the approximations inherent in the heuristic derivation of the stiffness, mass, and geometric matrices from static displacement functions.

The power series expansion of the dynamic stiffness matrix based on the Bernoulli-Euler beam theory does not account for rotary inertia and shear deformation effects. As an extension of previous work, in the present paper the derivation of the stiffness and mass matrices is obtained by expanding in power series the dynamic stiffness matrix based on the Timoshenko beam theory which includes rotary inertia and shear deformation. The Timoshenko beam equation may be written conveniently in the notation used by Snowdon (4) as

$$\frac{\partial^4 y}{\partial \lambda^4} + (na)^4(\alpha + \beta) \frac{\partial^2 y}{\partial \lambda^2} + (na)^4[(na)^4 \alpha \beta - 1]y = 0 \quad (1)$$

where  $k'$  is a shearing constant depending on the shape of the cross-section,

$$\begin{aligned} n^4 &= \frac{\omega^2 \rho}{Er^2} & \lambda &= \frac{x}{a} \\ \alpha &= \frac{r^2 E}{K' a^2 G} & L &= 2a \\ \beta &= \frac{r^2}{a^2} & I &= Ar^2 \end{aligned} \quad (2)$$

The dynamic stiffness matrix based on equation (1) is found by solving this equation and imposing the pertinent boundary conditions (3). The term in the fourth row and second column of this matrix is

$$S_{42} = \frac{EI(\theta^2 + n^2)(\theta^2 \eta S - \eta \theta s)}{2\theta^2 \eta^2(1 - cC) + (\theta^2 - \eta^2)sS\theta \eta} \quad (3)$$

where

$$\begin{aligned} (2\theta a)^2 &= (na)^4(\alpha + \beta) + \sqrt{(na)^8(\alpha - \beta)^2 + 4(na)^4} \\ (2\eta a)^2 &= - (na)^4(\alpha + \beta) + \sqrt{(na)^8(\alpha - \beta)^2 + 4(na)^4} \end{aligned} \quad (4)$$

$$s = \sin \theta a \lambda \quad S = \sinh \eta a \lambda$$

$$c = \cos \theta a \lambda \quad C = \cosh \eta a \lambda$$

For the sake of discussion the dynamic stiffness coefficient  $S_{42}$  is expanded in power series. In the derivation, operations with power series, including addition, subtraction, multiplication, and division are employed. The validity of these operations and convergence of the resulting series was proved by Knopp (5). The known expansions in power series about the origin of trigonometric and hyperbolic functions as well as the expansion of polynomial raised to a fractional exponent are used and substituted into equation (3) to obtain after considerable algebraic work the series given by equation (5)

$$S_{42} = \frac{EI}{a} \left[ 1 + n^4 a^4 \left\{ \frac{2}{35} + \frac{1}{15} (\alpha + \beta) + \dots \right\} + n^8 a^8 \left\{ \frac{4387}{2,182,950} + \frac{168}{18,900} (\alpha + \beta) + \dots \right\} + \dots \right] \quad (5)$$

The substitution of the symbols from equation (2) into equation (5), yields directly the dynamic stiffness coefficient,  $S_{42}$  in terms of the geometric and mechanical properties of the beam; namely,

$$S_{42} = \frac{2EI}{L} + \frac{mL^3 \omega^2}{140} + \frac{1097L^7 m^2 \omega^4}{69,854,400EI} + \frac{mL^3 \omega^2}{30} \left( \frac{r}{L} \right)^2 \left( 1 + \frac{E}{K'G} \right) + \frac{m^2 L^7 \omega^4}{14,400EI} \left( 1 + \frac{E}{K'G} \right) + \dots \quad (6)$$

It may be recognized that in equation (6) the first and second terms are, respectively, the stiffness and mass coefficients which are obtained from approximate displacement functions. The third term is a higher-order term involving the square of the mass and the last two terms represent the combined effect of rotary inertia and shear deformation. It should be pointed out that the terms of this series, with the exception of the shear factor, have been derived previously in a different formulation by Prezemieniecki (6).

In this paper the power series expansion for all the terms of the dynamic stiffness matrix based on the Timoshenko beam theory is obtained using the procedure described. Also the radius of convergence of the resulting series is determined from the theory of operations with power series.

#### REFERENCES

1. Archer, J. S. "Consistent Mass Matrix for Distributed Mass System," *Journal Structural Division, Pro ASCE* Vol. 89, 1963.
2. Henshell, R. D. and Warburton, G. B., "Transmission of Vibration in Beam Systems," *International Journal for Numerical Methods in Engineering*, Vol. 1, 1969.
3. Paz, Mario, "Mathematical Observations in Structural Dynamic," *International Journal Computers and Structures*. Vol. 3, 1973.
4. Snowdon, J. C. *Vibration and Shock in Damped Mechanical Systems*, John Wiley & Sons Inc., New York, 1968.
5. Knopp, K. *Theory and Application of Infinite Series*, Blackie, London, 1963.
6. Prezemieniecki, J. S. "Quadratic Matrix Equations for Determining Vibration Modes and Frequencies of Continuous Elastic Systems," *Proc. Air Force 1st Conference on Matrix Methods in Structural Mechanics*. Wright-Patterson Air Force Base, Ohio. October 26-28, 1965. AFFDL TR 66-80, 1966.

## EFFECT OF PHASE SHIFT ON SHOCK RESPONSE

Charles T. Morrow  
Advanced Technology Center, Inc.  
Dallas, Texas

Whereas the Fourier transform, complete with phase-versus-frequency information, uniquely defines a shock excitation time history and the corresponding response of any mechanical system, the shock spectrum does not. Any phase characteristic, compatible with the magnitude characteristic in the sense that it does not imply a negative time delay, can be assumed. Each choice would lead to a different time history. Concern that shock tests performed at different laboratories to the same shock spectrum requirement may lead to different failures of the same test item has led to various proposals for supplementary constraints on shock testing. At the 45th Shock and Vibration Symposium a suggestion was made that a phase curve with tolerances be provided to supplement the magnitude spectrum and its tolerances.

For the present theoretical investigation, an electromagnetically applied terminal step function of acceleration is selected as a starting point. It is simpler to analyze than a terminal peak sawtooth, but it induces similar responses. A simple all-pass phase shift network is assumed to be inserted in the electronic system. This permits a theoretical investigation of effect of phase shift on response peaks and on energy absorption by a procedure that could be approximated on a laboratory shaker.

The inserted phase shift network has negligible influence on the response transient of a simple resonator and negligible influence on the individual response transients of a two-degree-of freedom system. But it does alter the relative phase of the latter and thereby the timing and magnitude of the first maximum of their combined envelope. The energy absorption in the second resonator is also changed. Without the phase shift network, two transients nearby equal in frequency start out approximately opposite in phase, so that the first maximum of the envelope does not occur until they have experienced part of their decay. The influence of relative phase shift on their damage potential is greatest when the damping is highest.

It is not clear whether the study of phase effects will lead to a feasible way of controlling the possible variability of a shock test specified in terms of a shock spectrum or reveal some uncertainties the specification writer must accept. Some future steps toward settling the feasibility problem are outlined. If, however, there must be some uncertainty of effect regardless of the wording of the test specification, it is important to recognize this. Otherwise shock tests may be called upon to prove things they are incapable of proving about a test item.

## DYNAMIC BUCKLING OF SHALLOW IMPERFECT SPHERICAL CAPS UNDER STEP PRESSURE LOADS

Chatta Lakshmikantham and Tien-Yu Tsui  
Army Materials and Mechanics Research Center  
Watertown, Massachusetts

### BACKGROUND

The investigations of static buckling of shallow spherical caps have had a long history, dating back to the early thirties when Mt. Palomar Observatory was being designed. Starting with theoretical work of Karman and Tsien, they have progressed through several decades of experimental and theoretical work, their development keeping pace with the improvement of digital computer capabilities. Ref. 1, provides a fairly complete recent review of these investigations.

Despite such a long sustained interest in the static behavior, it has been only recently the dynamic response problem has been studied. As a result, there is a considerable gap in the understanding of the problem, especially with reference to the unsymmetrical buckling and the imperfection sensitivity. Also there has been no serious attempt to correlate the available theoretical results with test data.

Recently, a careful series of experiments was performed at Army Materials & Mechanics Research Center, Ref. 2, and as a result it was found that there is very poor correlation with the available theoretical results. Even more startlingly, the test results invariably were higher than the predicted results.

### AIM OF PRESENT WORK

The objective of this investigation has been to undertake a theoretical study of the problem including non-symmetric deformations and initial imperfections, so that a better correlation with the best results might be achieved.

### THEORETICAL FEATURES

The bulk of the theoretical results presented so far, has been invariably based on an axisymmetric formulation with the governing equations being a coupled system of nonlinear partial differential equations in terms of time and the radial coordinate. These equations are written in a finite difference scheme and integrated explicitly or implicitly with appropriate initial and boundary conditions. Such methods cannot successfully include initial imperfections and the equations being axisymmetric preclude unsymmetric behavior.

The present investigation deals with the more general problem of unsymmetric displacement including initial imperfections. Although the equations are in the familiar form Karman-Donnell Equations, they reflect the fact that as a second-degree curve the shallow cap could be parabolic or spherical and thus the present equations are not written with the spherical geometry in view.

The solution method uses a modal representation of both the normal displacement and the initial imperfections with coefficients being unknown functions of time. Both symmetric and non-symmetric terms are included to obtain a degree of generality. Based on experimental work on static behavior of shells it has been found that for values of shallow-shell parameter ' $\lambda$ ' up to 10, axisymmetric solution is valid and beyond that non-symmetrical terms govern.

The advantage of such a procedure is twofold: on the one hand, the chosen pattern has relevance to the observed phenomena and, on the other, one can take into account both symmetric and non-symmetric initial imperfections with relative ease.

Based on a buckling criterion that the dynamic buckling load corresponds to that critical load at which, for a small increment in the load, there is a very large increase in the response of the structure, the dynamic buckling load can be determined for a given shell parameter  $\lambda$  and a given imperfection, utilizing conventional methods as Galerkin's procedure, as have been done elsewhere, e.g. Ref. 3.

#### HIGHLIGHTS OF THE RESULTS

The results obtained for the axisymmetric buckling have shown excellent agreement with the test results of Ref. 2, for  $\lambda$  values up to 10 beyond which the asymmetric modes seem to dominate. For larger values, by including non-symmetric modes excellent agreement (within 5%) with the test results have been found.

This is a considerable improvement over the correlation with previous results.

#### REFERENCES

1. Fung, Y. C. and Sechler, E. E. (ed) Thin-Shell Structures, Prentice-Hall, Inc., New Jersey 1974 Ch 10.
2. Adachi, J. et al, Response of Shallow Spherical Shells to Pulse Pressure Loads, Proceedings of Army Symposium on Solid Mechanics, 1972, AMMRC MS73-2 Army Materials & Mechanics Research Center, Watertown, MA 02172.
3. Lakshmikantham, C. and Tsui, T., "Dynamic Stability of Axially Stiffened Imperfect Cylindrical Shells Under Axial Step Loading, *A.I.A.A. Journal*, Vol. 12, No. 2, Feb. 1974, pp. 163-169.

## FLUID - STRUCTURE TOPICS

### DETERMINATION OF DYNAMICS LOADS FROM MISSILE MODEL WIND TUNNEL DATA

P. G. Bolds and D. K. Barrett  
AFFDL, Wright-Patterson AFB, Ohio

The Air Force Flight Dynamics Laboratory has obtained unsteady pressure data on a model of an air-launched ICBM. The missile is required to fly at high angles of attack during the initial portion of the trajectory. During this portion of the flight, if Karman vortices are shed, there will be side loadings which could cause undesirable dynamic response of the missile structure.

Wind tunnel tests were conducted at AEDC on 1-5 July and 11-22 November 1974. With the use of the Air Force Flight Dynamics instrumentation van, unsteady pressure measurements were made on a missile model over a wide range of angles of attack and Mach numbers. The angles of attack varied in increments of  $5^\circ$  from  $-5$  to  $180^\circ$  and Mach varied from 0.3 to 1.5.

There were eight microphones at each of four missile model stations mounted on the leeward side of the model. There were eight missile model configurations varying in total length from 61.5 inches to 78.8 inches approximating a 10% scale missile.

Significant dynamic loading occurs when at any instant of time the pressure is positive on one side and negative on the opposite side of the missile and correlation along a larger portion of the length of the missile. When the frequency of the pressure changes and correlated lengths correspond to any of the missile free-free modes, then resonance of the missile in bending will occur. However, since damping is present in the missile structure, the amplitude or bending movement response will depend on the magnitude and frequency of the pressure and its distribution over the surface of the missile.

To obtain this information from the measured data, RMS pressure coefficients  $(\Delta C)_{rms}$  were computed thusly:

$$(\Delta C)_{rms} \equiv \frac{(\Delta p)}{q} \text{ rms}$$

where  $(\Delta p)_{RMS}$  is the measured dynamic pressure and  $q = 1/2\rho V^2$ . The RMS pressure coefficients were plotted versus  $\theta$ , the transducer location in degrees from the meridian. Power spectral density (PSD) values were calculated from the measured data. The  $(\phi_i)$  of the unsteady pressure coefficients were computed thusly:

$$\phi_i = \frac{\frac{|\Delta C_i|^2}{\Delta \omega D}}{V}$$

where  $\omega$  is the angular frequency ( $2\pi\Delta f_i$ ) and  $\Delta f_i$  is the broad (constant percentage of  $.23f_i$ ) bandwidth  $i$  under consideration,  $D$  is the diameter of the missile model and  $V$  is the measured velocity. Phi was plotted versus  $\omega D/V$ .

The value of  $\phi_i$  gives information as to the frequency distribution of the unsteady pressure coefficients. This information is useful in determining vortex shedding frequencies and ultimately determining potential coupling of the unsteady air load with natural modes of the missile. After examination of the broad-band analysis, narrow band (0.1 Hz) analysis of critical cases were performed to compute the cross-correlation and coherence function both radially and longitudinally.

An attempt will be made to relate the natural and dynamics response frequencies the model to a prototype of the missile. The unsteady pressure of the model should be observed at frequencies that are  $L_p V_m/L_m V_p$  times the value of those frequencies (Strouhal Number) of concern on the full scale prototype, where  $L$  and  $V$  are the length and velocity respectively.

## FEASIBILITY STUDY OF AN ACOUSTIC COVER FOR SHUTTLE PAYLOADS

M. Ferrante and C. V. Stahle  
General Electric Space Division

F. J. On  
NASA Goddard Space Flight Center

This paper presents the analysis, design and experimental evaluation of a viscoelastic laminated acoustic cover that will shield sensitive instruments from the high low-frequency acoustic environment of the Space Shuttle payload bay. The high low-frequency acoustic environment will result in a more severe dynamic environment than that of current launch vehicles. Consequently, it is anticipated that many new problems in experiment development will arise and that the use of existing experiment components and instruments will require qualification for the Shuttle environment. One method of circumventing this more severe dynamic environment is to provide protective covers for sensitive portions of the experiments. If this is accomplished effectively, generic experiment components can be used with a high degree of confidence in subsequent orbital operation and developmental costs will be substantially reduced. For this approach to be effective, a lightweight protective cover must be used. This study provides a cost effective method of reducing payload developmental costs and includes a preliminary design and experimental evaluation of a lightweight acoustic barrier.

A cylindrical configuration using viscoelastic laminated construction was selected because of its inherent stiffness and damping. Although a box configuration was considered, an order of magnitude increase in the cover resonant frequencies is obtained by the cylindrical configuration. This maximizes the frequency range over which acoustic attenuation is stiffness controlled. High damping extends the frequency range of effective attenuation by preventing large reductions in the acoustic attenuation at the cover resonant frequencies.

A cylindrical cover configuration with two face sheets joined by a viscoelastic shear layer was analyzed to determine the optimum wall construction. The wall construction was optimized for a three foot diameter considering a 500 Hertz minimum resonant frequency as a design goal. The analysis considered aluminum, magnesium and graphite epoxy materials for the face sheets. The results indicate that surface densities on the order of 0.25 to 0.5 lbs/ft<sup>2</sup> can be obtained using thin face sheets with a core made of strips of viscoelastic epoxy 1/4 inch wide on 5 inch centers. Although the design was optimized for a 3 foot diameter, the results indicate that larger diameter covers are also feasible.

A three foot cylindrical cover was designed for experimental evaluation. The test cover was made of two 20 mil aluminum face sheets with a half inch thick core of viscoelastic epoxy strips. A surface density of 0.75 lbs/ft<sup>2</sup> was obtained with an estimated composite loss factor of 0.6 and a fundamental resonant frequency of 500 Hertz. The end caps were fabricated using a conical aluminum face sheet joined to a flat bulkhead by viscoelastic wedges. A one inch thick removable fiberglass liner was included for absorption. Acoustic noise reductions were estimated considering the low frequency portion of the spectrum to be stiffness controlled and the high frequency portion of the spectrum to be mass controlled.

The experimental evaluation of the acoustic cover was performed in the NASA-Goddard Space Flight Center reverberant chamber and showed excellent agreement with predicted noise reductions. Two configurations were tested: one with the fiberglass liner and one without the fiberglass liner. The test cover was instrumented with 8 internal microphones and 9 accelerometers. The acoustic spectrum was shaped to that predicted for the Shuttle payload bay. Tests were performed at overall levels as high as 154 dB. Average reductions in the overall acoustic level of 20 dB and 12 dB were obtained with and without the fiberglass liner. In the low frequency range, attenuations were on the order of 20 to 30 dB. At high frequencies, attenuations were increased from approximately 25 dB to over 40 dB by the fiberglass liner. Minimum attenuations of 17 and 7 dB occurred in the 200 to 500 Hertz range with and without the fiberglass liner, respectively.

The results of the study verify the feasibility of using lightweight acoustic covers for Shuttle payloads and indicate that covers larger than the three foot test cover can be used effectively to protect sensitive payloads.

#### **LONGITUDINAL VIBRATION CHARACTERISTICS OF THE SPACE SHUTTLE SOLID ROCKET BOOSTER TEST SEGMENT**

D. L. Linton and J. C. Bartlett  
IBM Corporation, Huntsville, Alabama

Some of the liquid fueled launch vehicles in the Saturn program encountered low frequency longitudinal vibration anomalies which are called pogo. Pogo is a stability problem peculiar to liquid propellant vehicles with thin-skinned tanks which involves coupling between structural motions and the tank pressure regulation system. Although the Titan IIC vehicle has both liquid and solid propellant motors, the Space Shuttle will

be the first vehicle where the liquid motors burn before the solid propellant is depleted. In the Space Shuttle the liquid and solid propellant motors burn simultaneously and of special interest to the control and stability of the vehicle is the coupling between the pogo vibration mode of the liquid motor and the longitudinal vibration modes of the solid motor.

The primary longitudinal vibration modes of interest of the Space Shuttle Solid Rocker Booster (SRB) involve coupling between the rod modes of the motor case and the thickness shear modes of the solid propellant. The analysis of these coupled vibration modes is more complex than the analysis of other structural modes due to the properties of the propellant. Solid propellant is a highly damped viscoelastic material whose elastic moduli are complex quantities which vary with temperature, pressure, frequency, and strain. The dependence of the moduli on the latter two quantities results in the stiffness of the propellant being a function of the forcing frequency and the response deflection. Analytical techniques have been developed to analyze the longitudinal vibration characteristics of a solid rocket motor, but before any theory can be accepted it must be compared with test results. Because of the difficulty and cost of a vibration test of the entire SRB, a vibration survey test is planned for a segment of the SRB. This paper presents the analytical techniques that have been developed to analyze the longitudinal vibration characteristics of a solid rocket motor and the analysis of the longitudinal vibration characteristics of the modal survey test segment of the SRB.

The analytical techniques for vibration analysis of the longitudinal modes of a solid rocket motor were developed using the NASA Structural Analysis (NASTRAN) finite element computer program. Three different types of analysis from NASTRAN are used. First a normal mode analysis is used to determine the undamped eigenvalues and eigenvectors. Then a complex eigenvalue analysis is used to determine the damped eigenvalues and eigenvectors. Finally a frequency response analysis is used to determine which vibration modes can be excited by the forcing function and also what the shear strain will be throughout the propellant at the various vibration modes excited. An iterative procedure of changing the modulus to agree with the appropriate value consistent with frequency is used during the normal mode and complex eigenvalue analysis. An iterative procedure of changing the modulus to agree with the appropriate value consistent with strain is used during the frequency response analysis. The purpose of each of the three analyses and the iterative procedures used are presented in the paper in greater detail.

These analytical techniques were used to determine the vibration characteristics of the modal survey test segment. The iterative procedures were not used because of the limitation of propellant test data. The vast majority of propellant test data has been determined by test methods where the propellant shear strain was not a controlled test parameter. The analysis results show the vibration modes and the associated mode shapes for the test segment with both free-free and fixed-free boundary conditions. The analysis results also show which of these vibration modes can be excited by the proposed modal survey test.

The NASTRAN finite element model of the test segment is presented in this paper. Modal parameter results from normal mode, complex eigenvalue and frequency response analysis are tabulated and discussed. Computer generated mode shape plots and displacement versus frequency X-Y plots are also presented to supplement the results from the analysis.

**A STUDY OF THE DAMPING OF A CYLINDRICAL TANK PARTIALLY  
FILLED WITH LIQUID, AND APPLICATION TO THE FRENCH LAUNCH  
VEHICLE DIAMANT BP4 TO COUNTERACT THE POGO EFFECT**

P. Cochery, M. Vedrenne  
Centre National d'Etudes Spatiale Direction des Lanceurs  
Ervy, France

and

M. Poizat, R. Vialatoux  
Société pour la mesure et le traitement des  
vibrations et du bruit, Ecully, France

During the flight of liquid propellant launch vehicles many vibration problems occur, the main and more important one seems to be that of the "POGO" effect. It is characterized by an instability involving a low frequency longitudinal vibration mode of the vehicle structure, variations in the propellant flow rate in the supply-pipes, and thrust oscillations.

This effect has been observed on the French launch vehicle DIAMANT.

This paper is intended to show how it has been possible to suppress the "POGO" effect on DIAMANT launch vehicle using a locally spread damping technique.

The analysis of the phenomenon shows that the tank of the first stage plays the major part in the longitudinal vibration mode of the vehicle. Therefore, the dynamic behaviour of the tank partially filled with liquid was to be studied, this being considered as the coupling element between the structure and the liquid propellants.

Finite element methods, along with experimental investigation on a model-tank in order to improve the mathematical model of its dynamic behaviour, have been used to determine accurately the characteristics of the mode involved in the "POGO" effect, giving results necessary to isolate the mode, which is cylindrically symmetrical in shape and pressure field in the liquid, from other modes (e.g. circumferential ones).

Rather than pressurizing the tank as in an actual liquid propellant launch vehicle, this problem was solved by modifying the structure of the tank. This was achieved by using some circumferential stiffeners in order to move the circumferential modes towards higher frequencies taking care to change the longitudinal behaviour of the tank as little as possible. It should be noted that pressure transducers in the liquid were very helpful in finding the vibration mode looked for.

From previous flight data relevant to the rate of increase in vibration levels, it has been possible to evaluate what must have been the minimum damping factor of the actual tank to prevent the "POGO" effect from developing and therefore the level to which the gain of the feedback loop (structure-liquid propellants-pipes and thrust-structure) must be reduced.

The effect of damping on the model tank has been studied from two points of view:

- What could be obtained by damping only part of the tank? An experimental investigation and the computation of the dynamic behaviour of the damped structure were carried out concurrently.
- Which process to choose to achieve this? The single viscoelastic layer damping technique was compared with the constrained viscoelastic layer damping technique. Both of these were tested. Their efficiency and their technological problems were evaluated for this particular application.

From the transposition of the results to the actual tank and to the launch vehicle, the best trade-off between the surface of the tank to be treated, the technological difficulties, the increase in mass, and the efficiency of the damping treatment, has been determined.

The single layer damping technique has been chosen for use on the propellant tank of the first stage of the French launch vehicle DIAMANT B P4.

The analysis of the flight data obtained during its launching in February 1975 has shown that the process proved to be a good and efficient one: the "POGO" effect was completely suppressed. The efficiency of the process was confirmed during the launching of another DIAMANT vehicle in May 1975.

#### VIBRATIONS OF PERFORATED PIPES IN FLUID

Krajcinovic, D., Department of Materials Engineering  
University of Illinois at Chicago Circle, Chicago, Illinois

Chen, S. S. and Rosenberg, G. S.  
Components Technology Division, Argonne National Laboratory  
Argonne, Illinois

In many design applications it is necessary to study the dynamic response of a structural component embedded in fluid and subjected to various types of excitations such as earthquakes, acoustic and flow noises, etc. In case of long and slender beam-like components flow induced and sustained vibrations are even more important in view of possible instability. Several methods of suppression of excessive vibrations (including dampers, helical wires, surface modifications and shrouds) have been studied in the past. The objective of this paper is to present an analytical evaluation of the effect of orifices on the vibration response and suppression of instability.

The application of perforated pipes is indicated in at least two cases:

- When the separation of liquid inside and outside the pipe is not required.
- When  $t$  is used as a shroud.

Those two cases are analytically examined in the paper considering flow to be potential. The motion of the fluid through the perforations in the pipe wall is governed by Darcy's law. For example, the problem for case (1) can be stated as follows:

$$\left. \begin{array}{l} \nabla^2 \phi_1 = 0 \\ \nabla^2 \phi_2 = 0 \end{array} \right\} \quad (1)$$

$$\left. \begin{array}{l} -\frac{\partial \phi_1}{\partial r} \Big|_{r=a} - k\rho \left( \frac{\partial \phi_1}{\partial t} \Big|_{r=a} - \frac{\partial \phi_2}{\partial t} \Big|_{r=a} \right) = U \\ -\frac{\partial \phi_2}{\partial r} \Big|_{r=a} - k\rho \left( \frac{\partial \phi_1}{\partial t} \Big|_{r=a} - \frac{\partial \phi_2}{\partial t} \Big|_{r=a} \right) = U \end{array} \right\} \quad (2)$$

where  $\phi_1$  and  $\phi_2$  are velocity potentials inside and outside the pipe,  $U$  is pipe velocity,  $r$  is pipe radius,  $\rho$  is fluid density, and  $k$  is wall permeability coefficient. Equations (1) and (2) can be solved using separation of variables.

Under those assumptions of the hydrodynamic force acting on the pipe is derived in closed form for the case of harmonic excitation. It is found that the hydrodynamic force has two components:

- (1) one, in phase with acceleration, reflecting the increase in inertia, and
- (2) the other opposing the motion of the pipe and related to the damping mechanism.

Both components of the hydrodynamic force are derived in form of simple formulas containing fluid density, pipe mass, geometry permeability, and the excitation frequency.

From the hydrodynamic force, an added mass coefficient  $C_M$  and an equivalent viscous damping coefficient  $C_v$  are obtained. For case (1), they are

$$C_M = \frac{2}{1 + 4k^2a^2\rho^2\omega^2}$$

and

$$C_v = M\omega \frac{2ka\rho\omega}{1 + 4k^2a^2\rho^2\omega^2} \quad (3)$$

where  $\omega$  is oscillation frequency, and  $M$  is the displaced mass of fluid. Having the two constants, the dynamic response of a perforated pipe can be readily determined using conventional methods.

In a word, this paper presents an analytical study of perforated pipes vibrating in a liquid. The results demonstrate that perforations can be effectively used to suppress excessive vibrations of structural components.

## VIBRATION AND STABILITY OF FLUID-CONVEYING PIPES

H. C. Lin and S. S. Chen  
Argonne National Laboratory, Argonne, Illinois

Lateral vibration of tubes containing or surrounded by flowing fluid has received considerable attention in recent years. The dynamic behavior of tubes subjected to transverse loading is of importance in designing system components such as oil pipelines, heat exchangers, etc. In particular, the failure of a tube in a Liquid Metal Fast Breeder Reactor superheater or evaporator will result in a violent isothermal sodium/water chemical reaction and generate a large pressure pulse. To evaluate the effect of this pressure pulse on the structural integrity of the heat transport system, it is necessary to analyze the dynamic response of components in steam generators. Meanwhile, the estimation of the natural frequencies and stability limit of a system is necessary in designing a highly sophisticated component.

This paper presents the dynamics of a fluid-conveying pipe, clamped at the upstream end and elastically supported at the downstream end. First, the governing equations of the mathematical model are presented in universal dimensionless form. The stability/instability boundaries of the system are then discussed. Finally, an approximate solution is presented for transient response.

The stability of the system is determined using an exact solution, while the transient response is solved using an approximate solution. The technique is based on the separation of the original problem into two kinds of problems—"quasi-static" and "dynamic" problems, and on the properties of the linear differential operators intrinsic to the equations of motion and boundary conditions. The "quasi-static" problem is solved by a conventional method, and the "dynamic" problem is solved by an eigenfunction expansion. The stability/instability boundaries can be determined from the dynamic problem; while the transient response consists of the sum of the solutions of quasi-static and dynamic problems. Several numerical examples are presented to illustrate the method of analysis.

When the flow velocity is small, the system performs damped oscillation. As the flow velocity increases, natural frequencies decrease and damping increases; the reduction of natural frequencies is attributed to fluid centrifugal force and the increase of damping is associated with fluid Coriolis force. As the flow velocity is further increased, the pipe may lose stability by buckling, flutter, or both depending on the magnitudes of displacement and rotational spring constants at the end. In general, the critical flow velocity is very high; hence system components such as steam generator tubes in CRBRP (Clinch River Breeder Reactor Plant) are unlikely to lose stability in practical flow velocity ranges.

Designing to avoid large amplitude motion in subcritical flow velocity ranges and the prediction of component response require knowledge of the dynamic behavior of the components. Using the results presented in the paper, the response in subcritical flow velocity ranges can readily be calculated. The method presented can be used effectively to calculate the response of a system to an excitation with an arbitrary initial condition and time-dependent boundary condition. The method can also be applied to other non-conservative systems.

## **EXPERIMENTAL LIQUID FUEL/POSITIVE EXPULSION BLADDER DYNAMICS**

**Martin Wohltmann, Martin Marietta Aerospace  
Orlando, Florida**

An experimental program is presently underway at Martin Marietta Aerospace, Orlando, Florida, to 1) investigate fuel slosh effects on the stability and control of the Advanced Strategic Air Launched Missile (ASALM), and 2) to evaluate the performance of two candidate positive fuel expulsion bladder devices.

Due to general mission requirements, the ASALM missile executes thrusting climbs, constant altitude/velocity trajectories, thrusting or non-thrusting dives, and bank-to-turn maneuvers. As a result, the acceleration field direction seen by the bladder-encased liquid fuel varies over a significant range. Besides the usual lateral "coffee cup" type slosh effects, longitudinal "coffee cup" slosh induced by ramjet engine thrust variations causes pitch and yaw plane perturbations. Of significant interest is the effect on stability of the non-linear behavior of the liquid fuel during constant altitude/constant velocity flight and when pitching commands exceeding 1g are executed. For this flight condition, the entire fuel mass alternately impacts the upper and lower surfaces of the fuel tank.

Slosh testing will begin July 7, 1975, and be completed in four weeks. First phase slosh testing is limited to developing dynamically equivalent mathematical models for the "coffee cup" lateral and longitudinal fuel slosh. Slosh forces, moments, and damping will be used to generate mass-spring-damper models. If time permits, the impact condition will be tested during Phase I.

A full-scale fuel tank and positive expulsion bladder will be tested. However, the fuel tank will be fabricated from Plexiglass for ease of viewing the bladder/fluid motion.

Two candidate positive expulsion devices (hereinafter called bladders) will be slosh tested during Phase I. Because of the life requirements and extreme environmental conditions to be sustained by the bladders a materials evaluation study was conducted. Results of the study produced two candidate materials. A nitrile/nylon composite bladder (0.032 inch thick) has the capability of flexing but not stretching. As fuel depletes, the bladder wrinkles and folds due to external air pressure. The "pure" nitrile bladder has the capability of stretching as well as flexing. The empty bladder is cylindrically shaped and is 10 inches in diameter. As fuel is introduced into the bladder it expands "balloon-like" to fill out the tank volume. Cycling tests of two bladders similar in nature to the two above were conducted by Bell Aerospace Corp., Buffalo, New York. The wrinkling bladder tended to develop pin hole leaks at three corner fold points. No leaks were developed in the "balloonlike" bladder.

The Phase I slosh tests, while not classed as life cycling tests per se, will reveal, due to cycling at natural slosh frequencies, any basic structural weaknesses in the two bladder concepts. If time permits, life cycling tests will be performed.

The paper to be written (with photos) will include:

- 1) Test setup
- 2) Test instrumentation
- 3) Test procedures
- 4) Test results
- 5) Development of dynamically equivalent models
- 6) Bladder performance evaluation.

## FINITE ELEMENT SOLUTION OF FLUID-STRUCTURE INTERACTION PROBLEMS

Erwin A. Schroeder and Melvyn S. Marcus  
Naval Ship Research and Development Center  
Bethesda, Maryland

A general method using finite elements for computing natural frequencies of submerged structures was implemented using a large general purpose structural analysis digital computer program (NASTRAN).

This method represents the fluid and the structure with finite elements. Pressures are computed at grid points in the fluid and displacements are computed at grid points in the structure. The dynamic interactions at the fluid-structure boundary are the force on the structure due to the fluid pressure and the pressure gradient induced in the fluid due to the structure's motion. The finite element method produces a mass matrix and a stiffness matrix for the structure and similar matrices for the fluid. These two matrix systems are coupled by terms due to the interactions at the fluid-structure boundary. Natural frequencies are extracted by solving an eigenvalue problem for the coupled matrix system.

For a fluid of infinite extent, only a bounded region is represented by fluid elements. The outer boundary of this region was represented as a free surface. It may also be represented as a non-reflecting boundary. However, for the sample problem solved, using a non-reflecting boundary was neither necessary nor very successful.

To implement the method using a standard structural analysis program, the structure is represented by the usual structural finite elements. The fluid is represented using an analogy with structural elements. Elastic membrane elements are adapted to represent the two-dimensional acoustic fluid. The fluid-structure interaction is treated in two ways: by a consistent formulation and by a lumped formulation. For the consistent formulation, the interaction terms are computed using modified structural elements. For the lumped formulation, the interaction terms are precomputed and entered directly into the matrices.

For three-dimensional submerged vibration problems, a similar implementation using a finite element structural analysis program appears possible. Also, extensions of this method to solve transient problems are being explored.

An application of the method was demonstrated by solving a two-dimensional sample problem. The results agree well with an analytic solution of the same problem.

The sample problem consists of determining the natural frequencies of an elastic ring surrounded by an acoustic fluid. The motions of the ring and the fluid are assumed to be in the plane of the ring. The analytic solution was carried out for both bounded and unbounded fluid regions. The frequencies of bending modes for bounded regions converge rapidly with increasing radius to the frequency for an unbounded region. The frequency of the lowest mode for a fluid region having radius three times the radius of the ring is within 1% of the frequency for the unbounded region. For higher modes, even smaller radii suffice.

### **EXPERIMENTAL DETERMINATION OF ROCKET MOTOR STRUCTURAL RESPONSE TO INTERNAL ACOUSTIC EXCITATION**

F. R. Jensen, Hercules Incorporated  
Bacchus Works, Magna, Utah

Acoustic pressure oscillations in the combustion cavity of a solid propellant rocket motor can impose excessive dynamic loads on structural components and attached motor hardware. The problem of combustion instability has concerned the industry in recent years because of these structural effects. The Air Force Rocket Propulsion Laboratory at Edwards Air Force Base has initiated a program to develop analytical techniques for the prediction of motor component response to acoustic pressure oscillations.

One experimental task was included in the RPL Component Vibration Program to provide data for evaluation of the analytical techniques. The objective of the task was to measure the response of a motor to an acoustic loading that would simulate an unstable acoustic pressure oscillation. This paper describes the testing setup and the testing procedures used to obtain the motor structural response. The test results are also presented and discussed.

The acoustic excitation was provided by a cone-type loudspeaker placed in the centerbore of the motor. An oscillator was attached to the loudspeaker through an audio amplifier. Frequency sweeps were conducted by varying the oscillator frequency in the range from 0 to 1000 Hz. A microphone was placed in the combustion cavity to monitor pressure oscillation amplitude. The microphone was mounted on a shaft that could be moved along the motor centerline to map the acoustic modes. An accelerometer was used on the motor structure and components to map structural mode shapes. Double-backed masking tape was used to attach the accelerometer to the motor and components so that repositioning of the accelerometer would be fast and efficient. The use of tape was found to be a satisfactory method of accelerometer attachment for the low acceleration levels encountered in this test program.

The motor was pressurized to 50 psi so that the dome of the case would be forced out away from the propellant grain. Nitrogen gas was used to pressurize the motor for most of the testing; however, some studies were made using Helium gas in order to change the frequency at which various acoustic modes occurred. Since structural natural frequencies remain constant, variation of the acoustic natural frequencies simplified the problem of separating structural resonance from acoustic resonance in the test data.

Two types of tests were conducted: 1) frequency response, and 2) mode mapping. The frequency response tests were conducted by recording the accelerometer output on an  $x$ - $y$  plotter while the frequency was varied slowly over a certain frequency range. The accelerometer was then moved to another point and the frequency response test repeated. By examining results from the frequency response tests, major resonance frequencies were selected for mode shape mapping. The mode shape mapping was conducted by turning the oscillator to a particular frequency and then moving the accelerometer from one structural point to another to map the mode of response. The accelerometer signal amplitude and phase were recorded at each point.

Results from this experimental project are presented by way of frequency response plots and mode shape plots. The acoustic cavity resonances compare well with those determined previously by test and by analysis. No data were available for evaluation of the structural response data.

### EFFECT OF FLUID MEDIUM ON THE VIBRATION OF AN OPEN SHELL

J. L. Lai  
B. F. Goodrich Company, Akron, Ohio

The interaction of a vibrating open shell with its adjacent fluid medium is discussed in this paper. The emphasis herein is on the shell vibration rather than the sound radiation. The result of the study being reported is the effect of fluid and shell parameters on the vibrational frequency of the shell. Also, the estimation of the frequency of the shell in the fluid based on that in vaccuo is discussed.

In this study, the structure has been modeled as a thin, infinitely long, elastic, simply supported and open circular shell with a fluid medium on both sides. The shell is also under tension due to the fact of the pressurized internal fluid. The fluid is considered as linearly compressible, irrotational and inviscid. Free pressure boundary conditions, i.e. the fluid is enclosed by the soft membrane, are used for the fluid on circumferential boundaries. The continuities of the radial velocities and pressures of the shell and the fluid are used for the boundary conditions on the shell-fluid interface.

The thin shell theory in plane strain together with the normal mode method is used to derive the frequency equation of the problem. Due to the "added mass" effect, the natural frequency of the shell in the fluid medium  $\omega_f$  is found to be less than that in vaccuo  $\omega_v$ . The fluid factor,  $f$ , which contributes to the lower frequency of the shell is obtained as

$$f(x) = \frac{P_f R}{\rho_s h} \frac{1}{x} \left[ \frac{J_\rho(x)}{J_\rho(x)'} - \frac{H_\rho^{(2)}(x)}{H_\rho^{(2)}(x)'} \right]$$

where  $x = R\omega/c_f$ ,  $R$  is the shell radius,  $\omega$  is the circular frequency,  $c_f$  is the fluid sound speed,  $\rho_f$  is the fluid density,  $\rho_s$  is the shell density,  $h$  is the shell thickness,  $J$  and  $H$  are the Bessel and the Hankel function,  $\rho = n\pi/\alpha$ ,  $n$  is the mode number and  $\alpha$  is the shell extending angle. If  $f(x)$  equals zero, we have the case of being in vaccuo. In the low

frequency range, i.e.,  $x \ll 1$ , the fluid factor becomes frequency and sound speed independent, i.e.

$$f(x) = \frac{2\rho_f R}{\rho_s h p}$$

A concept of the "generalized added mass,"  $M_a$ , of the fluid is introduced to estimate the frequency ratio,  $\omega_f/\omega_v$ , from

$$\frac{\omega_f}{\omega_v} = \left(1 + \frac{M_a}{M_s}\right)^{-0.5}$$

where  $M_s$  is the generalized mass of the shell in vaccuo. A closed form solution for the mass ratio  $M_a/M_s$  is obtained for the low frequency range as

$$\frac{M_a}{M_s} = \frac{p^2 f}{1 + p^2}$$

Some numerical examples are given to show the effect of shell and fluid parameters on the  $\omega_f$  and the frequency ratio. Results show that the frequency ratio increases, if (1) shell extending angle decreases, (2) fluid mass decreases, (3) shall radius decreases, (4) shell area mass increases, (5) mode number increases. Discussion on the application of the results obtained to the structure which are surrounded by the fluid medium such as the sonar dome and the ship hull is given. The application of the mass ratio obtained together with the existing finite element computer code (say NASTRAN) to the estimation of the natural frequency of the structure of a complicated geometrical form in the fluid is also discussed.

## ACOUSTIC AND VIBRATION TESTING

### SIMULATING TACTICAL MISSILE FLIGHT VIBRATION WITH PNEUMATIC VIBRATORS

Don G. VandeGriff, Weston D. Ayers and John G. Maloney  
General Dynamics, Pomona Division, Pomona, California

The need has developed for a portable, simple to use and low cost vibrator system to approximate broadband random flight vibration for tactical missiles. The electronic complexity of these missiles is such that thorough functional checkout under vibration is required at the full missile assembly level during engineering development. The engineering checkout facilities at General Dynamics Pomona Division do not include large dedicated electrodynamic drivers for vibration testing.

When the test requirement for simultaneous three axis broadband random vibration first arose, the feasibility of using multiple electrodynamic drivers and a random vibration controller was explored. A literature search failed to reveal any documented evidence that such an approach would produce either well controlled or meaningful overall vibration levels on a test specimen which is slightly over one foot in diameter, nearly fifteen feet long and weighs several hundred pounds.

Further evaluation led to the conclusion that pneumatic vibrators offered the potential to fulfill the vibration equipment needs. Pneumatic drivers are commercially available in various sizes. They are used in parts sorters and grain conveyors. They consist of a cylinder, rigid end caps and a free piston. The piston is internally ported to obtain positive mechanical feedback. When driven by compressed air, above a threshold of about 20 psi the piston oscillates thru its full stroke. As the piston strikes the end cap a very sharp shock transient is generated at a repetition rate of 30 to 60 Hz depending on the pneumatic driver size and on the magnitude of the pressure supply. Additionally, the compressed air supply can be modulated in amplitude. This produces a smearing of the spectral content of the vibration response.

A cut and try approach was used in developing the pneumatic vibrator system for the tactical missile application. After numerous iterations it was found that mounting several of the drivers along the exterior of the missile produced the desired responses along the airframe. For example the following overall rms acceleration levels were achieved on a missile using nine pneumatic drivers.

Missile Region	Broadband Response—g RMS			Measurement Bandwidth—Hz
	Vertical	Horizontal	Longitudinal	
Forward End	6.8	6.5	6.5	20—5000
Mid-Section	8.9	11.2	4.4	20—5000
Aft End	8.9	8.7	6.0	20—2000

The acceleration spectral densities measured on the airframe during pneumatic vibration have the same general shape as those measured in flight at the corresponding locations.

Pneumatic vibrators have provided a means of producing broadband random vibration to simulate the flight vibration environment of tactical missiles. The pneumatic vibrators are low in cost, easy to use and do not adversely impact the missile checkout stations.

### A THREE DIRECTIONAL VIBRATION SYSTEM

Fred M. Edgington  
White Sands Missile Range, New Mexico

White Sands Missile Range (WSMR) has been interested in three directional vibration since 1960. At that time, a three directional vibration system was set up using a cube for the table. The cube having very smooth sides was driven by plates attached to the cube by only lubricating oil at atmospheric pressure. This system functioned very well at the lower frequencies but as the frequency was increased, the force transmitted through the oil to the cube was drastically reduced. Also as this was basically a feasibility study, there was virtually no satisfactory place to mount a test specimen without causing uncontrollable overturning movements.

In 1969, Wylie Laboratory at Huntsville, Alabama developed a three directional set-up for determining reliability of radios under helicopter vibration environments. The table for this system was approximately 16" square and its motion was restricted to three directions by the use of flexures having a circular design. This system was moved to WSMR for additional testing of radios and proved to be a considerable improvement over the first design in that hardware could be tested in three directions. The drive mechanism was relatively heavy compared to the table weight and flexure stiffness. This caused rocking modes to occur at 150 Hz and above. Therefore, at frequencies above this, the accelerations on the table were not uniform and good control of the test specimen input could not be maintained; particularly when more than one test item was to be tested. After an evaluation of this system, the decision was made not to use this system and to build one that would meet the WSMR requirements.

The criteria for the current three directional vibration system was:

- a. Have no resonance below 500 Hz
- b. Be usable to 2 kHz
- c. Have multiple uses
- d. Be capable of 1" DA in each of three directions
- e. Have an attachment surface of at least 3' X 3'
- f. Be capable of driving a 200 pound package of 10 g's
- g. Be isolated from the floor

Each of these criteria were met and exceeded in several cases. The first resonances of the drive table caused by the horizontal drive couplings is at 780 Hz and the system has been excited to 2.5 kHz. The system has been equalized with no load so that a flat spectrum exists in the three directions to 2 kHz.

The excitors are supported by a large L shaped frame made from 3' X 16" wide flange which is boxed in using 1" plate. This structure was then filled with sand to dampen any resonances and to provide more mass for low frequency operation. The excitors were purchased with only 6" diameter trunnions and no bases. To support the horizontal shakers, 6" thick plates were clamped to the trunnions and then the plates were welded to the main frame. The vertical exciter hangs from the multi-axis drive unit designed and built by Team Corporation. This unit allows the vertical forces of the exciter to be transmitted through 9 cylinders to two magnesium plates. The lower plate is 3-3/4" thick and the upper plate (the test table) is 5" thick. The 9 cylinders are restrained by the use of hydrostatic bearings so that motion is only in the vertical direction. This in turn restricts the lower plate to only vertical motion. The test table is held down by 9 long bolts which go through the lower plate and attached to the bottom of the cylinders to allow motion of the upper plate in any horizontal direction. Hydrostatic bearing surfaces are built in between the two plates. This also would allow rotation about the vertical axes but rotation is restricted by one of the horizontal shakers. Two spherical hydrostatic ball joints provide drive in one direction and the rotational restraint while only one ball joint is used to provide the motion for the third direction. To isolate the system from the floor, five Barry Stable-Level Air Support Units were used to obtain a 3 Hz resonance.

The two horizontal excitors can both be rotated into the vertical direction and used for driving relatively large test items in this direction. One of the horizontal excitors can also be rotated 180° from its original position and attached to a 4' X 6' table supported by Team bearings. This will provide good use of the equipment when it is not needed for three direction testing. Current planned uses of the system are to reproduce vibration environments on missile components and reproduce the vibration measured on avionic equipment in helicopters.

#### DUAL SHAKER VIBRATION FACILITY

Carl V. Ryden  
Pacific Missile Test Center, Pt. Mugu, California

The requirement for a dual shaker vibration facility was generated by the requirement for vibration testing of the PHOENIX and HARPOON missiles in the All-Up-Round configuration. This configuration is required for a more realistic simulation of vibration throughout the missile including the vibration level zoning for the section of the missile. Also in the case of the PHOENIX the missiles can not be disassembled for sectionalized vibration testing because of contractual requirements. Two shakers (one at the forward and one at the aft section of the missile) instead of the customary single shaker were needed because of the vibration transmissibility characteristics through the warhead and motor sections, and because of the different levels and spectrums required at the forward and aft missile sections. The transmissibility ratio varies considerably with frequency. These are low frequencies where the transmissibility ratio exceeds one. This is true for

both direction (from the aft control section to the forward guidance section, and from the forward to the aft section); however, the frequencies are generally different. At the higher frequencies the transmissibility decreases towards zero in both directions.

Two complete and independent vibration systems were utilized including random noise generators, equalizers, amplifiers and shakers. Since the signals from the two systems are random and independent there is no phase relation constant (continuously and randomly changing) between the two vibration inputs and their respective transmissibility through the missile and are therefore independently controlled assuming the system is essentially linear at the critical frequencies and amplitudes. The two shakers were identical in order to reduce set up complication and control problems.

Initial check out was performed using a "dummy" HARPOON missile which has similar over all dimensions and mass distribution, but dissimilar vibration and transmissibility characteristics. This test consisted of low level vibration input (1 grms with a flat spectrum) to each shaker one at a time and determining the response at the other shaker attachment point. No problems were encountered with this configuration.

Tests were then conducted using the actual HARPOON missile. These tests included:

1. Low level vibration (1 grms—flat spectrum) input to each shaker one at a time, and both shakers.
2. Intermediate level vibration (3 grms—flat spectrum) input to both shakers.
3. Full level vibration (5 grms—flat spectrum) input to both shakers.
4. Test level vibration with shaped spectrum input to both shakers.

Both system equalizers were under servo control. When both shakers were operated the vibration was applied first by one shaker and brought up to level, and then by the second shaker. Stability was established within the response time of the servo control. For the final test level with the shaped spectrum several of the lower equalizer frequencies filters were switched to manual control in order to obtain the desired test spectrum shape.

The results of the tests show a good simulation of vibration at the points monitored within the missile while controlling each vibration system by a control accelerometer mounted on the respective vibration fixture. Stability was established within the response time of the servo control system and the vibration levels were within the dynamic range of the control system.

## HIGH FREQUENCY VIBRATION ANALYSIS FOR INCIPIENT FAILURE DETECTION

David B. Board  
Manager, Diagnostics Technology  
Boeing Vertol Company, Philadelphia, Pennsylvania

During research of state-of-the-art diagnostic and prognostic techniques for potential application to helicopter transmissions, a new technique for high frequency vibro-acoustic emission analysis was evaluated on three transmissions in a regenerative test cell and on the Boeing Vertol Spur Gear Research Test Stand. Test results indicate that this new technique for high frequency vibro-acoustic analysis shows excellent potential for incipient detection and identification of faults in complex, high-speed, rotating machinery. Of the five bearing and shafting faults indicated and verified by teardown inspection during the transmission test, only one was known at the outset of the test and all five were detectable through analysis of test data without any need for baseline information. The gear research test stand evaluation demonstrated the capability to monitor progressive levels of gear tooth surface damage as well as the ability to detect a through-the-part crack originating at a tooth root and propagating through the gear web. This capability for IN-SITU fault detection and isolation without the need for baseline data and with decisions based on engineering rationale rather than rationalized pattern recognition, as well as the ability to detect non-debris generating failure modes such as cracks, indicates an important superiority over the more classical forms of low frequency vibration analysis that have been employed to date.

## ANALYSIS OF FATIGUE UNDER RANDOM VIBRATION

R. G. Lambert  
General Electric Company, Utica, NY

A closed form analytical solution has been derived to determine the average number of stress reversals to failure in a structural member which is subjected to a given root-mean-square (rms) Gaussian vibratory stress. The relationships are based on the commonly available reversed bending fatigue properties. All results utilize Miner's cumulative damage hypothesis.

$$S = A N^{-1/\beta}$$
$$\sigma = \left[ \frac{A}{\sqrt{2}} \right] \left[ \Gamma \left( \frac{(2 + \beta)}{2} \right) \right]^{-1/\beta} N^{-1/\beta}$$

where  $A$  and  $\beta$  are material constants.

An expression relating time to the average number of stress reversals is also given. Included is the damage probability density function (pdf) which shows that most of the damage is done by stress peaks between two and five times the rms stress.

Analytical results compare favorably with reported empirical results for both ductile and brittle materials. Evaluations of random fatigue curve constants have been made for several common materials.

The probability of failure  $F(N)$  as a function of number of stress reversals ( $N$ ) is also included in closed form. This includes the case where the rms stress or the material's reversed bending curve is a random variable. The expression is given by

$$F(N) = \frac{0.5 - \operatorname{erf} \left[ \frac{(k/n)^{1/\beta} - \bar{\sigma}}{\delta} \right]}{0.5 + \operatorname{erf} \left[ \bar{\sigma}/\delta \right]}$$

which can be readily evaluated.

The pdf of number of cycles to failure along with its median value is given in equation form.

Also included is the important effect on fatigue life of stress limiting. Results indicate that limiting at two times the rms stress level extends fatigue life by a factor of 13, three times rms level by a factor of 1.86, and four times rms level by a factor 1.08.

Also included is a closed form solution, readily evaluated in terms of Incomplete Gamma Functions, to predict fatigue life for materials having an endurance limit and for materials having a double slope fatigue curve. Numerical examples are given for all expressions.

#### RANDOM VIBRATION FATIGUE TESTS OF WELDBONDED AND BONDED JOINTS

F. Dandow and O. Manner  
AFFDL, Wright-Patterson AFB, Ohio

Recent interest in joining aircraft structural components has led to the development of new manufacturing processes. Two such processes are the metal bonding technique and the weldbonding process, the latter combines the processes of metal bonding and spotwelding. It is expected that savings in manufacturing cost and structural weight can be gained by usage of these methods. In order to further investigate the possibilities of these processes, the Air Force Flight Dynamics Laboratory is conducting several research and development programs in which the structural properties of these manufacturing processes are being studied. One structural aspect which required further investigation was the structural fatigue due to random dynamic excitation generally called sonic fatigue. For this purpose several experimental programs were conducted to evaluate the sonic fatigue properties of these two processes.

This paper presents the results of a series of random shaker experiments conducted with test articles consisting of thin beams fastened to a simulated stiffener by the weld-bond process using a so-called spot-weld etch surface preparation treatment and similar

test articles manufactured by the metal bond process using a metal bond (FPL) etch surface preparation. The test procedure is discussed. To establish base line data, a series of riveted samples of the same basic dimensions were also tested. Fatigue curves in the range of  $10^5$  to  $10^8$  cycles were established for skin thicknesses of .032 inch and .040 inch for each of the three joint constructions. Results are also compared to fatigue data obtained elsewhere.

The results of the tests indicate that the weldbond samples which are characterized by lower grade bond properties and higher class spot-welds, failed at higher stress response levels before the comparable riveted joints, while at lower stress responses the fatigue life was extended beyond that of the riveted samples. The basic fatigue mechanism in all spot-weld coupons was identical. Fatigue initiated as an adhesive failure at the highest stressed edge of the stiffener and propagated as such, until it reached the spot-welds. Skin cracks along the edge of weldspots followed. The weld cracks eventually joined through the skin for a complete failure of the test coupon. The thicker coupons exhibited a lower fatigue life in comparison to the thinner beams at the same stress levels due to the resulting higher peel stresses at the bond edge.

The metal bonded coupons with the FPL etch surface preparation exhibited an improved fatigue life. Three basic failure modes were encountered. The thinner coupons failed in the skin at the area of maximum stress. The thicker coupons, which have higher peel stresses for the same flexure stress levels, showed complete cohesive bond failures or partial cohesive bond failure with a final skin failure, also complete skin failures without bond failures were encountered.

The adhesive failure in the weldbonded article distinguished itself by a delamination from the metal, while the cohesive failure of the metal bonded specimens showed a separation within the bond without detachment from the metal. The cohesive separation propagated at a relatively low rate even at high stress levels. Although these results are presently being supplemented by panel tests in an acoustic environment, it can be concluded that weldbonding, despite its good static strength characteristics, should be employed only in aircraft structural components which experience very low vibratory stress levels, while structures bonded by the FPL method indicate an increased random fatigue life in comparison to riveted components.

#### **FATIGUE PREDICTION FOR STRUCTURES SUBJECTED TO RANDOM VIBRATION**

Paul J. Jones and William J. Kacena  
Martin Marietta, Denver, Colorado

Structures subjected to relatively long term or repeated random vibration exposure must be designed for fatigue. Although analytical techniques are readily available to estimate the structural response parameters such as rms and "peak" stresses for short term random vibration exposures, fatigue life prediction is primarily limited to a "single mode approach" coupled with Miner's Cumulative Damage Rule. This paper presents an extension to the existing short term random response methodology to predict the fatigue life for multiple degree-of-freedom structures with multi-modal response. This extended analytical tool is applicable where the assumption that the response occurs in a single and

predominate structural mode is no longer adequate to describe the response of complex structures exposed to a wideband random excitation.

The technique described is based on a finite element model of the structural properties in the form of normal modes, natural frequencies, stress transformations (relating stresses to inertial response), and stress combinations (to consider the net effect of bending, axial and torsional stresses at a point). Conventional random vibration analysis methods are used to predict the statistics (in this case the rms) of the combined stress response in each vibration mode. The total rms stresses are then determined by root-sum-squaring all the modal rms stresses, as would be done for short term random exposures.

The fatigue prediction can be accomplished as a function of exposure time if the number of cycles at each stress level can be defined for all possible stress levels. To this end, a Rayleigh Distribution of response peaks is assumed, and the basic response equations are extended to estimate the number of zero crossings in a given time associated with each stress parameter. This concept leads to the approximate number of cycles at all stress levels during the given exposure time. Structural damage or fatigue life is then estimated based on conventional S/N data for the structural material by summing the predicted divided by the allowable number of cycles over the stress levels in a truncated Rayleigh Distribution, as in Minor's cumulative damage approach.

This fatigue life prediction technique is a relatively simple combination of the analytical tools generally available in the fields of structural dynamics, statistics and fatigue. The approach is general enough that combinations of random levels and durations can be considered. In addition, there are no restrictions to preclude using the Goodman Diagram approach to account for combined random and steady stresses.

The basic development of the fatigue prediction equations for a multiple degree-of-freedom system are presented along with a description of a computer program written to implement the methodology. Throughout the development, the underlying assumptions are discussed to insure that all aspects of the approach are understood. In addition, a detailed example problem is furnished to illustrate and clarify the procedure. Finally, references are cited as sources of background information for a more detailed examination of the various analytical methods.

#### **MEAN LIFE EVALUATION FOR A STOCHASTIC LOADING PROGRAMME WITH A FINITE NUMBER OF STRAIN LEVELS USING MINER'S RULE**

G. Philippin, T. H. Topper, and H. H. E. Leipholtz  
University of Waterloo, Department of Civil Engineering  
Waterloo, Ontario, Canada

For the prediction of fatigue life of a specimen under cyclic loading with varying stress levels, Miner's rule has been widely applied. The most general kind of nonstationary loading with variable stress peaks is a stochastic loading. Therefore, attempts have been made to apply Miner's rule in such a loading case too, using the probability distribution of the stress peaks in that rule. Unfortunately, fatigue life predictions made in such a way were far from coinciding with true fatigue life observed experimentally.

In a first reaction, Miner's rule was blamed for the failure of the theoretical predictions, and many researchers have made great efforts in order to replace the rule completely or to modify it appropriately.

In this paper, it will be shown that the problem can be solved in a different way. First of all, it is proved that Miner's rule is sound from the probabilistic point of view if one assumes that a proper damage parameter has been chosen which is adequate to collect in classes all equally damaging load reversals. Secondly, it is concluded that stress cannot be such a proper damage parameter since using it in Miner's rule, which has been shown to be appropriate, leads to results of fatigue life prediction which are apparently erroneous. Therefore, the introduction of a new damage parameter having the dimension of an energy, and being related with each closed hysteresis loop of the stress-strain diagram, is advocated. Successful application of this new parameter in connection with deterministic loading programmes with varying stress levels have already been made elsewhere. Thirdly, an application of Miner's rule together with the new parameter to a stochastic loading programme is being made in this paper in order to generate data for an experimental verification which shall follow. The stochastic programme used is a simple one. It allows to calculate the damage parameter's probability distribution by means of combinatorial analysis in a way which is sufficiently transparent for educational purposes. However, the procedure used in the calculations makes a generalisation toward a more complex and sophisticated stochastic loading programme possible without severe restrictions.

#### **THERMO-ACOUSTIC SIMULATION OF CAPTIVE FLIGHT ENVIRONMENT**

W. D. Everett  
Pacific Missile Test Center, Point Mugu, California

A test facility and procedure has been developed wherein the combined thermal and vibration stresses of captive flight are accurately simulated.

The facility is essentially a large reverberant acoustic chamber within which is a small temperature chamber or shroud. The acoustic chamber is a 2000 ft<sup>2</sup> rectangular room driven by two air modulators with a combined capacity of 20,000 acoustic watts. The temperature chamber is more nearly a thermal shroud or bag of thin silicone rubber, through which hot or cold air is ducted. The flexibility of the thermal shroud is the novel feature of the facility. It contains the temperature conditioning air to the immediate vicinity of the test missile, yet is transparent to the acoustic energy which induces the vibration in the missile. The shroud is supplied by a closed loop air conditioning system driven by a 3 H.P. fan, heated by 9 KW heaters and cooled by a LN<sub>2</sub> refrigeration coil.

The test procedure is based on an estimate of the lifetime flight-use environment for tested missile in terms of percentage of life at various flight dynamic pressure ( $q$ ) conditions. For the current test program, on AIM-9L missiles, this estimate yields a  $q$  range of 125 to 525 psf. The acoustic test intensity is cycled through a sound pressure level range corresponding to the  $q$  range, with a representative percentage of time at each simulated  $q$  condition. The current test program combines with this acoustic intensity cycle a temperature cycle resembling that of MIL-STD-781B. In future tests it is expected that the

temperature cycle will be based on the temperatures corresponding to lifetime q environment of the missile.

Possibly this technique of accumulating simulated captive flight time at stress levels proportioned to combat flight use yields better fatigue rate and mode data than normal captive flight and more cost effectively.

### THE EFFECT OF SIGNAL CLIPPING IN RANDOM VIBRATION TESTING

Alfred G. Ratz  
Ling Electronica, Anaheim, California

An important aspect of wideband random testing using electrodynamic vibration excitors is the level of clipping applied to the random drive signal. The signal has a Gaussian probability-density characteristic, and clipping is therefore very difficult to avoid. It may occur either in the control electronics or in the power amplifier driving the exciter. Clipping is especially noticeable and significant when a vibration system is operated at its full force level.

That clipping is a significant aspect of wideband random testing is evident by the fact that many system performance specifications specifically define the acceptable values permitted of the peak factor of the drive signal.

This paper first reviews the influence of the clipping level of the drive signal on the force capacity of a given exciter system. It is shown that increasing the clipping level usually reduces the output force that can be obtained. The mechanism of how this occurs is explained. The conclusion is reached that one should plan to operate at full force with the drive signal clipping level held to as small a value as is permitted by the pertinent test specifications.

The specific test specifications of interest are those related to the statistical properties (amplitude probability density, power spectral density) of the force and motion waveforms at the output of the exciter. These are in their turn influenced by the level of clipping of the exciter drive signal, and it is the precise nature of the influences of signal clipping on the statistics of the motion which is worked out in this paper.

One important effect of clipping that affects the test is the way it modifies the power spectral density (psd) plot of the original unclipped wave. In dealing with this effect, the paper starts from first principles, and uses the techniques of Stieljes and Shepard to derive the modified psd plot. The ability to equalize specimen peak-notch resonances for various clipping levels is also explored. The presentation concentrates on giving an insight into (1) the mechanism by which clipping generates a new spectrum, and (2) the way the new spectrum influences test results.

The modified psd plot is shown to be made up of the original psd plot with a second psd function superimposed on it. The exact form of the second extraneous psd function depends on the form of the original psd plot; however, it has several general characteristics. It occupies a much wider spectrum than its progenitor. And it tends to have significant spectral components even at frequencies where the original spectrum has little or no

energy; thus, clipping can affect the ability of the control equipment to make the random signal conform to a specific test program.

For example, if an automatic random equalizer is used to control the psd of the acceleration waveform at the exciter table, the extraneous psd function generated by the clipping is in effect simply a background noise spectrum that is uncontrollable by the equalizer. This noise spectrum limits the magnitude of the resonance peak that can be handled, since it establishes a minimum value to the psd level at the resonant frequency.

The background spectrum usually covers a frequency range that is much wider than that of the test spectrum. This is important to most workers in the field, since it is usually desired to hold the energy content of the spectrum outside the test band to a very low value.

A second important phenomenon arising when a clipped signal is used, is the fact that the transfer characteristic of the exciter tends to "restore" the Gaussian nature of the signal. The peak factors of the acceleration, velocity or displacement waveforms at the shaker output are usually well in excess of the peak factor set for the clipped drive signal. The amplitudes of the motion signals exceed the clipping level "barrier" established for the drive signal. The phenomenon has been widely observed. And it is generally understood that the shaker transfer-function is chiefly responsible. However, the way the peak factor is restored does not seem to have been previously worked out, and it is the purpose here to describe the exact mechanism. The results are useful when one is trying to quantitatively establish the peak factor of the "restored" motion of the exciter table, for a given amount of clipping of the exciter drive.

The results of the investigation into peak-factor "restoration," together with the spectral effects described above, set criteria for the peak factor at which the drive signal is to be clipped, and so ultimately have a considerable effect on the capacity of a given system to perform random tests.

The theoretical developments lead to useful formulae which have wide application. The work is illustrated by a number of examples, based on practical test parameters. Finally, experimental work verifying the theory is also presented.

# IMPACT AND BLAST

## PREDICTION OF STANDOFF DISTANCES TO PREVENT LOSS OF HEARING FROM MUZZLE BLAST

Peter S. Westine and James C. Hokanson  
Southwest Research Institute, San Antonio, Texas

Whenever a gun is fired, a very intense blast wave is emitted from the muzzle with such severity that hearing loss is common in gun crews. In response to this and other hazardous noise problems, the Surgeon General's Office recently issued MIL-STD-1474(MI) specifying what maximum side-on sound pressure levels are tolerable for different durations of incident waves. This new MIL-SPEC either presumes that muzzle blast pressures and durations are known, expects blast pressures and durations to be calculated, and/or demands that blast pressures and durations be measured around all guns. In response to MIL-STD-1474, this paper presents empirically derived equations for estimating pressure, duration, and time of arrival for reflected shocks relative to incident shocks in the blast field around gun muzzles.

Both gun designers and field personnel share a fundamental question of where can crew members safely stand for a particular gun at an arbitrary angle of elevation, propelling charge, length of barrel, etc.? These individuals are more interested in determining safe standoff distance than they are in determining intermediate quantities such as pressures and durations. In response to their needs, two groups of design nomographs are presented which permit graphical predictions of safe standoff locations—one group for unprotected ears and the other group for ears protected with plugs and/or muffs.

The basis for all relationships is dimensional analysis and then a subsequent curve fit to test data. An extensive range of weapons is examined to obtain all curve fits and demonstrate the validity of this analysis. Among the guns evaluated are 105 mm Army howitzers such as the M102 with a zone 7 charge, the XM204 with a zone 5 charge, the XM204 with a zone 7 charge, the XM204 with a zone 8 charge; Naval guns such as the 8"/55, 6"/47, 5"/54, 5"/38, 3"/50; and cannons such as 40 mm, 20mm M3, 20 mm XM197, and 20 mm Mark 12. The results can be applied for any of 3 different angles of gun tube elevation to any closed breech gun without a muzzle brake or flash suppressor.

Many different comparisons between predicted and experimentally measured results are presented. To demonstrate the validity of both nomograph groups, experimentally measured blast waves are compared to the predicted safe standoff positions around XM204 howitzers with different propelling charges and gun tube elevation angles. Other successful comparisons are between predicted and experimentally observed pressures, durations, and times of arrival. This paper closes with recommendations for extending the solution to recoilless rifles or open breech guns, and indicates how the procedure could be extended to closed breech guns with muzzle brakes of various efficiencies.

## DYNAMIC RESPONSE OF THE HUMAN BONY THORAX TO FRONTAL IMPACT

Paul H. Chen  
TRW Systems Group, Redondo Beach, CA

Thoracic injuries play an important role in traffic deaths. Most of the severe thoracic injuries in vehical collisions appear to be caused by a direct blow to the chest. Clinical studies reveal that the severity of the trauma depends largely upon the injury pattern, location and number of injuries. These in turn depend significantly upon the pulse shape, magnitude, duration and spatial distribution of the input forcing function as well as structural characteristics of the bony thorax. There appears to be a direct mechanical link between the input force/acceleration field and the resulting injuries.

Cardiovascular rupture and other thoracic complications in general are directly attributable to multiple rib fracture wounds. In spite of the relative importance of the thoracic skeletal injuries, almost no analytical work pertaining to the dynamic response of the thoracic skeleton to impact is available in the literature of the present time. Most current research is either experimentally or clinically oriented. The experimental and analytical efforts are both necessary for the understanding, and the prevention of fatal thoracic injuries. This paper is focused on the analytical aspect of the problem.

A three dimensional finite element structural dynamic model (THORAX II) of a midsagittally symmetric human thoracic skeleton has been developed. The primary force transmitting skeletal members (costae, vertebral column, sternum), and the inertia effects of the thoracic and abdominal viscera as well as of the head and neck are represented. The detailed anatomical geometry and cross sectional properties of all elements measured experimentally are included. Bone and cartilage are idealized as linear elastic materials, and small deformation is assumed.

The complete system consists of 27 components or substructures and 1104 degrees of freedom. The finite element and component mode synthesis solution techniques were employed to analyze the response to an anteroposterior directed impact forcing function. This force was modeled as an equilateral triangular pulse of 40 ms duration and 1200 lb peak force, and is distributed at 24 frontal chest nodes located within a 6" diameter circle centered at the midsternal line and in the third interspace. Seventy-seven normal modes (frequency ranges from 6.25 to 317 Hz) and sixty-nine boundary modes were selected for final system synthesis. Displacement, internal forces and stresses were computed for a total of 40 ms, using the IBM 360 computer. Potential fracture sites along costae and sternum were located. The results compared favorably with available experimental data.

The motion of the frontal chest consists of a (+Y) rigid body rotation about the sternal angle and an (-X) anteroposterior (A-P) displacement. The A-P displacement of the sternum increases progressively from rib 4 to the xiphisternal junction where it attains a maximum of 3 in at 29 ms. The majority of the A-P displacement takes place in the costal cartilage inferior to the 4th rib. This displacement attenuates rapidly at points posterior to the costochondral junction (CCJ). The deformation posterior to CCJ represents a gradual transition from a predominant A-P motion to a large lateral motion at the midaxilla (MA). The maximum MA displacement of 1.25" occurs at rib 5. The amplitudes of the posterior rib cage motion is relatively small. The transient response frequency of the frontal chest wall is about 11 Hz which is in the range of reported experimental

data. The chest force a displacement ( $F-\delta$ ) relationship show a hysteresis phenomenon attributable to the inertia effect. This phenomenon was reported on all experimental  $F-\delta$  curves.

The maximum bending moment occurs in the CCJ to MA region, and has a predominant component about the minor principal axis of inertia. The frontal rib shafts are generally subjected to compressive axial forces whereas the posterior rib shafts are in tension. The stress distribution in the costae follow the internal force patterns. The greatest normal stresses occur in the CCJ-MA region. The maximum shear stress occurs in the angle-tubercle region. In the upper costae, fractures occur in the costal cartilage and anterior rib shafts. In the middle costae, it appears in the cartilage and Midaxilla. The lower ribs fractures occur merely in the cartilage. These computed results compared favorably with those from cadaver experiments.

The complexities and complications involved in the development of a structural dynamic human model are readily recognizable. Limiting the problem scope and simplifying the system parameters seems to be the first cut approach. In this context a linear elastic and conservative system was assumed. Anticipated future improvements will include material nonlinearities, damping, large deformations, improving joint conditions, and incorporating other structure effects such as those from diaphragm and skeletal musculatures.

#### A STUDY OF THE SPACE SHUTTLE SOLID ROCKET BOOSTER NOZZLE WATER IMPACT RECOVERY LOADS

Edgar A. Rawls  
Chrysler Corporation, New Orleans

and

Dennis A. Kross  
NASA, Marshall Space Flight Center, Huntsville, Alabama

NASA's Space Shuttle vehicle will employ two reusable solid rocket boosters (SRB's). Recovery will be achieved by utilizing a parachute deceleration system with terminal water impact down range of the launch site. The boosters will impact nozzle first to take advantage of the high drag characteristics of the nozzle/skirt/aft bulkhead projected area to minimize penetration depth, while utilizing the hydropneumatic piston damping effect of the motor case chamber to retard rebound and slapdown.

This mode of impact will subject the nozzle, aft skirt, and aft bulkhead surfaces to large impact pressure loads. The severe dynamic load applied to the gimballed nozzle presents a unique design problem as this load must be reacted by the nozzle/bulkhead interface flexible seal, actuators, and some tension-tie supporting system. The load transient initiates with an upward load applied to the nozzle as the exit plane ring makes water contact. As water fills the nozzle internal volume both lateral and axial load build up with flow converging to the nozzle throat. The nozzle external surface remains in a very low pressure turbulent cavity or wake through separation of the nozzle external flow from the exit plane stiffener ring and interaction: with the booster aft skirt internal

cavitation wall. The initial forward axial force and lateral load for oblique impact altitudes are predicted to exceed  $10^6$  pounds dependent on initial impact condition.

Water will completely fill the nozzle internal volume, jetting into the motor case chamber. As this occurs, flow in the nozzle/skirt annulus impinges on the aft bulkhead initiating stagnation of the annulus and a sharp rise in nozzle external surface pressures above the internal flow values creating a large tension or downward load tending to pull the nozzle away from the bulkhead. These loads will also reach maximums of over  $10^6$  pounds dependent on initial impact condition.

A theoretical analysis of the nozzle hydrodynamic flow field was originally conducted to define preliminary design pressures, loads, and TVC forces. Scale model water impact tests of the preliminary design SRB configuration were then conducted by Marshall Space Flight Center in the Hydroballistics Tank of the Naval Surface Weapons Center, White Oak, Maryland. The tests employed an 8.56% model of the SRB geometry Froude scaled for dynamic simulation. Ambient pressure in the test tank was reduced to 1.26 psia to simulate a scaled atmosphere. Pressure transducers were located on the nozzle internal and external surfaces, aft bulkhead, and skirt internal surface to provide definition of the initial water impact dynamic pressure load. A four (4) component force balance was also utilized to measure resultant loads at the nozzle/bulkhead interface with three (3) component accelerometers on the aft bulkhead to define vehicle reaction loads. Tests were conducted over a complete range enveloping the probable range of initial impact conditions of vertical velocities from 80 to 100 fps, horizontal velocities from 0 to 45 fps, and initial water contact attitudes of from 0 to  $\pm 10$  degrees. Real time multiplexed data was recorded and processed to provide time correlated values. These results have been analyzed, scaled-up to the full scale vehicle and provided as nozzle structural design and system dynamic response criteria.

This paper will present a summary of the Space Shuttle SRB nozzle water impact design loads study. Analysis of the hydrodynamic flow model producing the dynamic load transient will be presented along with correlations of local flow characteristics and pressures defined by the 8.56% scale model tests. Model test scaling requirements and procedures will be reviewed with comparison of results for scaled and unscaled conditions. Methods and procedures utilized in determination of the full scale SRB structural design criteria will be defined with illustrations of typical full scaled dynamic load response. A short movie film sequence of the scale model test program will also be presented to illustrate test set-up, operation, and resulting hydrodynamic flow fields.

#### **AN EXPERIMENTAL INVESTIGATION OF THE AXIAL FORCES GENERATED BY THE OBLIQUE WATER ENTRY OF CONES**

John L. Baldwin  
Naval Surface Weapons Center, Silver Spring, Maryland

Missiles which enter water from air experience a rapid change in velocity due to the substantial increase in fluid density. The forces present may damage or destroy the missile structure or internal components. The concept that the surface crossing may be replaced by an impulsive change in velocity has existed for some time and may still be used to advantage for some problems; however, for the dynamic analysis of the missile structure

and internal components, knowledge of at least the external forces as a function of time is required. Recent advances in instrumentation and test facilities have made possible the direct experimental determination of the water-entry forcing functions for many cases. A systematic investigation of entry forces has been part of the continuing investigation of water-entry phenomena at the White Oak Laboratory of the Naval Surface Weapons Center.

The constant speed vertical entry of a cone is perhaps the simplest case of water entry because a self-similar flow should exist during the wetting process. Circular symmetry also simplifies this problem as shown by equation (1):

$$U(X, Y, \theta, T) = T\phi\left(\frac{X}{T}, \frac{Y}{T}\right) \quad (1)$$

A similar simplification also exists for the oblique entry case. A direct consequence of self-similar flows is that the axial force acting on the cone during wetting is given by

$$F = Ks^2$$

up to a maximum. After wetting has been completed the force should decay to a steady-state value as the surface recedes.

An experimental program was conducted at the Naval Surface Weapons Center, White Oak to verify the theory and to determine the quantitative values of the axial force for the oblique entry of cones as a function of distance.

The test procedure consisted of launching a simple cone-nosed model containing an axially mounted crystal accelerometer from an air gun and recording the gage output during water entry. The transducer was connected to the fixed electronics by a trailing wire. A light screen located near the water triggered the recording system and a strobe lamp. An opened plate camera recorded the position of the model at several times just before water contact from which the entry velocity was obtained. Equations (2) and (3) were used to compute added mass of the fluid and the related infinite model mass drag coefficient from the data as functions of distance moved after water contact.

$$-\frac{dU}{dt}(M + m) + (Mg - B)\sin\theta = \frac{dm}{ds}U^2 \quad (2)$$

$$C_d = \frac{2}{\rho A} \frac{dm}{ds} \quad (3)$$

where  $A$  = model base area,  $B$  = model buoyancy,  $C_d$  = infinite mass drag coefficients,  $g$  = gravitational constant,  $M$  = model mass,  $m$  = added mass of the fluid,  $s$  = distance,  $t$  = time,  $U$  = model speed,  $\theta$  = entry angle from the horizontal, and  $\rho$  = fluid mass density.

The results showed that:

1. The axial force during the wetting of the cone was of the form  $F = Ks^2$  and the maximum force occurred when the distance penetrated was less than the cone length.

2. After penetration of several cone lengths, the drag coefficient approached the steady-state value at zero cavitation number.

3. Blunt cones had much larger drag coefficients and more rapid loading rates than fine cones.

4. For a fixed cone angle, the maximum drag coefficient occurred at vertical entry and the maximum loading rate at the shallow entry angle.

5. The maximum drag coefficient and loading rate were very dependent on entry angle for blunt cones and only slightly dependent for fine cones.

The transverse force function was estimated from consideration of boundary values, geometry and axial data. Possible errors of 35 percent were indicated for 90-degree cones. The exact direction of the total force vector and its location on the body should be the subject of a future investigation.

#### DELAMINATION STUDIES OF IMPACTED COMPOSITE PLATES

C. A. Ross and R. Sierakowski  
University of Florida, Eglin AFB, Florida

Impact resistance of one component materials in general depends on many material properties such as fracture strength, hardness, ductility; with particular properties being more important within certain impact velocity ranges. However, impact resistance of composite materials is not only dependent on the specific constituent material properties but also is dependent on the geometrical arrangement of the imbedded fiber arrays. The effect of fiber geometry and ply arrangement has been shown in previous tests to have a significant influence on the impact resistance of fibrous composite materials using both extensible and inextensible fibers. In the present studies the specific effect of controlled ply arrangement and orientation on impact resistance has been studied experimentally for both metal and non-metal fibers imbedded in an epoxy-matrix and is the major subject of this paper.

The two types of composites studied were tested by impacting six inch square plates with blunt ended circular cylindrical projectiles of different lengths. A notable difference in failure mechanisms due to impact was observed for plates using extensible (steel) fibers as compared to the relatively inextensible (glass) fibers. The steel-epoxy plates exhibit a very symmetrical and confined damage area with only localized fiber breakage apparent, and with radial cracking in the matrix. The glass-epoxy plates show some initial fiber breakage under the projectile, with delamination of successive plies extending out many projectile diameters from the impact point, and with total delaminated area and damage depending on the ply arrangement. Initial results indicate that the orientation and arrangement of the first few plies are very important in controlling subsequent failure and delamination patterns. To obtain these results a large number of cross-plyed plates of multiple layered combinations have been tested and results are reported in both tabular and graphical forms.

Also investigated has been the influence of boundary conditions and variable fiber length on the impact resistance of the composite plates tested. The former has been accomplished by testing large size panels of selected fiber geometries and comparing results with the six inch panel test. The latter effect has been studied by fabricating holder plates of different geometrical shape, and testing specific fiber geometries for observations of changes occurring in the failure and delamination patterns.

Finally, an assessment of single fiber, three fiber, and multiple fiber specimens sandwiched between continuous multi-filament lamina are reported on. Such tests, of a diagnostic nature, have been examined for their usefulness in projecting anticipated penetration mechanisms occurring in multiple lamina composites.

**SIMULATION OF X-RAY BLOWOFF IMPULSE LOADING  
ON A REENTRY VEHICLE AFT END USING  
LIGHT-INITIATED HIGH EXPLOSIVES**

R. A. Benham  
Sandia Laboratories, Albuquerque, New Mexico

The possibility of a Comprehensive Test Ban Treaty emphasizes the importance of nuclear effects simulation. This paper describes a method in which X-ray blowoff effects are simulated by the detonation of a sprayed coating of explosive initiated by an intense light. A specific experiment is described involving the curved aft surface of a reentry vehicle (flat-cone-torroid). The thickness of silver acetylide-silver nitrate explosive is varied to match impulse values calculated for X-ray blowoff. Surface initiation of the explosive layer produces a simultaneously applied impulse lasting for about two microseconds. Measurements of strain, displacement and acceleration during experiments at increasing impulse levels allow full understanding of structural dynamics with verification of a failure impulse. This experiment demonstrates for the first time that light-initiated explosive may be used for structural experiments involving large complex surfaces with step load discontinuities and represents a significant improvement in laboratory X-ray simulation capability.

**BLAST PRESSURES INSIDE AND OUTSIDE  
SUPPRESSIVE STRUCTURES**

E. D. Esparza, G. A. Oldham and W. E. Baker  
Southwest Research Institute, San Antonio, Texas

Suppressive structures are vented structures designed to attenuate blasts and thermal effects, and arrest fragments, from accidental explosions in hazardous operations in munitions plants. Considerable analytical and experimental effort has been recently devoted to predicting the initial shock loads and longer term quasi-static pressures generated by internal explosions in these structures, and the characteristics of the attenuated blast waves emitted from the chambers. This paper summarizes this work and gives a resume of prediction equations for internal and external blast wave properties. Related literature is also summarized.

Specific topics covered in the paper are:

- (1) Scaling of internal and external blast waves and quasi-static pressures.
- (2) The concept of an effective vent area ratio,  $\alpha_e$ , for suppressive structures.
- (3) Analytical and experimental studies of internal blast pressures and pressures between layers of vented panels in suppressive structures scaling.
- (4) Experimental and scaling studies of external blast waves. Effects of various panel configurations and  $\alpha_e$ .

This paper will include a number of figures and graphs which give some details of typical suppressive structure vent panel configurations, and functional relationships for scaled blast and quasi-static pressures.

#### **DEVELOPMENT OF STRUCTURES FOR INTENSE GROUND MOTION ENVIRONMENTS**

T. O. Hunter and G. W. Barr  
Sandia Laboratories, Albuquerque, New Mexico

The development of the technology to insure the survivability of deep buried structures subjected to short duration-high intensity ground motion environments requires the integration and utilization of numerous analytical techniques, design concepts, and material characterizations. Sandia Laboratories recently completed a program to develop a large structure designed to survive the ground motion environment resulting from a nuclear detonation in volcanic tuff. The free-field environment at the location of the structure consisted of accelerations which are typically in excess of 1000 g's and peak stress levels in excess of several kilobars (1 kilobar = approximately 15,000 psi).

The structure to be protected was an experiment chamber constructed of thick walled steel sections weighing approximately 75 tons. An integral part of this chamber was a high speed closure system which placed a 3500 lb. titanium door over a three foot opening in approximately 18 milliseconds. The chamber contained on-board recording systems to collect data for the assessment of system performance.

The design criteria for the chamber consisted of attenuation of the acceleration pulse to less than 200 g's and reduction of the surface stress applied to the chamber to less than 12,000 psi. The protective structure for the chamber consisted of a 30 foot diameter spherical shell with a wall thickness of eight feet of high strength concrete and a one inch steel liner. The chamber was placed in the center of the concrete shell and surrounded with cellular concrete. The concrete shell was utilized to limit the deformations of the interior cavity due to the free-field stress to below the locking-up deformation of the cellular concrete. With small deformations, the cellular concrete would transmit only small stresses to the chamber. A second major function of the cellular concrete was to attenuate the acceleration pulse level to below the chamber design criteria. Active data was taken to determine the system performance and recovery of the chamber was performed which allowed visual verification of survivability.

Numerous analytical techniques were utilized and developed as part of this effort. A one-dimensional finite-difference stress wave code with constitutive relationships accounting for dissipative material effects was utilized to develop the free-field stress wave characteristics. Finite element methods were used to determine the response of the large concrete protective structure. These methods had to account for non-linear material behavior, arbitrary dynamic loading, large deflections, and two-dimensional axisymmetric geometries. The inadequacy of existing finite element methods to account for behavior of structural and shock absorbing material under loading conditions of several kilobars required the development of new analytical techniques. A two-dimensional finite difference stress wave code was also utilized to determine the interaction between the structure and the stress waves in the rock. Comparison between these two analytical methods were made and sufficient agreement found to verify the design. Lumped parameter techniques were also employed to determine the motion of the structure.

The utilization and development of the analytical techniques were closely coordinated with a materials testing program which determined the appropriate material descriptions for both the analysis and field installation. High strength concrete was developed and utilized for the principal structures. Shear behavior was determined and modeled for mean confining pressures up to 3 kbars (50,000 psi). A cellular concrete with a crush strength of 1400 psi and an allowable deformation of 40 percent was developed.

The data obtained from the underground nuclear test indicated that the free-field pulse agreed closely both in amplitude and duration with analytical predictions. The concrete structure exhibited similar deformations to those predicted. The stress transmitted to the experiment chamber was limited to a few thousand psi and the chamber was structurally undamaged. The accelerations of the chamber were limited to those of the design objectives. A positive phase amplitude of 150 g's with a duration of 20 milliseconds was observed which agreed with calculated predictions.

In summary, the technology both in analytical techniques and design concepts for protection of structures in intense ground motion environments was developed and demonstrated in actual utilization.

#### DESIGN STUDY OF A NEW BRL EXPERIMENTAL BLAST CHAMBER

W. E. Baker and P. A. Cox  
Southwest Research Institute, San Antonio, Texas

This paper reports the results of a design study of a blast chamber intended for repetitive firings of explosive charges up to 30 lb weight with minimal disturbance to personnel in its vicinity. The study includes a survey of past work in blast chamber design, evaluation of several alternate design concepts and analyses to establish chamber material, spherical or cylindrical shape, size and thickness. Responses to initial and reflected blast waves were predicted, as well as stresses from internal static pressures. Effects of chamber evacuation on modification of loading and chamber stresses were considered. Other factors considered were chamber venting for unevacuated chambers, responses to charges detonated off-center, lining with shock-absorbing materials, and spalling effects.

The chamber design was found to be controlled by the initial and reflected blast loading, rather than static pressure. Partial evacuation to about 1/3 atmosphere markedly reduced blast loading and resultant chamber stresses, while off-center charge detonation increased stresses considerably. Reflected shocks were nearly in phase with chamber natural periods and therefore amplified stresses caused by initial blast loading. Stresses from static pressure rise were insignificant compared to those from blast loading, and no venting was necessary. Recommended construction material was mild steel, and recommended geometry was spherical. A steel vessel required no shock-absorbing lining and could not be spalled by any explosion other than a contact explosion. Chamber thicknesses were determined as a function of radius, and combinations for safe design were recommended.

## ANALYSIS OF CONCRETE ARCH MAGAZINE

John M. Ferritto  
Naval Construction Battalion Center, Port Hueneme, California

The Department of Defense has for many years stored explosives in earth-mounded arch magazines or igloos. Several varieties of reinforced concrete arch igloos have been used. One of the most prevalent has been the circular concrete barrel arch. The arch spans about 27 feet and has a height at the crown of about 13 feet. The thickness of the reinforced concrete varies from 16 inches at the base to 6 inches at the crown. Reinforcing steel in the direction of the arch consists of #5 bars at 12-inch centers on each face with a constant concrete cover of 1-5/8 inches. The arch igloos are covered with two feet of soil forming an earth berm sloping outward at 2 horizontal to 1 vertical.

The objective of this study was to examine and upgrade the blast resistance of this arch to long duration loading effects produced by a detonation of a nuclear weapon. The relatively steep slope of the earth berm results in an increase in loading from the reflection of the side-on overpressure blast wave and from the dynamic drag forces caused by the blast wind pressure. Further the loading is principally on the side of the structure producing a significantly antisymmetrical loading condition on the arch. An approximate analysis indicated that the structure in its existing configuration would fail at a very low overpressure (less than 10 psi side-on overpressure, 25 psi total dynamic pressure). To upgrade the hardness of the structure, it would be necessary to decrease the reflected pressure wave, the dynamic drag pressure, and/or the antisymmetrical characteristics of the load applications. To achieve these results, it was proposed to flatten the slope to as near horizontal as possible (less than 4:1) and to increase the height of soil cover over the arch. The hardness level of the modified structure was evaluated using the finite element technique. This paper presents the results of a finite element analysis and the recommended modifications to the existing structure to upgrade its hardness to a side-on overpressure level of 100 psi.

The finite element method idealizes a continuum as an assemblage of a finite number of discrete structural elements interconnected at a number of joints or nodal points. The program used in this study was NONSAP, a structural analysis program for static and dynamic analysis of nonlinear structural systems. Several elastic and inelastic analyses were performed of arches with and without soil cover. An eigenvalue analysis was performed to determine mode shapes and natural periods.

It was found that soil mass increases the natural period from 72 msec to 118 msec, but the low mode shapes of the arch with soil were similar to that of the arch without soil. However, higher mode shapes differed somewhat because the soil mass restrains the arch.

A linear dynamic analysis was performed using the direct intergration method. A 100-psi traveling wave was used to load the arch covered by soil. Thrust-moment diagrams and pressure loads were computed for various time increments from which the peak loading was determined. The moving wave produced a loading which was more anti-symmetric than the static loads. By use of the thrust-moment loadings it was determined that the load at which the structures became inelastic (formed a first hinge) was 80 psi. Points of high stress (hinge formation) were determined. Since the stresses approach the ultimate capacity of the concrete (thrust rather than moment), the probability of failure over large areas of the arch is high. Therefore, it is necessary that the allowed ductility factor must be low—1.3 to 1.5. Using the computed structural resistance and a ductility factor of 1.4, the maximum total load capacity of the arch was found to be 105 psi. The arch would be able to carry about 100 psi side-on overpressure on the ground surface. This represents the maximum pressure that can be carried without structural modification to the arch. The deflection history of the crown of the arch, and the deflection, velocity, and acceleration of the floor slab centerline were determined.

Ground motions as high as 20 g would be expected on the floor slab. The finite element analysis was successful in representing the arch structure and loading.

The front entry structure, rear wall, and blast door must be upgraded to equal the 1-psi capacity of the arch. This can be accomplished by constructing an entry structure housing a new blast door and a new cantilever rear wall.

## MEASUREMENTS AND CRITERIA DEVELOPMENT

### BOUNDARY LAYER FLUCTUATING PRESSURE DATA OBTAINED IN A HIGH BACKGROUND NOISE ENVIRONMENT ON A SMALL SCALE WIND TUNNEL MODEL

G. L. Getline  
General Dynamics Corporation, San Diego, California

During preliminary design studies of a lift-lift/cruise engine V/STOL fighter aircraft, it was realized that it might be necessary to crop the trailing edge of the canopy because of the close proximity of the vertical lift engines which were located immediately aft of the cockpit. Flow visualization studies on a small wind tunnel model of the aircraft indicated the possibility of aerodynamic flow separation over the cropped canopy in the transonic flight regime and under some maneuvering conditions. One result of such flow separation could be an increase in cockpit interior noise levels so as to interfere significantly with electronic communications. It was planned, therefore, to instrument an available small scale (1/14.92) model with external flush mounted high frequency pressure transducers in order to obtain boundary layer fluctuating pressure data in the transonic and supersonic flight regimes. These data could then be used as a basis for estimates of cockpit interior noise levels for the full scale aircraft during high speed flight.

Supersonic test data were obtained in the Convair supersonic wind tunnel at San Diego, California and transonic data were obtained in the CALSPAN transonic wind tunnel at Buffalo, New York. Three technical areas which required circumspection in attainment of program objectives were:

- a. Obtaining of very high frequency (up to 80 KHz) fluctuating pressure data in the presence of a high background noise and turbulence environment.
- b. Demonstration that the test data was representative of boundary layer pressure fluctuations and did not merely reflect ambient wind tunnel noise and turbulence.
- c. Conversion of wind tunnel model data to the full scale aircraft with appropriate geometric and aerodynamic scaling parameters.

The high frequency data requirement was established by the small scale of the model. The 80 KHz upper limit, however, was dictated by available instrumentation and scaled up only to about 5400 Hz. Availability of ambient noise and turbulence data from both of the test tunnels enabled pre-filtering of signals from the pressure transducers. This, along with the large (Strouhal) frequency separation between the full scale tunnel pressure data and the small scale model data enabled extraction of the model boundary layer pressure data from the composite signals.

The above technical areas are discussed in detail. Test data are presented which describe wind tunnel ambient noise and turbulence, and separation of boundary layer

pressure data from background noise. Comparison is made of test data obtained in this program with data obtained in special facilities by other institutional and government researchers. It is demonstrated that it is feasible to obtain valid, high frequency boundary layer fluctuating pressure data at low cost on small scale models in unmodified wind tunnels with characteristically high level background noise and turbulence.

### THE DYNAMIC MEASUREMENT OF THE LOW FREQUENCY COMPONENTS OF TRACK INDUCED RAILCAR WHEEL ACCELERATIONS

Steve Macintyre, Tom Jones and Bob Scofield  
ENSCO, Inc.

In characterizing the overall shock and vibration environment to which a railcar may be subjected, the complete acceleration spectrum must be measured. Track induced railcar wheel accelerations cover a broad frequency band and include both short duration (2-3 ms) high level (600 g's) shock as well as low level (.1 g's) low frequency (0-30 hz) vibrations. In order to measure wheel acceleration without causing transducer saturation, an accelerometer with a wide dynamic range (1000 g's) must be used. Piezoresistive, piezoelectric, or strain gage accelerometers are the usual choices in picking a transducer for this application. But their accuracies are at best  $\pm 1\%$  of full scale and in the case of the piezoelectric accelerometer only respond to signals above a low frequency limit. As a result, the low level low frequency signals become lost in the transducer and conditioning amplifier noise.

Measurement of the acceleration components within the 0 to 30 Hz frequency range can be accomplished by mounting a servo-accelerometer on a linear spring-mass-damper mechanical isolator designed to attenuate the high frequency accelerations applied to the wheel. A linear mechanical system should be used since its mechanical impedance (and thus its transmissibility) can be fairly well controlled; its responses to applied accelerations are accurately known; and generation of harmonics of the applied acceleration are minimized. The transmissibility function for a second order spring-mass-damper system expressed in Laplace Transform notation can be written as:

$$\frac{A_o}{A_i} = \frac{w_n^2 (1 + 2\delta s/w_n)}{s^2 + 2\delta w_n s + w_n^2} \quad (1)$$

where

$A_o, A_i$   $\equiv$  mass and applied accelerations respectively,

$w_n$   $\equiv$  nature frequency of the mechanical system,

$\delta$   $\equiv$  damping ratio of the mechanical system.

Because of the zero at  $w = w_n/2\delta$ , it is difficult to establish a  $\delta$  that will prevent the transmissibility of the system from peaking within the bandwidth of the mechanical system at a value greater than unity. To prevent this acceleration amplification from saturating the accelerometer and to flatten the overall measurement system frequency response, a combination inductor-resistor-capacitor (LRC) network can be placed in the

servo-accelerometer feedback loop and tuned to minimize the effect of the mechanical zero in the overall system transfer function. The effect of the LRC network is to adjust the feedback current to the torque coil of the accelerometer suspension system such that the accelerometer's range changes with frequency in proportion to the changes in mechanical transmissibility.

A system that can be mounted on the journal bearing adapter of a standard freight car truck was designed, built and tested. Four 1/2" radius helical coil springs made from 1/8" diameter Music Wire and having a total spring constant of 144 lbs/in were used to suspend the mass and accelerometer from the top and bottom of a 20cm X 19.5cm X 5cm aluminum container. In parallel with the four springs was a gum-rubber spring damper combination. The container cavity was fabricated by milling out the center of a solid piece of aluminum. A 1" diameter cylindrical hole bored into the mass acted as the cavity for the damper piston. Mounting holes for both a longitudinal and transverse servo accelerometer were also provided on the mass structure.

The assembled measuring system was tested in the laboratory with silicon damping fluids ranging in viscosity from 50 to 12,500 centistokes using a shaker table. A constant 4g peak acceleration was applied to the unit while its frequency was swept from 10 to 1000 Hz. Best system response was achieved with 3000 centistokes fluid. The container had a fundamental resonant frequency of 265 Hz with a secondary resonance at 650 Hz. Both resonances were sufficiently above the 30 Hz bandwidth of the system that their effects were negligible. The results of these tests indicated that the basic concept was sound. Field tests with the measuring system mounted on a freight car will be conducted this summer.

#### **DEVELOPMENT AND APPLICATION OF A MINIATURE RECORDER/ANALYZER FOR MEASUREMENT OF THE TRANSPORTATION ENVIRONMENT**

AFPEA, Wright-Patterson AFB, Ohio

The Air Force Packaging Evaluation Agency contracted with Bolt, Beranek & Newman, Inc. to develop a miniature electronic transportation environment recorder to determine the environments and hazards that packaged items experience in handling, shipment, and storage. The key to the significant reduction in volume of this recorder is the use of metal oxide semi-conductor (MOS) technology circuitry coupled with the use of miniature sensors. This technology yields compact circuitry with low power requirements.

Three piezoelectric accelerometers are used, one for each of the principal axis of the recorder. The shock data acquired from the triaxial accelerometer is separated by shock polarity for each of the three recording channels. Data is analyzed in real time and the results stored in the MOS memories. The data can be readout on request by a digital readout device. The recording range is from 2.5 G to 90 G. Twenty-four amplitude windows are used for storing acceleration peaks for one polarity and one channel. The first 19 windows are 2.5 G wide, the next 5 windows are 10 G each while the last window is an overflow window for shocks greater than 90 G.

The recorder also has the capability of measuring temperature and humidity. The recorder's temperature range extends from -20 to +140° F. Sixteen amplitude windows are employed for the temperature measurements, each 10° F wide. The recorder's relative humidity range is 0 to 100%. A total of eight windows are used for the humidity measurements; one window for 0 to 30% RH; and seven windows for 30 to 100% RH, each 10% wide. Temperature and humidity readings are made once each minute. The recorder also contains an elapsed time clock which measures time in one minute increments. The elapsed time clock makes possible the determination of the percentage of time specific temperature and humidity ranges are experienced.

One of the prime advantages of the recorder is that the data as readout are already analyzed. It is not necessary to perform magnetic tape analysis or to feed data into a computer. The statistical analysis has already been accomplished.

Using internal batteries, the recorder can operate continuously for over two weeks. External battery packs can be connected to the recorder for longer operation. The total volume of the recorder including batteries for two-week operations is 168 cubic inches (4-7/8 X 5-7/8 X 5-7/8 inches) and the weight is six pounds. If required, the triaxial accelerometer can be separated from the recorder package and mounted on smaller test articles.

Prototype recorders have been subjected to extensive in-house calibration and operational testing by the Air Force Packaging Evaluation Agency. Vibration testing has revealed the need for additional filtering to eliminate spurious signal inputs due to shock resonances in the recorder housing. Programmed shock tests also revealed the need to increase the low frequency response of the system.

Current applications of the recorder involve measurement of the shock environment experienced a set of standardized cushion packs extensively used by Air Force as well as other DOD activities in the shipment of fragile items. Data collected has been used to establish reliable pack selection criteria to insure safe delivery of critical high value weapons system components. In addition to the measurement of item response in terms of peak G, additional data was obtained on the shipping environment by placing the miniature shock recorder in a specially designed shipping container which provided approximately equivalent response regardless of the orientation of the container at impact. Prior to shipment, the instrumented pack was calibrated in the laboratory to correlate peak shock values with container drop heights. The information obtained on drop height was used to verify the reliability of previously developed design criteria. Future plans involve a more ambitious program to measure environmental conditions experienced by Air Force equipment in world-wide distribution. This information is required to improve design techniques and the reliability of performance testing.

## **ADVANCES IN SHIPPING DAMAGE PREVENTION**

H. Caruso and W. Silver, II  
Westinghouse Electric Corp., Baltimore, Maryland

For several years now, Westinghouse Electric Corporation has been studying the transportation of loose cargo in tractor-trailers to determine how products are damaged in shipment and how they can be better designed to resist this damage. This work has been the joint effort of Westinghouse' Corporate Traffic Department in Pittsburgh, its Defense and Electronic Systems Center's Product Qualification Laboratory, and Jones Motor of Spring City, Pennsylvania.

There is good reason to be concerned with shipping damage: In the past 5 years, more than \$350 million worth of manufactured goods were damaged in truck shipments. Last year alone, this figure exceeded \$75 million. The following outlines the progress that Westinghouse has made in measuring the road transportation environment and how it has developed test methods and specifications for evaluating product survivability.

A number of tractor-trailer types were instrumented with accelerometers at several points along the trailer loading beds and on the front and rear axles. Measurements were also made at the fifth wheel. During the road test phase of these studies, each factor that might have contributed to shipping damage was investigated:

- Various types of suspension systems were tested. Among these were conventional single leaf springs, air bags, damped coil springs, and rubber isolators.
- Trailers were tested with varying degrees of load, from lightly loaded to half and full loads. Measurements showed that the worst ride occurs in a lightly loaded trailer over the rear axle.
- Measurements were made with the rear wheels in their forward, rear, and center positions. This information is currently being analyzed.
- Rides were measured over various road types including city streets, unimproved back roads, interstate highways, and special test tracks. It was found that high-speed driving over interstate highways produces the worst ride in the trailer.
- The man in the cab was found to have very little effect on the ride in the trailer. Road type, speed, suspension system, and load are the major factors in determining ride quality.

Analysis of the road data led to two major conclusions:

- First, it was found that certain suspension systems could not only prevent shipment damage, but also reduce the road stresses that lead to trailer fatigue and excessive tire wear. In addition, handling would be improved and driver fatigue reduced due to improved rear wheel tracking.
- Second, a shipping test specification was developed to evaluate product and package designs under simulated road conditions.

In a typical loose cargo shipping test, the product is placed on a simulated trailer bed mounted to a vibration exciter. Although barriers are used to limit sideways travel, the product is in no way tied down to the vibration fixture. The simulated trailer bed is then subjected to a random vibration input that produces a "ride" equivalent to the worst conditions measured during the road studies. These conditions are found over the rear axle of a lightly loaded trailer travelling at high speed.

Laboratory tests can also be used to evaluate package designs and the behavior of reasonable loading configurations. In addition, similar tests are being used to investigate the behavior of the trailer bodies themselves and to evaluate new trailer designs and construction techniques. When testing is completed, the test report serves several important and distinct purposes:

- It evaluates product, package, and truck designs;
- It provides specific recommendations to increase product survivability and improve package and truck design; and
- Because it documents product and package behavior under realistic shipping conditions, it can help to settle claims disputes that result when shipments are damaged.

The road transportation environment is no longer a completely unknown quantity. It has been measured, analyzed, and duplicated in the test laboratory. The road studies made have been developed into shipping test standards that can be incorporated into industrywide regulations. Using technology that is available today, it is possible to improve tractor-trailer ride quality, increase product survivability, and substantially lower shipping damage. The same technology can also decrease shippers' overhead expenses by stretching useful trailer life and reducing tire wear.

#### **EXPERIMENTAL VERIFICATION OF DETERMINING IN-FLIGHT VIBRATORY LOADS ON HELICOPTERS USING ACCELEROMETER DATA AND IMPEDANCE MEASUREMENTS**

Joseph H. McGarvey and Felton D. Bartlett, Jr.  
Langley Directorate, USAAMRDL, Langley Research Center, Virginia

and

Thomas W. Forsberg and William G. Flannelly  
Kaman Aerospace Corporation, Bloomfield, Connecticut

The accurate determination of the magnitudes and phases of forces and moments of various harmonics acting on a helicopter in flight is necessary for practical fatigue and reliability testing of entire helicopter fuselages on the ground and important to stress analysis, corroboration of rotor loads predictions, the design of rotor isolation systems and the design of dynamic absorbers and other methods of vibration reduction. This paper describes the theory of determining operational forces and moments and their phasings from in-flight fuselage accelerations and shows results of laboratory testing on a sixty inch

long dynamic model of a typical helicopter in which simultaneous forces were determined to within 5 percent error on magnitude and 4 degrees error on phase.

The method consists of first ground shaking the suspended helicopter fuselage, on which a greater number of accelerometers than vibratory loads to be determined have been mounted, so that the mobility of each accelerometer coordinate to each excitation coordinate at the desired harmonics is measured. This dynamic calibration may also be accomplished by shaking the aircraft at only one point. The second step is to record the signals of each accelerometer during the flight conditions of interest. The forces and moments and their phase angles at each harmonic are determined by multiplying each harmonic of the accelerations by the pseudoinverse of the rectangular mobility matrix of that harmonic.

To test this theory, a sixty inch long, fifty pound dynamic model of a typical helicopter was dynamically calibrated from 7.5 to 50 Hz both by direct hub excitation and by single-point-shaking theory. Center of gravity shifts and gross weight changes, simulating payload variation and fuel burnoff, were made during the tests on the dynamic model. Fifteen accelerometers were distributed along the model to measure both vertical and lateral responses and were oriented to give independent measurements for the applied vibratory loads. Simultaneous vertical and lateral forces of various magnitudes and phasings were then applied to the dynamic model at frequencies both near and distant from the natural frequencies. The pseudoinverse of the mobility matrix and the accelerations measured under simultaneous excitation were used to determine the magnitudes and phasings of the excitation forces and these determinations were compared to the measured magnitudes and phasings of the excitation forces. The testing showed errors of less than 5 percent on magnitude and 4 degrees on phase of the excitation forces in all practical cases. The highest error was approximately 16 percent in a case of an uncorrected shaker restraint peculiar to the laboratory setup which, in this instance, did not accurately reflect flight.

The paper will present the basis of single-point-shaking (SPS) theory showing the conveniences and cross checking advantages of using SPS theory at an additional point. Test results showing that SPS theory can be applied at a point or points of convenience to accurately produce the mobilities relative to excitation points which have not been excited will be presented. The method of using SPS theory for the separation of proximate modes will be described along with actual test data illustrations.

#### COHERENCE METHODS USED TO DEFINE TRANSMISSION PATHS OF AIRBORNE ANTENNA VIBRATION

Jerome Pearson and Roger E. Thaller  
Air Force Flight Dynamics Laboratory, Wright-Patterson AFB, Ohio

To develop secure, reliable communication for airborne command posts, the Air Force Avionics Laboratory has been investigating the use of super-high-frequency (SHF) terminals to communicate between aircraft and synchronous satellites. At these frequencies, near 8 GHz, Doppler effects from the aircraft motion may shift the signal frequency by several kilohertz. These Doppler effects are removed by a computer operating on the inertial navigation system outputs. The additional Doppler effects due to antenna

boresight vibration are not corrected. The angular vibrations of the antenna in elevation and azimuth cause pointing errors that reduce signal strength. These effects can severely degrade airborne communications, and thus are limiting factors on system performance.

To measure the antenna vibration and to determine the vibration transmission paths, the Air Force Flight Dynamics Laboratory flight tested a transport aircraft equipped with an Avionics Laboratory SHF terminal communicating with a synchronous satellite. This paper is a discussion of the determination of the vibration transmission paths performed on test data acquired during cruise.

The data were analyzed to determine the source of the vibration by using coherence functions. The responses of the antenna in pointing (elevation and azimuth) and the response along the line of sight (boresight) were considered to be the outputs of a linear system. The vibrations of the antenna pedestal in three linear directions (vertical, lateral, and longitudinal) and in two angular directions (roll and pitch) and the noise in the antenna fairing were considered to be the inputs to this linear system. The relative importance of all these inputs in causing the antenna responses was evaluated by using the following types of coherence: pairwise, multiple, marginal multiple, conditional pairwise, conditional multiple, and marginal conditional multiple.

The results of multiple coherence analysis show that the responses of the antenna at its important resonant frequencies are well accounted for by the chosen inputs of pedestal vibration and fairing noise. The results further show that the main antenna boresight excitation is a function of the pedestal longitudinal vibration, and that the responses in elevation and azimuth are due to excitation produced by the other pedestal inputs. The fairing noise input has little effect on any of these low-frequency modes. The results of this flight vibration test and coherence function analysis show that these techniques can be applied to practical flight vibration problems and can produce the necessary information to proceed with effective vibration reduction.

#### **DEVELOPMENT OF COMPONENT RANDOM VIBRATION REQUIREMENTS CONSIDERING RESPONSE SPECTRA**

C. V. Stahle and H. R. Gongloff  
General Electric, Space Division, Philadelphia, PA

and

W. B. Keegan  
NASA, Goddard Space Flight Center, Greenbelt, MD

A method of determining component random vibration requirements from measured data is presented which enables the final specifications to be placed on a statistical basis. The statistical analysis of measurements has become the accepted method of developing component vibration requirements although several approaches have been proposed. The early work of Condos and Barrett statistically analyzed the peak PSD values in frequency bands while the more recent work of Keegan analyzed PSD values at discrete frequencies. After completing the statistical analysis of the PSD values, a selected percentile was enveloped to determine the component random vibration requirements. The above

procedures lose their statistical significance and usually employ arbitrary factors to assure the adequacy of the components for the vibration environment. The purpose of this paper is to present a method of developing component vibration requirements which retains the statistical significance of the procedure so that more meaningful requirements are specified.

The random response spectra (RRS) of the ensemble of measurements is used to determine the best method of analyzing the PSD data. The RRS is defined in a similar manner as shock response spectra. The RRS is the RMS response of a single-degree-of-freedom oscillator as a function of the oscillator frequency. The RMS response is considered to reflect the damaging effects of the random vibration environment. Because it is not practical to develop RRS data for the large amount of existing measurements, the objective of this study is to develop a method of analyzing PSD spectra such that the resulting RRS preserves the statistical characteristics of the RRS of the ensemble of measurements.

Four methods of sampling PSD spectra are evaluated. The spectra were measured at subsystem mounting locations during spacecraft level acoustic tests. The spectra are analyzed using one-sixth octave frequencies to define frequency bands or sampling frequencies. The PSD spectra are sampled using (1) the peak value in a band, (2) the average value in a band, (3) a reduced peak value in a band, and (4) the actual PSD value at discrete frequencies. The reduced peak value provides a 3 dB reduction of narrow band peaks or the selection of the peak value if it is not a narrow band. For each sampling method, the PSD values are statistically analyzed. Although both Weibul and Log Normal distributions were evaluated using the method of residuals, the Log Normal distribution provides the best fit to the data.

Random Response Spectra obtained for the ensemble and from the four sampled PSD spectra were used to evaluate the best sampling method. The individual PSD curves were digitized using an APPLICON Tabletizer to provide a replica digitization of the curves. These curves were analyzed digitally to determine the one-sixth octave RRS for each measurement and the RRS were analyzed statistically. For each sampling method, the sampled PSD spectra were statistically analyzed and for various probability levels, the RRS were computed. The comparison of these RRS with the ensemble RRS at several probability values indicates that the best sampling method is using discrete frequency sampling.

Smoothed spectra having a desired probability value are obtained using the sample or ensemble RRS statistical properties. Considering components to have a single failure mode which can occur with equal likelihood at any frequency, the RRS of the smoothed spectrum is placed on a statistical basis. The smoothed spectra are then shifted and shaped to obtain the desired probability value with a minimum deviation from the desired spectrum.

## STATISTICAL DETERMINATION OF RANDOM VIBRATION REQUIREMENTS FOR SUBASSEMBLY TESTS

John M. Medaglia  
General Electric Company, Valley Forge, Pennsylvania

A method for determining random vibration requirements for subassembly level testing is presented and applied to the Japanese Broadcast Satellite Experiment (BSE) Transponder. The BSE Transponder assembly is a two-tiered, 2.5 foot by 4.5 foot structure which supports numerous electronic components and weighs approximately 175 pounds. The structure is magnesium sheet stiffened with extruded and formed members. It forms one side of the box structure of the satellite. A test at only the component level is not adequate for the Transponder assembly because of the many waveguide connections between components and the numerous small devices embedded in the waveguide itself. Performance evaluation of the Transponder can be done only as a complete assembly. Therefore, a subassembly test of the Transponder is necessary. The purpose of this paper is to present a method for specifying the random vibration requirements for hardmount testing of the assembly which are compatible with the vibration requirements applied to the individual electronic packages.

The need for a practical, realistic method for specifying the random vibration requirements for the assembly was confirmed by the Engineering Model (EM) test of the Transponder. The EM test inputs were partially defined analytically by enveloping the predicted PSD responses to the 1-G transfer functions and shaping the inputs using component test specifications as a guide. The final test input levels for each axis were defined during the test since the finite element model was not sufficiently accurate. The inputs were adjusted so that the  $G_{RMS}$  of the maximum responding accelerometer was within 10% of the  $G_{RMS}$  of the component specification, but the Power Spectral Density (PSD) peaks were allowed to exceed the component specification by 10 dB. No minimum response levels were set. The responses were characterized by large variations in PSD and no location resembled the component specification environment in PSD shape. Better matching of the PSD response to the component specification would have required impractical input shapes. The response behavior of the subassembly in the hard mounted EM test should represent the major subassembly modes which will be excited on the spacecraft. The input levels of the EM test provided the data base for the behavior of the Transponder. The unsatisfactory accuracy of the analytic model and the confusing variety of response data from the EM test demonstrated the need for a method to develop conservative but realistic inputs that simulate the effect of flight environments on components.

The Random Response Spectra ( $G_{RMS}$  damage potential) due to the subassembly response and due to the component random vibration test specification were compared at several probability levels to establish test input levels. The component test specification was developed by enveloping data from several previous spacecraft at selected probability levels and as such represents a realistic PSD environment across the frequency band of interest (20 to 2000 Hz). The equivalent damage of component piece-parts was quantized by calculating the  $G_{RMS}$  responses of Single Degree of Freedom oscillators. Each resonance was considered to have equal probability of being the critical failure mode. The PSD of the component specification and the PSD response of the Transponder assembly were stimuli to the SDF oscillators. When the  $G_{RMS}$  responses due to each stimulus were satisfactorily matched, the input levels were defined. This method considered points on the assembly with high response and low response to represent actual flight conditions.

There were several distinct steps in developing the random vibration test input specification for the BSE Transponder. The environment was statistically defined by the Component Acceptance Test specification, consisting of data from several previous spacecraft. The PSD responses of 59 accelerometers at component mounting locations on the EM Transponder were replicated by digitization for each of the three axes of vibration. The SDF  $G_{RMS}$  response to the replicated PSD's was computed at 41 discrete (1/6 octave) frequencies for each of the 59 accelerometers. The  $G_{RMS}$  values were fit to lognormal distributions and a mean ( $\mu$ ) and standard deviation ( $\sigma$ ) obtained for each of the 41 frequencies. The PSD replicas were sampled at the 41 discrete frequencies and the  $\mu$  and  $\sigma$  of the PSD response was obtained. At several probability levels, the  $G_{RMS}$  due to the sampled PSD was compared to the  $G_{RMS}$  due to the replicated PSD and good agreement was found. The  $G_{RMS}$  due to the component specification PSD was compared at several probability levels to the  $G_{RMS}$  due to the EM Transponder PSD response. The ratio of these two  $G_{RMS}$  levels was used to analytically reshape the EM PSD input (and thereby the EM PSD response) until the  $G_{RMS}$  due to the EM data satisfactorily matched that due to the Component Environmental Specification. The preliminary input levels used in the EM test were found too high below 250 Hz and too low from 500 to 1200 Hz. After reshaping, the  $G_{RMS}$  ratios averaged less than 1.05 and at discrete frequencies the ratios showed less than a 40% difference. This is analogous to the component specification which allows a  $\pm 10\%$  tolerance on the overall  $G_{RMS}$  and a  $\pm 3$  dB tolerance on the PSD peaks. The comparison of the Transponder PSD shape and the component specification PSD showed an average ratio of 1.19 and peak ratios of from .26 to 3.68 even though the  $G_{RMS}$  levels matched satisfactorily.

A method has been developed and applied to the BSE Transponder which will enable realistic subassembly random vibration requirements to be specified. Close matching of PSD's is apparently not required to obtain equivalent damage. With sufficient data, the PSD response may be sampled, statistically defined and used to calculate the  $G_{RMS}$  of a subassembly, eliminating the costly calculation of the  $G_{RMS}$  spectra from replicas and then getting a statistical definition to the  $G_{RMS}$  values. Subassembly testing has several advantages:

- Does not limit environment to prescribed level.
- Represents dynamics of assembly.
- Enables better performance monitoring and assembly qualification.
- Can be less expensive than requiring many component tests.

#### Summary of Method

- Sample PSD responses on subassembly.
- Statistical analysis of sampled PSD responses.
- Calculate  $G_{RMS}$  from sampled PSD.
- Calculate  $G_{RMS}$  from component specification.
- Compare  $G_{RMS}$  values and shape test input until  $G_{RMS}$  agree at various probability levels.

## EVALUATION OF THE HARPOON MISSILE AIRCRAFT LAUNCH EJECTION SHOCK ENVIRONMENT

James A. Zara and John L. Gubser  
McDonnell Douglas Astronautics Corp., St. Louis, MO

and

Allan G. Piersol  
Bolt, Beranik & Newman Corp., Canoga Park, CA

and

William N. Jones  
Naval Weapons Center, China Lake, CA

Extensive shock environment measurements were made on the Harpoon missile during simulated aircraft launch ejections conducted at the Naval Missile Center Ground Ejection Test Facility, Pt. Mugu, California. A series of eleven ejections were performed on the test missile using both the MAU-9A and the ZERO-7A ejection racks. Two different cartridge sizes (10 klbs and 20 klbs) were evaluated. Up to three ejections were performed for some of the rack/cartridge combinations to obtain a measure of repeatability in the test results. A total of 30 accelerometers were used to obtain shock response measurements of major equipments installation and of structure at points along the length of the missile. The shock response time histories were reduced to shock spectra and in some cases energy spectra. The shock spectra were then statistically analyzed.

The results yielded some conclusions which are of general interest to the high impact shock environments of structures other than Harpoon. For example, an evaluation of data from repeated tests using the same ejection rack and charge size revealed close agreement, on the average, in the shock spectra values at frequencies below 1000 Hz, but significant differences in the values at higher frequencies. These results illustrate that the response of structures to an impact type loading can be very sensitive at the higher frequencies to minor changes in the manner in which the initial load contact is made. On the other hand, when the ejection charge size was doubled, the shock spectra of the missile response increased significantly at frequencies below 1000 Hz, as would be expected, but did not increase at the higher frequencies. Again, the results indicate that the high frequency response is dominated by factors other than just the total impact energy.

Other conclusions of the study are: (a) the structural response at a given location is not significantly different among the three orthogonal axes, (b) the response does diminish rapidly with distance from the point of impact, and (c) the response is not significantly different for different ejection racks, given the same charge size. The paper concludes with suggestions on the shock testing of missile components.

## **DEVELOPMENT OF SHIP SHOCK LOAD TEST FOR RGM-8A MISSILE (HARPOON)**

T. L. Eby

Pacific Missile Test Center, Point Mugu, CA

The environmental design criteria for the HARPOON missile specified ship shock loads for the three principal missile axis. The shock load is specified as a trapezoid acceleration pulse of thirty-five milliseconds, with ten millisecond ramps to the peak acceleration level. This paper discussed the development of the device to verify these missile design load requirements. The design verification test was developed and performed using a large shock facility at the Pacific Missile Test Center. The specified shock pulse shape was obtained by using a combination of Belleville (disk) springs as the impact energy transferring device.

Belleville springs are characterized by non-linear load deflection curves. The load deflection curve requirements were determined by graphical techniques. A series combination of two sets of nested Belleville springs were designed. The first set was designed to develop the pulse ramps. The second set was designed with pre-loads to develop the maximum acceleration level. The conservation of energy and conservation of momentum equation were used to determine the correct parameters for the shock machine and spring devices.

The Belleville spring device was mechanized, using commercially available springs. The springs were selected and installed on a threaded cylinder. The lower set of springs was pre-loaded to the desired load characteristics. The upper set of springs was held in place with a retaining ring and impact surface. The impact resulted in the initial compression of the upper springs until the pre-load level of the lower springs was overcome. At this point the entire spring arrangement acted as a single series non-linear spring until the energy of the impact was absorbed.

A test vehicle was used to verify the results of the analytical and graphic work. This inert test vehicle was used to resolve test configuration, test eccentricities and instrumentation problems. The design data and actual test results compared favorably with the design criteria.

## ISOLATION AND DAMPING

---

### THE MEASUREMENT OF DAMPING AND THE DETECTION OF DAMAGES IN STRUCTURES BY THE RANDOM DECREMENT TECHNIQUE

J. C. S. Yang and D. W. Caldwell  
University of Maryland, College Park, Maryland

When physical structures are subjected to random forces, certain internal vibrations are set up within the structure as it absorbs the energy imparted to it. In some cases, the energy imparted may cause stresses which exceed the strength limitations of the structure and which may result in a failure of the structure. To prevent the failure of a structure two areas of engineering need to be more thoroughly investigated. One such area is structural damping. Small cracks and localized failures of the structural elements often have a significant effect on the vibration response characteristics of the structure long before they are significant enough to be visually detectable. Damping is one of the characteristics which changes. Damping is the means by which structures absorb energy and significant changes in damping is therefore very meaningful. The precise measurement of damping is therefore highly important to the economic design and reliable analysis of large structures.

Various attempts have been made to provide means for obtaining structural damping information used in the design of structures and used in the monitoring of the response to the applied forces. Although various types of apparatus and techniques are available for measuring structural responses to random vibrations, the data obtained is usually so complicated that an observer cannot readily determine when a significant change in the structural response occurs. Most of these techniques are only suitable for use under controlled laboratory conditions and are of little use for structures in service.

A simple, direct, and precise method is needed for translating the response time history into a form meaningful to the observer. The parameter chosen to examine the structure should be sensitive to changes in natural frequency and damping factor. Spectral power density has been considered, with damping measured by the half-power point bandwidth method, but this was found to have a large measurement variance, especially when the bandwidth was small. In addition, when two modes are close this method cannot be applied. Erroneous answers were obtained when assumed linear systems were actually nonlinear, a problem which could not be detected unless the input was also measured. The autocorrelation function was investigated as an alternative wherein damping data was obtained from the logarithmic decrement. The problem with the use of autocorrelation signatures is that the level of the curve is dependent on the intensity of the random input, and in a natural environment this can seldom be measured or controlled. If the structure is a linear system, the level changes can be compensated for by normalizing the curves, but if the structure is nonlinear (as is often the case), a different signature will be obtained with each level of excitation. Therefore, correlation functions can only be used with linear systems and by knowing the input.

Another area that needs development is the detection of crack initiation and growth. Present methods of crack detection include visual inspection and acoustic emissions. Although acoustic emissions can detect flaws in assembly line comparisons it is highly unlikely that under conditions of high ambient noise level such as is encountered in aircraft flight that this method can be applied. In addition, it is obvious that visual inspections are useless when cracks develop within the interior of a structural material.

#### RANDOMDEC ANALYSIS

A technique called "Random Decrement" has been developed and explored which advances the state-of-the-art in measuring precise damping values and in the detection of crack development and extension in structures subjected to random excitation when only response data is available. The analysis of the output of a system subjected to an unknown random input yields a signature similar to the autocorrelation function in that it is the free vibration decay response of the system. However, the main difference is that the amplitude of the signature can be chosen independently of the output level. Therefore, innumerable signatures, each at a different amplitude, can be obtained from a given time history and the shape of each signature is independent of the level of the input. Non-linear effects such as amplitude dependent damping can be measured and a repeatable signature for damage detection can be obtained. The ability to obtain signatures for different modes enables one to measure damping precisely and to detect damage before the overall structural integrity is affected.

Damping ratios were computed using this technique for several modes of randomly excited panels, beams, and bones. These damping ratios compared satisfactorily to damping ratios which were computed from the power spectral density method. Standard randomdec signatures were established for all the structures. Damages were detected by observing the changes in the established signatures. Notches which simulated cracks were induced into two of the beams. The effects of these notches on the beams' signatures were presented.

#### SURFACE VIBRATION REDUCTION OF MARINE PROPULSION GEARBOXES

E. V. Thomas and A. J. Roscoe, III  
Naval Ship Research and Development Center  
Annapolis, Maryland

The gear induced noise from high power marine propulsion systems causes a hearing health hazard to the ships crew. Generally, gearboxes are resonant in large areas a condition which amplifies the vibration at specific speeds. The resonant case is easily attenuated by application of a damping treatment. The reduction of the airborne noise due to the gearbox can be accomplished by reducing the vibration of the radiating surface. The best way to accomplish vibration reduction of the gearbox is to apply a continuous mass cover suspended on a soft isolating spring. A constrained layer of damping material with sealed edges on the constraint plate can be designed to carry out structural damping and

vibration isolation. The evaluation of the acoustic transmissibility is simplified to vibration transmissibility measurement and measurement of covered and uncovered areas.

To design an effective noise reduction, a damping spring like material is utilized to produce a viscoelastic shear layer between the gearbox and the constraining plate. The constraining plate is edge-sealed with a rubber caulk to contain the acoustic energy radiated from the gearbox. The constraining plate mass is designed to have a low resonant frequency when mounted on the spring-like material. The composite produces a moderate level of structural damping and a vibration isolation of the constraining plate above 300 Hertz.

Additional vibration reduction will result if a second layer of isolated mass is applied over the damping layer velocity isolator. This layer is developed with a closed-cell, fire-resistant foam as the spring layer, and a limp lead loaded vinyl sheet as the mass layer. The combination is designed as a compound mounted system with the resonances well below the frequencies of maximum attenuation desired. Standing wave resonances are designed to be above maximum attenuation frequencies. The compound isolator design produces effective attenuation over a decade of frequency.

As in any radiating surface attenuation, the total proportion of noise reduction varies as the sum of surface velocities squared per unit area of treated and untreated surfaces to the average velocity squared per total area. One hundred per cent coverage is not possible since some areas must be left uncovered for inspection, shafts, gauges, and piping. This limitation results in a coverage of about 97% which reduces the attenuation of the treatment to 25 dB.

#### RESPONSE ANALYSIS OF A SYSTEM WITH DISCREET DAMPERS

G. K. Hobbs, D. J. Kuyper, and J. J. Brooks  
Santa Barbara Research Center  
Goleta, California

The NASA-sponsored SMS Spacecraft is a Synchronous Meteorological Satellite having as the primary instrument a Visible Infrared Spin-Scan Radiometer (VISSR). The infrared channels of the radiometer use HgCdTe detectors which must be cooled to less than 90°K for operational use. A two-stage passive radiation cooler is used to obtain the low temperature.

The radiation cooler which supports and cools the two infrared detectors is optically aligned to the radiometer telescope axis. The major cooler components are an ambient housing and sun shield, intermediate stage, and cold stage. The sun shield specularly reflects to space unwanted solar energy entering the cooler during summer solstice. The intermediate stage supports the cold stage (detector stage) and thermally decouples the cold stage from ambient source radiation. High emittance radiators on both stages emit long-wavelength energy to low-temperature space, thereby lowering the temperature of each stage until thermal equilibrium is reached.

The cooler interstage support members have severely contradictory design requirements. Interstage heat transfer (radiation, conduction) must be reduced to very low

levels if the detectors are to reach their operational temperature, but a rigid interstage support structure is needed to raise the cooler vibration mode frequencies above the principal launch excitation frequencies. Also, large thermal gradients between stages ( $250^{\circ}$ K, overall) must be accommodated during operation, while maintaining detector alignment within 0.001 inch.

A glass-epoxy composite material was selected for the interstage support members, because of its high strength/conductivity ratio. The interstage support members were arranged like pretensioned spokes in a wheel. The use of six tension members per stage maintained a statically determinant system.

Each member was fabricated in a configuration much like a rubber band—a continuous structure wrapped around a cylindrical support at each end. This configuration was selected to minimize the stress concentration at the end attachments. The unidirectional glass-epoxy bands were fabricated from continuous "S" glass rovings pre-impregnated with epoxy resin. This design yielded a typical strength of about 220,000 psi, with a tensile modulus of about  $9 \times 10^6$  psi.

Creep relaxation during service was not found to be a problem, but the duration and level of vibration exposure were found to be critical to the fatigue life of the fiberglass bands. Random vibration was found to be particularly critical.

The analysis and test of a structural model cooler showed very high dynamic magnification factors, as much as 100 to 1 between stages. Survival of launch was not expected. Discreet dampers were inserted into the mathematical model and parametric analyses run to determine the optimum placement, type, and value of the dampers. In addition, stiffnesses were varied in the search for maximum fatigue life. The structure was found to be very sensitive to small parameter changes due to the interplay between the five principal participating modes of vibration and the frequency dependent input vibration levels. Final selection of damping was to use a tuned elastomeric auxiliary mass damper on the cold stage and to mount the sun shield on elastomeric bushings. The elastomeric bushings allowed the sun shield to vibrate out of phase with the intermediate stage at the critical frequency and, in so doing, to flex the elastomer and dissipate energy.

Tests run on the configuration which evolved showed good agreement with analytical results, and to date, two flight units have been launched with complete success.

#### THE APPLICATION OF ELASTOMERIC LEAD-LAG DAMPERS TO HELICOPTER ROTORS

D. P. McGuire, Lord Kinematics, Erie, Pennsylvania

Ground resonance is a potentially destructive instability which can occur in helicopters with fully articulated or soft in-plane rotors. This instability results from coupling of the in-plane motions of the rotor blades with the natural roll mode of the fuselage. Energy derived from rotation of the rotor makes the motion unstable. Current practice calls for incorporating sufficient damping in the lead-lag mechanism to control the blade motions and preclude instability. This is done by means of hydraulic or friction devices.

The use of a high hysteresis viscoelastic material to perform this function has significant advantages over other types of dampers in eliminating maintenance and improving reliability.

Suitable mathematical models are considered to represent the spring and damping characteristics of an ideal viscoelastic material. Hysteresis damping with the damping force proportional to displacement, but in phase with velocity is used. The equations of motion are developed for the rotor/fuselage system incorporating hysteresis damping. By assuming axial symmetry of the rotor ( $N \geq 3$ ) and using the method of multiblade coordinates, the system is reduced to four degrees of freedom, two representing the effective center of gravity of the rotor and two for the fuselage motions.

A computer program (HGRSA), which solves repetitively for the eigenvalues of the characteristic polynomial, is used to define the stability boundaries of the system and functions of system parameters, such as rotor speed, blade damping coefficient, etc. The equations of motion are also transformed to state-space variable form to allow time and frequency response of specific systems to be calculated using available computer programs.

The stability boundaries are determined for a base line system with the conventional viscous damping. The effects of the blade spring restraint provided by a viscoelastic damper on these boundaries is evaluated. The effects of hysteresis damping versus viscous damping and changing the loss factor of the viscoelastic material are also determined. All of this analysis is based on the linear ideal model of the viscoelastic material.

Nonlinear characteristics of two highly damped elastomers (BTR and BTR IV) are determined experimentally as functions of dynamic amplitude. The reduction in elastic and damping modulus with increasing dynamic amplitude is shown to be potentially destabilizing. The change in the stability boundaries as functions of dynamic amplitude are determined using the measured material characteristics. The effect of material non-linearity is shown to be within design limits.

#### EVALUATION OF ISOLATION MOUNTS IN REDUCING STRUCTUREBORNE NOISE

Thomas F. Derby, Barry Wright Corporation  
Watertown, Massachusetts

The increased concerns with reducing structureborne noise caused by shipboard equipment has raised questions concerning the evaluation of isolation mounts.

One problem seems to be what is measured according to MIL-STD-740B and how this relates to what the ultimate purpose of the Navy is in reducing structureborne noise. The reason for MIL-STD-740B is to evaluate the noisiness of a machine without taking into consideration the foundation on which it is to be mounted. The ultimate problem is the amount of ship deck or hull vibration caused by the machinery.

The impracticality of having real conditions is recognized because a) ships have not been built, b) different locations on the ship have different structural responses, and

c) the same machine can go into different ships and/or different locations on the ship.

Even if real conditions are present there are some questions concerning which response quantities should be used in evaluating the effectiveness of isolation mounts in reducing structureborne noise. Isolation mount effectiveness should be determined by the value of the response ratio, which is defined as the vibrational amplitude of concern when equipment is hard mounted, divided by this same amplitude when the equipment is isolation mounted. Isolation mounts have been evaluated on the basis of the value of the ratio of the acceleration on the foundation side of the mount divided by the acceleration at the equipment side.

The purpose of this paper is two-fold: (a) to compare structureborne noise, determined according to MIL-STD-740B, to structureborne noise transmitted to a ship deck or hull; and (b) to compare the ratio of accelerations on either side of an isolation mount to the response ratio. Both theoretical and experimental results are used.

The theoretical results are based on a one directional model of the equipment, isolation mount, and foundation. The mathematical formulation is presented in terms of modified four-pole parameters. The four-pole parameters are determined from the theory of longitudinal vibration of internally damped rods as presented in Chapter Six of *Vibration and Shock in Damped Mechanical Systems*, by J. C. Snowdon. Although this is a simple model, it is felt that its essential features (i.e., impedance versus frequency curves having alternate sharp peaks and troughs) are adequate in showing the effects of equipment and foundation structural responses. Also, various isolation mount characteristics are easily accommodated by this model (e.g., a two-stage mounting with a rigid mass included within the isolator).

The theoretical results are presented graphically for various combinations of system parameters. The parameters used are mass, fundamental standing-wave frequency, and damping factor. These results are generated by a computer program which is also presented.

Some experimental results are also presented and compared to the corresponding theoretical results.

#### THE ANALYSIS OF SHOCK ISOLATION OF A FLEXIBLE BODY PROTECTED BY ELASTOMERIC MATERIALS

Richard Bolton and Charles W. Gilson  
Westinghouse Electric Corporation, Sunnyvale, California

The problem of the protection of flexible bodies from shock through the use of elastomeric materials has long attracted the interest of many investigators. Early attempts concentrated on the application of energy techniques and attempted to bound the problems. Later various mathematical models were proposed to describe the instantaneous response. Of these, one of the most popular was that proposed for foam elements by Volz<sup>1</sup> which utilized numbers of maxwell elements to describe the isolator responses to shock inputs. Included in the Volz model was a nonlinear spring, which characterized the typical isolator elastic performance, and a variable area orifice air spring, which characterized the

pneumatic induced air force. This model is very similar to those recently proposed by Sepcenko<sup>2</sup> and also by Liber<sup>3</sup> for foam which differed basically in the form of the equations used for pneumatic damping.

Models utilizing maxwell or similar elements essentially model the material as an ideal viscoelastic material with superimposed air damping. The increase in isolation forces under the high strain rate conditions consistent with shock loadings on elastomeric isolators are easily represented by such models as has been shown in the previous works. These ideal models, however, also have their disadvantages. First, any elastomeric material can be modeled by a suitable number of ideal elements used in series or parallel forms. For example, Sepcenko has used twelve such parallel maxwell elements in his foam model while Hoover<sup>4</sup> has used five similar elements in his model of structured elastomeric pads. In the actual analysis of flexible missiles isolated by a large number of these isolators, however, both investigators were forced by numerical difficulties and cost considerations to use as few as a single element per row or ring of such isolators instead of the ideal model. Such a simple model was shown by Volz to adequately model the behavior under known inputs, i.e., when a simple model can be tuned to a known input, it can adequately predict the response. Unfortunately, such models cannot always satisfactorily predict the response for a general shock input. Liber has shown, for foam for example, that the maxwell element constants themselves and the single isolator "bottoming" behavior are velocity dependent. Hence, the model derived from static and dynamic tests depend to a degree on how accurately the test approximates the design shock; clearly this is not a desirable condition. Finally, the model constants are generally derived from tests which consider a single static load cycle and only the loading portion of the dynamic cycle. However, elastomeric materials have a pronounced cycle dependence which is significant especially for flexible bodies, whose peak responses are usually associated with modal responses which occur after the peak rigid body responses are achieved. These problems can limit the utility of analysis models using simple maxwell elements when used for the analysis of flexible bodies.

This paper discusses a new and alternate approach to such analyses. This method is based on computed system loads at discrete times using strain, strain rate, and cycle dependent functions of the isolator, rather than modeling the material behavior as ideal. It is shown that many of the difficulties associated with the simple maxwell element analyses are removed with this new approach. Test data is then used to define the isolator itself rather than material constants. The single element and full ring static and dynamic tests which involve both loading and unloading cycles are described in support of these methods. Analyses for polyurethane foam and structured elastomeric pad designs are discussed. Finally, the applications of these analyses to the lateral shock isolation of the Trident I and MX missiles are described.

<sup>1</sup>Volz, W. A., et. al., Foam Shock Isolation Feasibility Study, WEC, RSD-TR-66-11, Feb. 1966, Air Force Contract AF04(694)-568. (Also 39th, S. & V.B., 1967).

<sup>2</sup>Sepcenko, V., Analysis of Open Cell Polyurethane Foam Under Impact Loadings, 45th Shock and Vibration Bulletin, 1974.

<sup>3</sup>Liber, T., et. al., Shock Isolation Elements Testing for High Input Loadings, SAMSO TR 69-118, June 1969, Air Force Contract F04694-67-C-0076.

<sup>4</sup>Hoover, G. D., Mathematical Model of an Upper Linear Pad, WEC TN 69-18, 1969.

## FOCALIZATION OF SEMI-SYMMETRIC SYSTEMS

Alan J. Hannibal, Lord Kinematics  
Division of Lord Corporation  
Eire, Pennsylvania

Focalization, as treated in the literature, has been limited almost exclusively to symmetric systems in which four axisymmetric, in-plane isolators are positioned in a rectangular pattern about the c.g. of the suspended item. Unfortunately, the solution normally provided for this problem does not decouple the modes in both the fore-aft-vertical and lateral-vertical planes simultaneously unless the isolator pattern is square. One exception to the treatment of symmetric systems is the paper by Derby (1), in which the c.g. is arbitrarily placed with respect to the rectangular isolator pattern. The isolators are still all the same and in-plane whiel their directional characteristics are manipulated to de-couple the modes.

The approach described in this paper removes most of these limitations for it assumes that the suspended package has two different isolator sets, front and rear, having different elevation and lateral spreads. To the designer, this means greater freedom to specify desirable isolator locations or to utilize those structurally available. In each set, the isolator's stiffness and damping characteristics are the same while their locations and directions are symmetric about the  $X-Z$  plane. It is also assumed that the body has one plane of symmetry ( $X-Z$  plane), which is not a serious limitation as most systems to which this analysis is applicable, has a plane of symmetry, such as prop-driven aircraft engines, cabs on trucks and tractors, shipping containers, optical and guidance systems, etc. . . .

Another important feature of this analysis is its ability to decouple the system while constraining the shear spring rate and  $L$ -value of the isolators, their toe-in and elevation angles and the natural frequencies of the system.

### SYSTEM DESCRIPTION AND SOLUTION METHOD

The linear form of the system described above is represented mathematically as

$$M\ddot{\mathbf{x}} + C\dot{\mathbf{x}} + K\mathbf{x} = \mathbf{F}$$

where

$$\mathbf{x}^T = (x, y, z, \alpha, \gamma)$$

$$M = \begin{bmatrix} m & 0 & 0 & 0 & 0 & 0 \\ 0 & m & 0 & 0 & 0 & 0 \\ 0 & 0 & m & 0 & 0 & 0 \\ 0 & 0 & 0 & I_x & 0 & I_{xz} \\ 0 & 0 & 0 & 0 & I_y & 0 \\ 0 & 0 & 0 & I_{xy} & 0 & I_z \end{bmatrix}$$

$$C = \begin{bmatrix} c_x & 0 & c_{xz} & 0 & c_{x\beta} & 0 \\ 0 & c_y & 0 & c_{y\alpha} & 0 & c_{y\gamma} \\ c_{xz} & 0 & c_z & 0 & c_{z\beta} & 0 \\ 0 & c_{y\alpha} & 0 & c_\alpha & 0 & c_{\alpha\gamma} \\ c_{x\beta} & 0 & c_{z\beta} & 0 & c_\beta & 0 \\ 0 & c_{y\gamma} & 0 & c_{\alpha\gamma} & 0 & c_\gamma \end{bmatrix}$$

$$K = \begin{bmatrix} k_x & 0 & k_{xz} & 0 & k_{x\beta} & 0 \\ 0 & k_y & 0 & k_{y\alpha} & 0 & k_{y\gamma} \\ k_{xz} & 0 & k_z & 0 & k_{z\beta} & 0 \\ 0 & k_{y\alpha} & 0 & k_\alpha & 0 & k_{\alpha\gamma} \\ k_{x\beta} & 0 & k_{z\beta} & 0 & k_\beta & 0 \\ 0 & k_{y\gamma} & 0 & k_{\alpha\gamma} & 0 & k_\gamma \end{bmatrix}$$

The zeros in the stiffness and damping matrix are a consequence of symmetry about the  $X-Z$  plane.

In order to decouple the system statically, the submatrix

$$\begin{bmatrix} 0 & k_{x\beta} & 0 \\ k_{y\alpha} & 0 & k_{y\gamma} \\ 0 & k_{z\beta} & 0 \end{bmatrix}$$

must be made identically zero. That is,  $k_{x\beta} = k_{y\alpha} = k_{y\gamma} = k_{z\beta} = 0$ . In most cases, "identically" zero is an impossibility and in the light of practical parameter identification "approximately" zero is sufficient. Dynamic coupling is viewed in the following manner. The arbitrary focal point will always be the center of gravity so that the system is automatically inertia decoupled. The coupling due to viscous damping, rather than make an unrealistic definition, like  $C = uM + vK$ , will be considered small and, therefore, unimportant. In the case of loss factor damping, if all isolators are of the same material, it is represented as  $j\eta K$ , in which case the damping decouples simultaneously with the stiffness matrix. As a consequence of these assumptions static and dynamic coupling are equivalent.

The solution method is one of constrained minimization. An objective function is formed as the sum of squares of the four non-zero coupling terms. That is,

$$\text{obj. funct.} = k_{x\beta}^2 + k_{y\alpha}^2 + k_{y\gamma}^2 + k_{z\beta}^2,$$

which is minimized with respect to an arbitrary subset of the following eight parameters: toe-in angles, elevation angles, and the isolators' shear spring rates and  $L$ -values. Constraints can be placed on these parameters as well as the natural frequencies of the system.

The natural frequencies are derived in closed form by assuming that minimization of the objective function has already been affected; that is,  $k_{x\beta} = k_{y\alpha} = k_{y\gamma} = k_{z\beta} = 0$ . For an arbitrary set of parameters, the natural frequency constraints do not truly represent the natural frequencies of the system. However, as the optimization progresses, they become more representative.

The above constrained minimization problem is, then, submitted to an efficient computer program, called CONMIN\*, for solution. The program is designed to selectively eliminate design parameters if so desired. For instance, if the designer wishes all four isolators to have the same characteristics, they can enter into the analysis as fixed values.

## DISCUSSION

Some of the aspects of this analysis discussed in the paper are as follows:

1. Multiple solutions—There are a number of local minima for most problems, which can be obtained by varying the starting values. Derby [1] alludes to this phenomenon in his paper, but because of technique only solutions for the e.g. above the center of the mounting pattern are used as starting values for the offset system.
2. Sensitivity to parameter variations—practical applications are plagued by fabrication tolerances, which are closely linked to system cost. Therefore, if a optimum solution is sensitive to small changes in system parameters, it is of little or no use to the designer. This problem will be discussed at length in the paper as well as exemplified.
3. Effect of constraints—constraining the system parameters has the advantage of producing a system which can be practically manufactured, but, has the disadvantage of providing a lesser degree of focalization and, in some cases, no solution. To aid in

---

\*Available from CHI Corp. in Cleveland, Ohio.

overcoming this difficulty, an attempt has been made to measure the degree of coupling statically by relating the off-diagonal elements of the stiffness matrix to the diagonal ones. For example,  $k_{y\alpha}/k_\alpha$ .  $k_{y\alpha}$  is a measure of roll response to a lateral disturbance.  $k_\alpha$ , on the other hand, is a measure of roll resistance to roll input. Therefore, the moment  $k_{y\alpha}y$  must be balanced by  $k_\alpha\alpha$ , or,  $\alpha/y = k_{y\alpha}/k_\alpha$ . In other words,  $k_{y\alpha}/k_\alpha$  is a measure of how much roll the designer is willing to endure for a given amount of lateral motion.

## BIBLIOGRAPHY

1. Derby, T.F., "Decoupling the Three Translational Modes From the Three Rotational Modes of a Rigid Body Supported by Four Corner-Located Isolators," *The Shock and Vibration Bulletin*, No. 4, Part 4, June, 1973.
2. Pechter, L.S. and Kamei, H., "Design of Focalized Suspension Systems," *Shock and Vibration Bulletin*.
3. Timpner, F.F., "Design Considerations in Engine Mounting," SAE 650093, January, 1965.
4. Himelblau, H. Jr. and Rubin, S., "Vibrations of a Resiliently Supported Rigid Body," *Shock and Vibration Handbook*, Edited by C. M. Harris and C. E. Crede, McGraw-Hill, New York, 1961, Vol. 1, Chapter 3.

## USE OF GENERAL PURPOSE COMPUTER PROGRAMS TO DERIVE EQUATIONS OF MOTION FOR OPTIMAL ISOLATION STUDIES

W. D. Pilkey and Y. H. Chen  
The University of Virginia, Charlottesville, Virginia

This paper presents methods for using general purpose structural computer programs to derive the equations of motion for limiting performance studies of isolation systems. This new approach selects the design parameters on the basis of information furnished by a limiting performance study of the dynamical system being designed. In the process the system dynamics need be solved only once and thus greatly reduces the computation burden. This technique has been successfully applied to problems ranging from an infinite degree of freedom system with two design parameters (a beam) to a five degree of freedom system with six design parameters (an automobile model). Typically, it leads to an optimal design using about 1 ~ 2% of the computer time required by a conventional computational design technique.

Currently, the new method is being applied to the design of structures that are suitable for analysis by general purpose finite element (FE) computer programs. This can be accomplished by having the FE codes generate the equations of motion in a form suitable for the limiting performance study which in turn provides information needed for identifying the design parameters.

Consider a structure subjected to base excitations. The system equation of motion written in matrix form is

$$[M] \{ \ddot{X} \} + [C] \{ \dot{X} \} + [K] \{ X \} = [F] \{ \ddot{Y} \} \quad (1)$$

where  $[M]$  is the mass matrix,  $[C]$  the damping matrix,  $[K]$  the stiffness matrix,  $[F]$  the coefficient matrix associated with the forcing function vector  $\{ \ddot{Y} \}$ , and  $\{ X \}$  is the displacement vector. If now portions of the structure are replaced by generic (or control) forces  $\{ U \}$  as required for the limiting performance study, then the system equation of motion takes the form

$$[M] \{ \ddot{X} \} + [C] \{ \dot{X} \} + [\bar{K}] \{ X \} + [V] \{ U \} = [F] \{ \ddot{Y} \} \quad (2)$$

where now a new stiffness matrix  $[\bar{K}]$  is obtained and a coefficient matrix  $[V]$  associated with the generic forces  $\{ U \}$  is added. While standard FE codes will provide all the information in Eqn. (1) with no or minor modification, Eqn. (2) is the one in the form suitable for the limiting performance study. Thus, the task of coupling the indirect synthesis method to a FE code essentially amounts to having the FE code develop the matrices  $[\bar{K}]$  and  $[V]$ . Two approaches have been developed:

#### APPROACH 1:

This approach makes use of the fact that the matrices  $[\bar{K}]$  and  $[V]$  are related to the original stiffness matrix  $[K]$  and thus can be derived from the latter. The replacement of an isolator element  $k_i$  by a control force  $u_i$  amounts to making the substitutions in the equations of motion

$$u_i = k_i \sum_j a_j x_j$$

where the summation is over the degrees of freedom that are connected with isolator  $k_i$  and the  $a_j$ 's are the kinematical factors that are associated with each degree of freedom. This implies that isolator  $k_i$  no longer contributes to the assembly stiffness matrix  $[K]$  and instead an additional matrix  $[V]$ , whose individual column consists of the coefficients of the term  $k_i \sum a_j x_j$  in the equation of motion, must be assembled. In other words, the new stiffness matrix  $[\bar{K}]$  is obtained by simply removing those contributions from  $[K]$  and the controller matrix  $[V]$  is formed by taking as its column the coefficients of  $k_i$  in a row (or column) of  $[K]$ , the row or column number being that of a translational degree of freedom which is enacted by the isolator.

#### APPROACH 2:

This approach obtains  $[\bar{K}]$  and  $[V]$  by treating the control forces  $\{ U \}$  like applied loads. Rewrite Eqn. (2) as

$$[M] \{ \ddot{X} \} + [C] \{ \dot{X} \} + [\bar{K}] \{ X \} = [F] \{ \ddot{Y} \} - [V] \{ U \} = [F] \{ \ddot{Y} \}$$

$$= \begin{Bmatrix} V_{11} \\ V_{21} \\ \cdot \\ \cdot \\ V_{N1} \end{Bmatrix} U_1 - \begin{Bmatrix} V_{12} \\ V_{22} \\ \cdot \\ \cdot \\ V_{N2} \end{Bmatrix} U_2 - \dots - \begin{Bmatrix} V_{1j} \\ V_{2j} \\ \cdot \\ \cdot \\ V_{Nj} \end{Bmatrix} U_j$$

where  $N$  = number of DOF, and  $J$  = Number of controllers. It is seen that  $\bar{K}$  is now the stiffness matrix of the structure less  $J$  portions or isolators and the columns of  $[V]$  are simply the influence coefficients of the "loads"  $\{U\}$ . Thus to obtain the  $i$ th column of  $[V]$ , one sets all  $U$ 's equal to zero but  $U_i$  which is set equal to 1 so that unit loads are applied at modes that are connected to the  $i$ th isolator. The resulted load vector is the desired column.

The paper contains the development of the theory and application of the approaches to several example problems using the SAP IV general purpose program.

# DYNAMIC ANALYSIS

## DYNAMIC RESPONSE OF LAMINATED COMPOSITE CYLINDRICAL SHELLS

C. T. Sun  
Engineering Research Institute  
Iowa State University, Ames, IO

Composite materials are in current use in a wide variety of applications. Important examples include composite materials for aircraft structural components, composite ablative materials for ABM and re-entry vehicles, filament-wound solid-propellant motor cases and nozzles, fiber reinforced rotor blades for helicopters, composite turbine blades for jet engines, and fiber reinforced gun tubes.

An element common to all of these applications is that the composite materials are subjected to dynamic loads. In particular, they are vulnerable to dynamic impact loading in these applications. In order to perform adequate design studies for such usage, methods are needed which will make it possible to determine the response of composite materials to dynamic loads. The solutions to dynamic boundary value problems, however, are often very difficult and time consuming compared to corresponding static problems. Thus, the establishment of dynamic load factors (DLF) (the ratio of dynamic response to static response) which would allow dynamic problems to be analyzed statically is of considerable importance to materials engineers and structural designers.

In this paper, the classical method of separation of variables [1] is employed to analyze the dynamic response of composite cylindrical shells under time-dependent uniform pressure at the inner surface of the shell. This method was first developed by Mindlin and Goodman [1] and was subsequently used by Yu [2] and Sun and Whitney [3].

Numerical results for maximum deflection  $w$ , maximum normal moment resultants  $M_x$  and  $M_\theta$  and maximum normal stresses  $\sigma_x$  and  $\sigma_\theta$  are evaluated for eight layer 0/0/ $\phi$ - $\phi$ /0/0 laminates. The maximum dynamic response is then compared with the corresponding static response for graphite-epoxy and glass-epoxy composites.

A detailed examination of the numerical results reveals that the DLF can be grouped into two categories: one for  $w$ ,  $M_\theta$  and  $\sigma_\theta$  and another for  $M_x$  and  $\sigma_x$ . In order not to duplicate the results, only the numerical values for  $\sigma_x$  and  $\sigma_\theta$  will be presented. The numerical results are presented by plotting the DLF for  $\sigma_x$  and  $\sigma_\theta$  as a function of  $\phi$ , where  $\phi$  in each ply is the angle between the axis of the shell and the directions of orientation of the fibers. Numerical results show that, contrary to the classical prediction, the DLF for the composite materials under various dynamic loading conditions may be greater than two. For example, the maximum value of DLF for  $\sigma_x$  and  $\sigma_\theta$  occurs in the neighborhood of  $\phi = 45^\circ$  under rectangular pulse. For graphite-epoxy it is about 2.75 for  $\sigma_\theta$  and 7.5 for  $\sigma_x$ , and for glass-epoxy it is about 2.38 for  $\sigma_\theta$  and 4.1 for  $\sigma_x$ . These results may be significant in design considerations.

## REFERENCES

1. R. D. Mindlin and L. E. Goodman, "Beam Vibrations with Time-dependent Boundary Conditions," *Journal of Applied Mechanics* 17: 377-380 (1950).
2. Y. Y. Yu, "Forced Flexural Vibrations of Sandwich Plates in Plain Strain," *Journal of Applied Mechanics*, 27: 535-540 (1960).
3. C. T. Sun and J. M. Whitney, "Forced Vibrations of Laminated Composite Plates in Cylindrical Bending," *Journal of the Acoustical Society of America* 55: 5, 1003-1008 (1974).

## SPECTRUM AND RMS LEVELS FOR STRESSES IN CLOSELY SPACED STIFFENED CYLINDRICAL SHELLS, SUBJECTED TO ACOUSTIC EXCITATION

G. Maymon, Armament Development Authority, Haifa, Israel

A method, by which the calculation of rms values of stresses in cylindrical shells with closely spaced stiffeners, subjected to acoustic noise excitation, is presented. Donnell type equations are used to analyze the stiffened shell. Effects of eccentricity of stiffeners (stringers and rings) and the existence of constant axial stress in the structure are also included. Analysis of the deformation is done by "smearing" the stiffeners over the whole surface of the shell but calculations of stresses include the effect of discrete stringers, thus rms values for stress in the shell, in the ring and in the stringer are obtained separately. The response analysis is based on scanning the wave number diagram of the examined shell, determining the modes in each bandwidth. In order to make the analysis useful for engineering purpose, a digital computer program was written, based on the analysis presented. At this stage of development, the acoustic efficiency of the shell is to be given as input data to the program. As the acoustic efficiency of closely space stiffened shell is not available at present, numerical example were calculated only for unstiffened shells using the present analysis with "zero stiffeners." Parametric study of power spectral densities of stresses, displacements, velocities and accelerations are presented.

As a by-product of the analysis, noise reduction of the shell is also obtained. The results were satisfactorily compared to experimental results available in the literature. In the near future, calculations of acoustic efficiency of the stiffened shells will also be included in the analysis.

It is believed that the present analysis may serve well as a tool in the primary design of externally carried stores, which are subjected to acoustic environments during the captive flight, and for high speed missiles and reentry bodies.

## THE USE OF COMPUTER GRAPHICS IN EVALUATING THE DYNAMIC RESPONSE OF STRUCTURES

by

Dr. George H. Workman  
Applied Solid Mechanics Section

and

William C. Bruce, Jr.  
Data Management and Computer Graphics Systems Section  
Battelle's Columbus Laboratories  
Columbus, Ohio

Engineers have traditionally preferred the graphic medium in which to conceptualize problems and express the results of analysis. One merely has to sift through several hundred pages of computer output to appreciate the impact of solutions translated into graphics. Passive graphics in the form of drum and microfilm plotters have been used for some years and many analysis programs have had a "graphics package" added to them. Interactive graphics go even further by providing a means of control over the development and synthesis of a problem that would be practically unachievable using passive graphics. One not only looks at a picture but also manipulates it to obtain the most informative view.

*This paper describes an application of interactive graphics utilizing a state-of-the-art graphics terminal for the purpose of evaluating the dynamic response of structures. The hardware and software combination provide an environment in which the structural engineer can interactively formulate his problem and interpret the results of the analysis faster and more effectively.*

The software described in the paper is used on a continuing basis utilizing real problems and is built around a hardware system consisting of

- a 24-inch CRT with a viewing area 20 inches in diameter and a nominal refresh of 50 Hz
- 8 zoom levels each a factor of 2
- dynamic sissoring
- multiple independent virtual pictures
- lightpen tracking, picking, and intensification.

The basic operating configuration consists of a minicomputer to act as a display file processor and a large central computer to serve as the host machine. The minicomputer is also capable of doing some programmable functions independent of the host such as picture rotation.

The problem at the beginning of the software task was basically one of defining a system that would make full utilization of the hardware characteristics, display meaningful engineering data, and yet be efficient and effective when applied to practical dynamic structural response problems. The research engineer in consultation with the systems analyst defined the objectives of this effort which was centered around an existing large general purpose finite element code already operational on the host computer.

The initial effort was divided into two general areas: pre and post-processing of the data. In the pre-processing stage, basic geometric data of the structural model were to be displayed. This include two- and three-dimensional static plots in addition to three-dimensional rotational plots. In the post-processing stage, deformed shapes, either static or dynamic, or the dynamic response of the structural model were to be displayed.

Many of the hardware features were utilized in the design of the software. The user can use the lightpen and translation features to focus his attention on a certain area of the structure and have the area enlarged to provide a large amount of detail. Multiple line styles provide ability for showing the undistorted and the distorted cases on the same image in addition to displaying the relative displacement vectors of a specified grid point under load. The ability to vary the intensity along a vector was used to produce a three-dimensional effect: intensity was decreased in proportion to the depth in the view. A rotation capability performed entirely on the display processor was added to enable the user to be able to look at the model from any vantage point of his choosing without increasing host computer central processor time.

To demonstrate some of the capabilities of the resulting graphical system, several actual practical engineering analyses are given. This includes the ability to generate a motion picture of the predicted dynamic response of an actual structure, in this case an offshore platform subjected to wave action.

#### A GENERAL PURPOSE COMPUTER GRAPHICS DISPLAY SYSTEM FOR FINITE ELEMENT MODELS

H. N. Christiansen, Brigham Young University/University of Utah, Provo, Utah,

B. E. Brown, University of Utah, Provo, Utah,

and

L. E. McCleary, Naval Undersea Center, San Diego, California

The paper describes a Fortran Computer Program which generates displays of finite element models in line drawing and/or continuous tone format. The system reads data generated by other analysis routines, accepts a variety of control commands, and produces line drawings with hidden line removal and/or black and white or full color continuous tone images with hidden surface removal. The display features are appropriate to both static and dynamic math models and allow output in single frame or smooth animation movie format.

A session begins with user initiated commands to READ the geometry, displacement and/or special function files. The geometry file consists of the nodal coordinates, an element connectivity array, and a definition of the division of the connectivity array into separate smooth surfaces and/or parts. Special function files are used to read scalar

functions such as stress or strain components and temperature. These files may be later used as the basis for "pattern type" displays using color fringe and/or surface warping techniques. The user then RESTores the geometric which initializes the translation, rotation, and explosion options. A command SCOPE is utilized to select output devices and prescribe ambient light conditions. The content of the scene is controlled by specifying the PARTs to be displayed and EXPlosion patterns. Commands are available to specify the COLOR of the various parts, to invoke and define color FRINges and surface WARPing techniques. The viewing positions are controlled by ROTAtion, TRANSlation, CENTERing, and DISTance to origin commands. These commands also allow control of perspective parameters and "z-clipping." Displacement amplitude is controlled by a SCALe command, and the format of continuous tone pictures is controlled by the instructions FLAT (which allows linear variation of the light intensity over the individual elements but preserves interior element boundaries), UNIForm (which precludes intensity variation over individual elements), and SMOOth (which invokes the Gouraud method of smooth surface simulation). Smooth animation and the generation of a sequence of frames (which may include harmonic motion) for MOVies is also available. At appropriate times, the user will request a VIEW of the scene he has defined. All four letter commands either result in completion of the request or ask specific questions before returning to a command wait status. An extra carriage return or an unrecognized instruction produces a list of the commands available. The result is a system for which minimum training is required.

The system was originally written at the University of Utah and used to produce raster driven displays with the option of a "Visible Surface Processor" to solve the hidden surface problem in hardware. Later the programs were implemented at Lawrence Livermore Laboratories by Christiansen, Brown, and Michael Archuleta. Archuleta had previously been a programmer at the University of Utah where he had written an implementation of the Watkin's Algorithm. This routine was optionally called by the display program if the hardware processor was "down." At Lawrence Livermore Laboratories, Archuleta produced an improved version of his program and it has been used mainly to produce line drawings. The installation of the system at the Naval Undersea Center has further generalized the system and made it as machine independent as possible. It is currently used to produce line drawings on a Tektronix 4012 scope and continuous tone images on a Comtal 8300 display system. The general purpose digital computer being utilized in both a batch and time sharing mode is a Univac 1110.

The development of the system has been sponsored by ARPA, ERDA, and the Naval Undersea Center. The documented system is available upon request to both governmental and private users. Although considerable effort has been made to achieve as much machine independence as possible, some changes will be necessary to drive other display devices.

It is believed that the system provides a versatile display tool for panel systems which can be readily implemented on most display configurations. The Naval Undersea Center (San Diego) version provides output on low cost line drawing and continuous tone display terminals.

## VIBRATION CHARACTERISTICS OF THE 1/8-SCALE DYNAMIC MODELS OF THE SPACE SHUTTLE SOLID ROCKET BOOSTERS

Sumner A. Leadbetter

Joe W. Majka,

Wendell B. Stephens

John L. Sewall,

NASA Langley Research Center

Hampton, Virginia

and

Jack R. Bennett, Rockwell International

The structural dynamic characteristics of all launch structures must be predicted and understood during vehicle development and operation to assure a design which will properly account for flutter and pogo instability as well as dynamic loads. The space shuttle vehicle is a particularly complex configuration to understand since it is composed of four separate elements joined asymmetrically at discrete interfaces. These basic elements are the orbiter, external tank, and two solid rocket boosters (SRB). As a fundamental step toward understanding the dynamic behavior of these elements scale models which are nominally one-eighth the actual size of preliminary vehicle concepts have been fabricated for test and analysis at Langley Research Center. The purpose of these tests is to assess the adequacy of analytical procedures which can be used to predict full-scale behavior. The purpose of this paper is to present the results of these comparisons as applied to the scale model SRB.

The SRB models used in the study are designed to represent three different stages of deployment; that is, the lift-off, mid-burn, and burn-out flight times. The models are circular cylindrical shells with end-rings attached. The primary structure is an aluminum shell with an L/R ratio of approximately 150 and an R/t ratio of 52. This shell casing has attached to it concentric solid propellant layer which at lift-off has a thickness of about .7R. The modulus of the propellant simulant, however, is only about 30 MN/m<sup>2</sup>. Experimental data are presented for the free-free vibrations of this configuration at the three aforementioned flight times for longitudinal, torsional, beam, and shell modes. The experimental data are then compared with three different analyses. First, a shell of revolution approach is used in comparing the basic shell modes with experimental data. However, the membrane frequencies are overestimated by shell theory since the propellant layer tends to interact somewhat with the aluminum shell motion. A finite element model comprised of beam elements and interlayer springs is used to model this behavior. Another finite element model composed of plate bending elements to represent the casing and hexagonal solid elements to represent the propellant is used to determine all modes of behavior. This third analytical approach is necessary in order to properly account for asymmetries which are present on the full-scale model and the remaining space shuttle elements undergoing test and analysis.

Additional analytical studies are presented which show the effect that the high internal pressures expected to occur at burn-out will have on modal frequencies. Also an analytical evaluation of the free-free vibration frequencies of the full scale SRB are presented for the burn-out flight time using the shell of revolution analysis.

The study shows that the proper application of analytical approaches described can adequately predict the SRB behavior for all the fundamental membrane, beam, and shell frequencies. Even the thick propellant layer can be modeled with thin shell behavior if the total propellant mass is accounted for.

## MECHANICAL IMPEDANCE TECHNIQUES IN SMALL BOAT DESIGN

B. E. Douglas and H. S. Kenchington  
Naval Ship Research and Development Center  
Annapolis, Maryland

The objective of this paper is to demonstrate the utility of mechanical impedance technology as an aide in evaluating small boat structural designs. The role of mechanical impedance in identifying vibration problems associated with the hull and decking as well as in diagnosing airborne noise problems in small boats is discussed and an example of the application of these techniques to a small boat vibro-acoustic problem is presented.

Small boat designs, especially those for military applications, place a high premium on weight in order to achieve high performance (i.e. speed, maneuverability and payload). As a result, extensive use is made of lightweight hull and deck plating which can give rise to severe low frequency vibration problems from resonance amplification of "high Q" plating modes. When these resonances coincide with major forcing frequencies, such as blade rate, piston firing frequency, tooth contact frequency and their harmonics, the hull and decking experience significant dynamic loadings which, at a minimum, causes crew discomfort leading to reduced efficiency and, at most, could ultimately result in hull *structural failure*. Thus, the identification of hull and decking resonances and associated modal loss factors together with modal density and vibration transmission path strength measurements are important considerations from which the designer can better select appropriate hull design modifications to provide optimum ship performance.

This paper will discuss the application of mechanical impedance technology to obtain (1) measurements of hull and decking resonance frequencies and associated loss factors from driving point impedance spectra, (2) relative vibrational path strength determinations from transfer and driving point impedance spectra, and (3) hull and decking radiation factors to characterize the role of modal radiation from small boat structures in airborne noise. Limitations to obtaining these measurements on small boats are briefly examined including modal density considerations in measuring damping loss factors and transducer mounting effects.

Application of these techniques to solve a small boat vibro-acoustic problem is made on a 36-foot landing craft, LCP (L). The LCP (L) is currently used by the Navy as a personnel and patrol boat as well as a guide and control boat in amphibious operations. High airborne noise levels were observed in the forward cabin of this craft which were deemed detrimental to its performance. Subsequent analysis revealed that several low frequency discrete lines dominate the "A"-weighted sound pressure levels in the cabin. Since low frequency acoustic problems are difficult to control through direct application of barrier or absorptive treatments without detrimentally affecting ship performance, a structural modification appeared to offer the best alternative for solution. Therefore,

impedance and airborne noise radiation factor measurements were made to identify structural contributions to the airborne noise. As a result of this analysis, several alternatives for corrective action became apparent which otherwise may not have been considered. An example of such action is the selective application of structural damping thus lessening the impact on performance due to added weight.

It is concluded that the application of impedance technology as an aid in diagnosing low frequency vibro-acoustic problems on high performance craft offers the designer information at relatively modest cost from which appropriate re-design modifications can be selected.

#### DYNAMIC BALANCING OF ROTORS—AN ORDERLY PROCEDURE (SUMMARY)

D. M. Janssen  
International Business Machines Corporation  
Boulder, Colorado

A technique is described to systematically balance a rotating device in two planes simultaneously. Straightforward mathematics is used to determine the position at two locations along the axis of rotation. These measurement locations do not necessarily coincide with the two balance planes.

Conceptually, the imbalance can be thought of as a series of force vectors distributed along the axis of rotations ( $Z$ ), and rotating in synchronism with the rotor at an angular velocity  $\omega$ . Generally these force vectors will not be in phase with one another. The net result of these imbalance forces can be measured as displacements (velocities or accelerations in two axial positions) represented by  $Z^1$  and  $Z^4$ . These imbalance forces can be cancelled by adding a mass at the proper radius and phase in two planes, say  $Z^2$  and  $Z^3$ .

The desired correction forces are analytically determined through the measured deflections. To determine what the imbalance forces are, we must find out what relationship the imbalance forces in planes  $Z^1$  and  $Z^3$  have with the displacement measurements taken in planes  $Z^1$  and  $Z^4$ . Assuming the system behaves linearly, we can correlate a displacement in plane  $Z^1$  with the imbalance forces in planes  $Z^2$  and  $Z^3$  as

$$x^1 = c_2^1 F_x^2 + c_3^1 F_x^3$$

and

$$y^1 = c_2^1 F_y^2 + c_3^1 F_y^3$$

where the  $c_j^i$ 's are compliant influence coefficients that relate the displacement at position  $i$  to the force applied at position  $j$ .

Likewise, the displacement in plane  $Z^4$  due to imbalance forces in plane  $Z^2$  and  $Z^3$  can be represented by

$$x^4 = c_2^4 F_x^2 + c_3^4 F_x^3$$

and

$$y^4 = c_2^4 F_y^2 + c_3^4 F_y^3$$

The four unknown imbalance forces  $F_x^2$ ,  $F_y^2$ ,  $F_x^3$  and  $F_y^3$  are found using linear algebra.

If the balancing is performed at a rotational velocity  $\omega$  that is much lower than the resonant speed  $\omega_n$ , then the force and the mass can be adequately related through the radial acceleration, i.e.

$$W = mg = -Fg/a = -Fg/r^2$$

As the balancing speed approaches the natural frequency of the system, the imbalance forces become amplified. To take this into account, based on the equation of motion for a rotating unbalance,<sup>1</sup> we have

$$W = -Fg \left[ \left( \frac{1}{\omega} 2 - \frac{1}{\omega_n} 2 \right)^2 + \left( \frac{2\xi}{\omega \omega_n} \right)^2 \right]^{1/2} / r,$$

where  $\xi$  is the damping ratio which can be experimentally determined or ignored if neglectable.

Information which must be experimentally obtained are the compliant influence coefficients and the rotating displacement vectors in planes  $Z^1$  and  $Z^4$  at a known rotational speed.

With the amplitude and phase information, the  $x$  and  $y$  components are readily obtainable through

$$x^i = A^i \cos \phi^i,$$

and

$$y^i = A^i \sin \phi^i,$$

where  $A^i$  are the displacement magnitudes and  $\phi^i$  are the phase angles between the peak amplitude of  $A$  and the  $x$  axes.

Very accurate dynamic balance can be achieved by repeating this balance procedure several times. That is, obtain the experimental amplitude and phase of the imbalance at  $Z^1$  and  $Z^4$  then analytically determine the size and position of the correction masses for  $Z^2$  and  $Z^3$ , then repeat.

---

<sup>1</sup>Thomson, W. T., *Vibration Theory and Applications*, Prentice-Hall, 1965 (p. 58-61).

An example is presented in which a total of three iterations are required to obtain the desired balance. By comparing the vector magnitude of the initial imbalance moment (weight times radius of weight placement) at  $Z^2$  and  $Z^3$  to the final imbalance moment, we obtain a figure of merit. A reduction by a factor of 125 is obtained. Thus, each iteration improves the balance on an average by a factor of five. It should be noted that this procedure does not independently reduce imbalance in each plane, but couples these corrections together. Reviewing the balancing data shows that the cross-coupling between the two balance planes is hard to detect intuitively.

### FREQUENCIES AND MODE SHAPES OF GEOMETRICALLY AXISYMETRIC ROTATING STRUCTURES. APPLICATION TO A JET ENGINE

P. Trompette and M. Lalanne  
 Institut National des Sciences Appliquées  
 VILLEURBANNE, FRANCE

Axisymmetric structures may be made out of various parts such as thin shells, thick elements and rings. They have been extensively studied by Dr. D. Bushnell and Dr. E. Wilson using Finite Element techniques and a Fourier's series development [1], [2]. Here we present the introduction of rotation effects into the calculations. As in the previous work, Fourier's series and Finite Element are used. Supposing an axisymmetric state for initial stresses the dynamical behaviour of the structure is given for each Fourier term  $n$  by:

$$M_n \delta^{oo} n + C_n \delta^o n + |K_{en} + K_{gn}(\sigma_0) - \Omega^2 M_{gn}| \delta = F(\Omega^2) \quad (1)$$

where

$F(\Omega^2)$  is equal to zero for  $n \neq 0$ ,  
 $\Omega$ , speed of rotation,  
 $M_n$ ,  $K_{en}$ , classical mass and stiffness matrices,  
 $K_{gn}(\sigma_0)$ , geometric matrix function of initial stresses,  
 $\Omega^2 M_{gn}$ , additional stiffness matrix.

The coriolis matrix  $C_n$  will be neglected for each  $n$ . The initial stresses  $\sigma_0$  are obtained in solving the equation (2):

$$|K_{eo} + K_{go}(\sigma_0) - \Omega^2 M_{go}| \delta_0 = F(\Omega^2) \quad (2)$$

and for each  $n$  frequencies and mode shapes are calculated in solving the classical eigenvalue problem (3),

$$\omega^2 M_n \cdot \delta_n = |K_{en} + K_{gn}(\sigma_0) - \Omega^2 M_{gn}| \delta_n \quad (3)$$

The method and the computer program, written in Fortran IV, are tested with simple known examples. Then the dynamical behaviour, frequencies and mode shapes of a part of

jet engine is predicted. Calculation are performed for about ten terms of the Fourier's series. The agreement between theoretical and experimental results is good.

#### REFERENCES

1. D. Bushnell, "Stress, stability and vibration of complex branched shells of revolution: analysis and user's manual for Bosor IV." Contract n° 00014-71-C-002.
2. E. Wilson, "Dynamic stress analysis of axisymmetric structure under arbitrary loading," Report E.E.L.C. 69-10.

#### EIGEN SOLUTION SENSITIVITY TO PARAMETRIC MODEL PERTURBATIONS

Charles W. White and Bruce D. Maytum  
Martin Marietta Corporation, Denver, Colorado

The basis for all dynamic analyses is the mathematical model used to simulate the structure under consideration. Energy methods by which these models are generated are well known. Application of existing modeling techniques is always subject to the engineering judgment of the analyst to the extent that the original mathematical simulation seldom duplicates the observed dynamic behavior of the hardware. Additional modeling uncertainties arise from evolutionary configuration changes that occur in the normal design cycle. Material and manufacturing tolerances introduce other uncertainties. The size of most mathematical dynamic models makes parametric evaluation of these uncertainties prohibitively expensive.

In this paper, a study of the general eigenproblem is undertaken to develop economical methods for the evaluation of mode shape and frequency sensitivity to dynamic model changes.

The initial approach taken was to approximate the perturbed eigenvalues and eigenvectors by a first-order Taylors series expansion. It was observed that results obtained in this manner are valid for small perturbations. Higher-order derivatives are required to predict large perturbation effects. However, difficulties in obtaining these derivatives led to the search for an alternate approach.

The alternate approach is a formulation of the eigenproblem in terms of perturbed nominal model element data and nominal model modal coordinates. The extent of coupling produced by elemental stiffness and/or mass matrices between the nominal modes determines the distribution of modal strain energy and kinetic energy among the model elements. The extent of this coupling produced by elemental stiffness and/or mass matrices between the nominal modes determines the distribution of modal strain energy and kinetic energy among the model elements. The extent of this coupling is limited by

AD-A037 182

NAVAL RESEARCH LAB WASHINGTON D C SHOCK AND VIBRATION--ETC F/G 20/11  
THE SHOCK AND VIBRATION BULLETIN. PART 1. SUMMARIES OF PRESENT--ETC(U)  
OCT 75

UNCLASSIFIED

BULL-46-PT-1

NL

2 of 2  
ADA037182



END

DATE  
FILMED  
4-77

orthogonality of the nominal model eigenvectors with respect to the unperturbed finite element data. This property is utilized in the methodology to decrease the size of the eigenproblem required to calculate modal perturbations produced by a given element perturbation. Thus, the sensitivity of a particular mode to perturbation of a specific model element can be determined economically. The size reduction is significant in terms of eigensolution computer cost. In certain instances, the method allows reduction to the point where a hand solution provides reasonably accurate results for many practical dynamic model perturbation problems.

A comparison study was conducted which identified the equivalency of the initial Taylor's series expansion approach and the modal coupling approach. It was determined that the diagonal terms of the modal coupling formulation are the partial derivatives of the eigenvalues with respect to the specific model element perturbation as obtained from the first order Taylor's series. Inclusion of the modal coupling effects, therefore, is equivalent to providing higher order derivative terms in the Taylor's series.

The methodology is applied to a sample aerospace type structure. It is shown that orthogonality divides the system modes into strongly coupled sets clearly identifying the reduced eigenproblem. It is then shown that the reduced-size eigensolutions yield results that match exact solution results with considerable savings of computer time.

It is concluded that the economical evaluation of dynamic model sensitivity is provided by the methodology defined.

#### DYNAMIC RESPONSE OF LAMINATED COMPOSITE PLATES UNDER INITIAL STRESS

C. T. Sun  
Iowa State University, Ames, IO

It is a well known fact that an initial stress will modify the mechanical properties of a medium. As an example, a homogeneous and isotropic medium in the unstressed state may become nonhomogeneous and anisotropic under initial stress. In general, a tensile initial stress will stiffen the rigidity of the medium, while a compressive initial stress will reduce its rigidity. When the compressive initial stress reaches a critical value, the rigidity of the medium becomes very small, and instability will occur.

The stability problem of plates and shells under compressive initial stress have been investigated by many distinguished researchers. The objective of this talk is to investigate the effects of initial tensile stress on the dynamic response of an infinitely long, simply supported composite plate. The investigation is carried out by using a method previously developed by the author (1) to analyze composite plates under time-dependent dynamic pressure. The initial tensile stress is assumed to be uniformly distributed over the thickness of the plate.

Numerical results for maximum bending stress and maximum interlaminar shearing stress are evaluated for eight-layer  $0/0/\phi/-\phi/\phi/\phi/0/0$  graphite epoxy laminates. The angle  $\phi$  in each ply is the angle between the fiber direction and the geometrical axis of the plate. The numerical results are presented by plotting the ratio of the maximum dynamic response to the corresponding static response as a function of the initial tensile stress for the cases  $\phi = 45^\circ$  and  $90^\circ$  respectively. In each Figure, three kinds of dynamic

loadings-rectangular pulse, sine pulse and triangular pulse-are considered. We observe that the rectangular pulse always produces the maximum dynamic response. The numerical result also shows that the effects of initial tensile stress to the dynamic response of composites depend not only on the type of dynamic pulses applied but also on the angle of lamination of the composites. Initial tensile stress will reduce the dynamic response considerably for the laminates when the direction of the fiber is parallel or close to the direction of the initial tensile stress. This result may be important to materials engineers and structural designers.

1. Sun, C. T. and Whitney, J. M., "Forced vibrations of laminated composite plates in cylindrical bending," *J. Acoust. Soc. Am.*, 55(5), 1003-1008 (May 1974).

# CLASSIFIED SESSION I

## MINUTEMAN DYNAMICS

### AN INTRODUCTION TO THE DESIGN AND QUALIFICATION OF LARGE SHOCK ISOLATION SYSTEMS

Loren L. Luschei  
Boeing Aerospace Company, Seattle, Washington

The recent design of new shock isolation systems for military applications required an extensive program of dynamic testing and analysis. Shock and vibration environments for which these isolation systems had to be designed ranged from those associated with distant earthquakes to those associated with nearby nuclear weapon explosions. Design specifications placed requirements on rigid body motions as well as dynamic response up to 2000 cps. Space envelopes for the shock isolation system hardware were restricted due to the fact that existing equipment was to be shock isolated within existing facilities. This paper provides an introductory description of the test programs, test facilities and test verified analytical methods that were used to design and qualify these shock isolation systems.

Individual shock isolation system component types were selected based on data obtained from a comprehensive program of concept development testing. Components tested included mechanical springs, liquid springs, elastomeric foams, rubber springs, steel cables, and floors of several types of construction. Static and dynamic force-deflection tests, impact tests in shear and compression, and acceleration transmissibility tests were included. Dynamic data from these tests were used to develop the analytical models of components. In this manner, test verified dynamic characteristics were incorporated in system analyses at an early time and this in turn allowed an accurate evaluation of each design concept.

Component testing was done using ordinary test laboratory equipment plus specially built test fixtures. New test facilities were required for system level testing. Essential to these facilities would be large force actuators capable of precise control. The actuators that were developed are pneumatically powered, hydraulically controlled, and with a peak force capability of one and one-half million pounds. Concurrent with the development of the actuators was the development of an analysis that would accurately predict their performance. Historically, performance of this type of actuator has been established, prior to the actual testing, by calibration runs. Development of the analytical model enabled system level tests to be run without expensive and time consuming calibration runs and in all cases, other than a few where mechanical malfunctions occurred, the actual performance was well within tolerances allowed.

The force actuators developed are used in two facilities capable of full sized shock isolation system tests. One facility is designed to test a full scale missile and its shock isolation system to simulated nuclear weapon ground shock environments. The other facility is designed to test shock isolated equipment floors to these same environments.

Three test programs were conducted in these facilities where the data obtained were used to define physical parameters and to verify the analytical models that were subsequently used to qualify two shock isolation systems.

The first program was to test a full scale ground test missile and missile shock isolation system. In this program vertical and horizontal inputs corresponding to nuclear weapon air blast induced ground motions were produced by the previously described force actuators. In addition, horizontal direct induced motion were provided by a secondary force activation system. The total weight of the test article (missile and missile shock isolation system) was 125,000 pounds. This test series provided additional confirmation, over and above that obtained from component testing, that the analytical models to be used for qualification were adequate.

The second program, using the same facility that was used for the missile shock isolation system test, was the test of an equipment floor segment. Actual electronic cabinet structures, with mass simulated electronic components were mounted on the floor segment. Vertical and horizontal shock isolators were identical to those that were to be incorporated in the full scale shock isolation system.

The full-scale test series of the shock isolated equipment floor was conducted at the second described facility. These tests were conducted using electronic cabinet structures with both mass simulated and actual operating electronic components. Nuclear air blast induced input motions were simulated by four of the large force actuators previously described. Test data were again used to verify the analytical models of the floor and thus ascertain that this shock isolation system would meet all dynamic design requirements.

All the above tests, in conjunction with the analytical models developed, were necessary to show compliance of these very non-linear shock isolation systems with the dynamic design requirements imposed upon them.

#### POLYURETHANE FOAM ISOLATORS FOR SHOCK ISOLATED EQUIPMENT FLOORS

William C. Gustafson  
Boeing Aerospace Company, Seattle, Washington

This article presents the results of a large analytical and experimental program that was undertaken in the design and verification of a horizontal isolator set for shock isolated equipment floors. Polyurethane foam blocks were chosen for the isolator set because of their unique shock absorption characteristics, reliability, and near optimum properties for the imposed design requirements. The operating environment which controlled the system design was ground motion induced by nuclear weapons and the major design constraints were the available space in an existing facility for dynamic floor excursions and the level of shock attenuation that had to be achieved to ensure equipment survival. One additional constraint was imposed by the requirement that the foam blocks had to form a continuous platform which could be walked on by maintenance personnel while servicing equipment.

Practical limitations imposed by the size of the operational equipment floors precluded full scale testing with inputs to the horizontal foam isolator set. In order to achieve a high degree of confidence in the system design, a qualification program was configured where the analytical design models would be qualified by correlation with a smaller floor segment test and then the operational floor would be qualified by detailed analytical data evaluation with these models. The floor segment test specimen consisted of a 5' × 10' steel floor suspended vertically by three cable/liquid spring assemblies, isolated horizontally by large foam blocks, and two electronic cabinets were mounted on the floor. A series of approximately twelve tests were conducted with combined vertical and horizontal inputs to the vertical isolators and simultaneous shock input to the horizontal foam blocks. Test instrumentation recorded 84 active data channels which measured test inputs, floor excursion histories, and floor response environment experienced by the equipment cabinets.

The analytical model used for the floor excursion analysis predicts three dimensional excursions of an arbitrarily shaped floor supported by an arbitrary number of isolators and excited by a specified ground shock. The mathematical modeling uses six rigid body degrees of freedom with the option of an additional five freedoms for flexible body modes. The vertical liquid springs are modeled as line elements comprised of a nonlinear spring, a friction element, and a velocity squared damper. The foam isolators are modeled by three elements suggested by Sepcenko (1974); these are a nonlinear spring, a Maxwell element, and a pneumatic element. The nonlinear spring exhibits a stress which is a double-valued function of strain with separate loading and unloading branches; the functional values are derived from the static test data. The Maxwell element approximates the visco-elastic dynamic effects exhibited by the foam. The air flow in and out of the foam block is considered to be independent of the visco-elastic effects and is modeled as a pneumatic element consisting of a chamber with an air-tight piston, a strain dependent variable area orifice, and an air friction function. The modeling parameters for the three elements of the foam isolator idealization were derived in accordance with the techniques described by Sepcenko (1974). The equations of motion for the model were solved by numerical integration using a Runge-Kutta variable step procedure.

Extensive analysis/test correlation work was done to verify the analytical idealization of the foam isolators. The results indicated excellent agreement between the measured excursions and those determined analytically. Tests and analysis were conducted for several levels of ground motion. Both the air induced and direct (cratering) induced ground motions encountered in nuclear weapons effects phenomenology were examined in the testing and analysis. The good correlation that was achieved between the analysis/test results indicated the validity of the foam modeling that had been done by Sepcenko (1974) on the basis of component level sled testing. The confidence that was established as a result of this work permitted subsequent qualification of the operation floor.

An important observation made from the floor environment response data indicated that the foam isolator did not represent a significant transmission path for response environment above 100 cps. This was observed in the comparison of response data for tests with and without inputs to the foam isolators. The conclusion reached was that the liquid springs used for vertical isolation provided the principal transmission path for high frequency environment. This fact validated the response environment data gathered on a subsequent full scale test where only inputs to the vertical isolators were employed.

Analysis and test data indicated that polyurethane foam provided an excellent means of reducing large low frequency relative displacements that result from direct induced

motions. The effectiveness for air induced motions which are much more severe in terms of acceleration and peak velocity is somewhat limited unless the allowable floor environment is quite high. The foam effectiveness is most dramatically seen where the accelerations associated with the ground motion are on the same order of magnitude as the allowable floor acceleration as often the case is with direct induced ground motion.

## REFERENCE

Sepcenko, Valentin, "Analysis of Open Cell Polyurethane Foam Under Impact Loading," 44th Shock and Vibration Bulletin, August, 1974.

## ACTUATOR DEVELOPMENT FOR SYSTEM-LEVEL SHOCK TESTING

G. Richard Burwell  
Boeing Aerospace Company, Seattle, Washington

Concurrent with the recent development of shock isolation systems for military application, the design and development of two new force actuators were accomplished. The development was required as all known existing shock test devices were inadequate in producing the required forces, input motions and other performance parameters. The primary actuator, the design and development of which is the subject of this paper, was to provide the high velocity ground motion associated with the air blast created by nuclear weapon explosions. A secondary actuator was to stimulate the much lower velocity ground motion associated with the direct-induced (cratering) effects of nuclear weapon explosions.

Performance requirements for the primary actuator design were in terms of shock levels defined by response shock spectra, synchronization requirements for multiple actuator use and repeatability requirements. The actuator was required to be capable of providing a large number of specific shock spectra levels within a tolerance band for each level. The specified shock levels represented a very wide range with the highest level being approximately twenty times the magnitude of the lowest level throughout the frequency range. The actuator was required to be capable of producing two simulated ground shock motion types: positive-only and positive followed by partial return.

Preliminary design efforts resulted in the selection of a pneumatically-powered and hydraulically-controlled actuator as the basic design. The expansion of high-pressure gaseous nitrogen ( $\text{GN}_2$ ) would be used as the energy source to power a piston and piston rod inside a cylinder. The kinetic energy (the piston's motion) would be absorbed by controlling the flow of hydraulic fluid displaced by the piston from the main cylinder through piping to a series of capped cylinders called shaping accumulators. Four fluid exit ports would be provided in the base of the cylinder, three for connection to shaping accumulators and one for connection to a return accumulator.

Concurrent with design efforts, an analytic model of the actuator concept was developed. This model is described later and was instrumental in establishing the various volumes, diameters, lengths and other geometric parameters that would allow the actuator

to produce the required range of test levels. In addition, many details contained in the final design were selected after the effects were considered in the model.

The actuator includes a piston whose diameter is twenty inches and an eight-inch diameter piston rod the end of which attaches to the test article. Shaping accumulators containing threaded orifice plates accept the fluid displaced by the piston. The size and spacing of these plates control the flow of hydraulic fluid and are therefore critical in controlling the piston motion. Piping with either a two inch or five inch flow path and with a pipe orifice connects the main cylinder to each shaping accumulator. Motion initiation is achieved by firing one, two or three ordnance valves in the piping leading to the three accumulators.

The same type of cylinder used for the shaping accumulators is used for the return accumulator but with a return piston separating the GN<sub>2</sub> from the hydraulic fluid that replaces the orifice plates. A pipe connects the volume above the return piston to a separate GN<sub>2</sub> accumulator. The inside diameter of the pipe was selected to provide a "choked flow" condition during tests requiring a high return displacement. This was done to provide the required return velocity history which is low in peak value but longer in duration than the positive motion. The same type ordnance valve used for flow to the shaping accumulators is used to initiate the return motion. A locking unit arrests and holds the residual piston motion following pulse generation.

As stated earlier, an analytic model was developed for use as an aid in the design of the actuator. In addition to supporting the design task, the model has been used in test programs to define the actuator configuration that would provide the desired input motion to the test article. Thus the requirement to conduct numerous and costly "calibration" tests, which up to this time was the primary means of obtaining actuator configurations for smaller pneumatic/hydraulic actuators, was eliminated. Also, isolation system responses could be predicted using the predicted input motion.

The analytical model is idealized by four degrees of freedom that contain second order time derivatives. In addition, four variables with first order derivatives are necessary to describe the gas flow through the return pipe. The motion of the piston and piston rod is idealized as one degree of freedom. This variable and the time history of its derivatives are the input to a test article. Fluid flexibility is idealized by a spring and a viscous damper between the piston degree of freedom and the fluid degree of freedom. The isolator or connection between the piston rod and test article is idealized as a non-linear spring, viscous damper and coulomb damper in parallel connecting the test article mass with the piston rod. The return piston motion is assigned a degree of freedom and the first and second time derivatives of this freedom are set equal to zero until the return fire time is reached. The gas pressure above the return piston is dependent upon the gas flow through the return pipe. Four first-order freedoms (pressure and density in each chamber) are needed to adequately describe this flow.

During the model development period, assumptions were made, the equations were derived and model parameter values were assigned. The data gathered from the first test programs using the actuator were used to improve the model representation and parameter values. This model improvement effort has resulted in a model that accurately predicts the piston motion histories for actuator configurations corresponding to a very wide range of test levels. The basic model could also be used with modified parameter values to predict the motion histories of other existing pneumatic/hydraulic actuators or to develop new actuators.

## **COMPONENT TESTING OF LIQUID SHOCK ISOLATORS AND ELASTOMERS IN SUPPORT OF RECENT SHOCK ISOLATION SYSTEM DESIGNS**

John P. Ashley  
Boeing Aerospace Company, Seattle, Washington

Over the past six years, considerable component testing has been accomplished to support the design of new shock isolation systems. Larger yield and more accurate nuclear weapons, producing higher overpressures and increasing the direct-induced ground motion effects, has resulted in more severe nuclear weapons effects ground motion criteria. This paper describes the dynamic testing of candidate isolation system components and the subsequent development testing of components selected for consideration in the detail system design.

Early concept development transmissibility testing, introduced by Grant (1), provided dynamic response characteristics for the most suitable candidate shock isolation systems. These concept tests provided information which supported a basis for early elimination of concepts with undesirable characteristics and influenced design details where concept feasibility was demonstrated. Empirical data and improved techniques for the prediction of shock isolation system dynamic performance were also obtained. From these test results, optimum characteristics for shock isolation systems were established and subsequently directed toward specific design requirement and weapons system design specifications. Five general shock isolation element categories were subjected to candidate component testing under conditions of shock, vibration, and impact loading. Tested elements included elastomeric foam, rubbers, cables, liquid isolators, and candidate floor structures. Test data were used to determine acceleration transmissibility for varying input levels for each of these elements.

Within required design constraints, prototype hardware was then selected based on the most suitable transmissibility characteristics. This hardware was subsequently subjected to development testing to provide design and analysis data in support of the system design. Specific isolation system designs for which dynamic response characteristics are presented in this paper include: polyurethane foam blocks, rubber spring assemblies, single chamber liquid isolator assemblies and a liquid/mechanical shock isolator concept.

Considerable testing was conducted on flexible foam specimens and rubber spring assemblies. Force-deflection data were obtained from tests of: static compression, impact drop in compression and shear, and shock testing with varying vector impact angles and velocities. Variations in specimen densities, sizes and formulation techniques, and effects of a teflon antifriction impact surface were also investigated.

A prototype liquid shock isolator and cable assembly, duplicating functional characteristics of the isolator design for a shock isolated equipment platform, was fabricated and tested to verify the functional performance of the isolator. The structural integrity of the liquid isolator pressure cylinder and seal assemblies were demonstrated while load-deflection tests confirmed the isolator predicted spring rate and established the seal friction hysteresis. Vertical and horizontal shock test results were used to correlate dynamic isolator response with pre-test predictions. The source of the transmitted accelerations were identified and the transmissibility characteristics of the liquid shock isolator

were defined for use in predicting the isolation system dynamic environment from 0 to 2000 cps, and ultimately the equipment capability requirements.

A similar test program was conducted on a single liquid/mechanical isolator and cable assembly, proposed as a possible shock isolation concept for a missile suspension system. Load-deflection, vertical shock and impact tests were conducted to evaluate isolator performance and transmissibility. The high frequency performance of the system was equal to or better than expected and the environment due to mechanical spring surge modes were not significant. Test results demonstrated the feasibility of the design and it was ultimately incorporated into the detailed design of the suspension system.

Subsequent to the satisfactory performance exhibited during the single liquid/mechanical isolator tests, dynamic development tests were conducted on a prototype design missile suspension system. The test specimen consisted of three liquid/mechanical shock isolators each supported by a cable, but only one of which was excited by a single force actuator. The liquid spring portion of the shock isolator was from an operational shock isolation system and was tested as part of the concept development tests described above. The mechanical spring portion of the isolator was prototype hardware. The missile cage assembly was representative of the final design with the exception of foam blocks and elastomeric springs which were eventually incorporated in the final system configuration for shock isolation from large horizontal motions. A simulated missile mass of 78,000 pounds was used supported by a "boilerplate" skirt. Specific objectives accomplished with this test program were: 1) establishing the full stroke load-deflection characteristics of the composite isolator assembly, 2) determining the high frequency and low frequency transmissibility, and 3) determining the rigid body dynamic response characteristics, and the associated loads, when the upper cable attachment point of the prototype missile suspension system was subjected to a range of vertical and horizontal simulated weapon system ground shock motions. It was concluded from the test program that the suspension system performance was quite satisfactory and that final design verification testing should be accomplished with the full scale suspension system and missile.

The most recent series of component tests consisted of a series of single isolator tests to determine the performance limits of the liquid isolator assembly. Ground shock parameters which were investigated included variations in test level, shock type (positive only or positive with return) and vertical to horizontal input components. The effects of isolator preloads were also investigated. Test results established a basis for comparison of single isolator component testing with full-floor shock test programs. Test results supported qualification of the new shock isolation system as well as compliance with the final liquid isolator design specification. This program provided data with which to assess isolator transmissibility up to fragility level input conditions. Data from these tests were used in fragility analyses conducted on the system. Isolator assembly failure thresholds and actual failure conditions were established through cable assembly failures. On tests where cable failure was achieved as planned, the minimum cable dynamic failure loads were not significantly greater than the certified static load capability.

Computer analysis models were developed to calculate selected responses associated with the new shock isolation systems. These models were initiated during the candidate component tests and design phases of the programs described above, and were subsequently developed and improved as test data from the component development test programs became available.

Examples of the component analysis models derived for this program were published by Sepcenko (2) on the "Analysis of Open Cell Polyurethane Foam," and by Vail (3) on the "Effects of Additive Damping on Transfer Function Characteristics of Floor Structures."

An effective single liquid isolator analysis model has been developed, demonstrating excellent test/analysis correlation for the single isolator tests, and providing confidence in the system analysis models.

#### REFERENCES

1. Grant, Richard L., "Initial Design Considering Statistical Fragility Assessment," 41st Shock and Vibration Symposium, December, 1970
2. Sepcenko, Valentin, "Analysis of Open Cell Polyurethane Foam Under Impact Loading," 44th Shock and Vibration Symposium, December, 1973
3. Vail, Curtis F., "Effect of Additive Damping on Transfer Function Characteristics of Structures," Research Publication GMR-1255 Dated October 1972, Published by the Society of Automotive Engineers, Inc.

#### ANALYSIS AND TESTING OF FULL SCALE SHOCK ISOLATED EQUIPMENT FLOORS

William R. Milne  
Boeing Aerospace Company, Seattle, Washington

Increased nuclear threats identified during the past decade have resulted in the need to design an improved equipment floor to insure survival of electronic equipment critical to a silo based ICBM system. The improved equipment floor design requirements limited loads on the sensitive equipment during the period when the suspension system was exposed to facility motions considerably in excess of those used for the previous equipment floor design. The design problem was compounded by two design constraints which were to fit this new equipment floor into the existing facility and to limit the floor response loads and environment to current equipment capabilities. The design criteria associated with this increased facility motion was expressed in terms of a shock spectrum which represented a composite shock requirement including motions induced by the airblast and ground transmitted effects induced by the cratering. Air (blast) induced motions are characterized by a high velocity and acceleration and a relatively low displacement. The direct induced (cratering) motions are characterized by a low acceleration, low velocity and a large displacement relative to that of the air induced pulse.

A simplified analytical model for an equipment floor with idealized vertical and horizontal isolators was established to support the selection of a candidate concept. It became obvious as the study progressed that the air induced motion had a significant influence on the floor loads while the direct induced motion had a significant influence on the overall system motions. To accommodate both of these response conditions, a system concept was selected which was an annular steel equipment floor with vertical

isolation provided by four liquid isolators attached by cables to the facility ceiling and horizontal isolation provided by polyurethane foam blocks mounted on the sides of the floor. Existing equipment racks were mounted on the upper surface of the floor and batteries and a motor generator set were suspended by structure from the underside of the floor.

A detailed review of the analysis and testing requirements indicated the feasibility of dividing the activity into: (1) component analysis and testing which could be developed separately and subsequently integrated into the system design and (2) the overall system analysis and testing which utilizes results from the component level work. The component analysis of the liquid isolator and the horizontal foam restraints were developed separately and systematically improved by a series of component test programs. The overall system analysis was accomplished using a three dimensional (6 degree of freedom) loads and excursions analysis known as the "N" isolator program and a linear transmissibility analysis using Fourier transform techniques which relates floor response to input motion or to responses at other floor locations.

In the "N" isolator model the vertical isolation system (liquid spring) is modeled by a force-deflection curve and appropriate dissipation functions derived from the single isolator analysis/test results and the horizontal isolation system is represented by using the foam component model analysis/test results. System inputs are provided by velocity time histories or the associated displacements which are defined at the facility/isolator and the facility/foam interfaces. System responses are computed by integrating the nonlinear equations of motion to establish transient time histories of floor motions at the system stiffness center. These responses are used with a geometric transfer function to compute the motions and loads at any location on the equipment floor. Displacements are generally calculated relative to the facility for easy assessment of the available rattlespace.

During the early design phase, a transmissibility analysis using Fourier transform techniques was developed to predict floor environments up to 2000 cps. This analysis technique established a system transfer function using a finite element modal analysis for responses below 50 cps and a transfer function based on small floor segment tests for the range 50 cps to 2000 cps. This effort was necessitated by a system requirement specifying an absolute upper bound on the operating environment that could be present at the floor/equipment interface.

As the analytical activities progressed, the requirement for a full scale system level test program was identified. The major goals of the test were to verify the vertical suspension system performance when it was exposed to criteria level inputs to the liquid isolator set. Key parameters that were evaluated were isolator and floor loads, isolator set damping and floor high frequency environment. The test program would also provide transmissibility data for a prototype floor structure which was then used to update the transmissibility analysis model. Uncertainties in the transmissibility analysis and the importance of the floor/equipment interface environment were the most important requirement for full scale system testing. An additional goal was to evaluate the system response to input values at and in excess of the nominal design criteria without risking failure of the floor and with the electrical equipment operating.

A two part test program was planned for conduct in the full scale test facility designed specifically to test a complete shock isolated equipment floor. The horizontal foam isolators were not driven during the test since a prior floor segment test program had verified the ability to analytically predict the influence of the driven foam on the

floor responses. The first part of the test program (the Block I test program) varied input levels, input azimuth and input angle with vertical and determined the floor responses at the interface with mass simulated electronic equipment. The second portion of the test program (the Block II test program) repeated and then increased input velocities and displacements over those input in the Block I test and utilized operating electronic equipment.

The Block I test program was successfully completed in May 1973 and it verified the ability of the shock isolated equipment floor to meet its design requirements. The sensitivity of the floor response to input angle with vertical and to input azimuth was established. It was shown that the floor transmissibility was a nonlinear function of input amplitude with a lower threshold level of floor environment caused by the breaking of isolator friction. Isolator loads were generally found to be lower than loads experienced during the prior floor segment test program.

The Block II test program was successfully completed in October 1973 and verified the ability of the electronic equipment to perform at and in excess of the nominal design criteria. Comparison of floor responses with responses from tests using mass simulated electronics confirmed the adequacy of the mass simulation approach used during Block I testing and the floor responses were found to generally be proportional to isolator loads and not necessarily to exact input level.

The full scale floor test programs contributed significantly to the development of a fully verified analysis which was then used to qualify the operational suspension system for all aspects of the design criteria. The analytical models were subsequently used along with data from the single isolator failure tests to establish the fragility levels of the shock isolated equipment floor.

#### EQUIVALENT AXISYMMETRIC STRUCTURAL LOADING FOR A TRAVELING OVERPRESSURE PULSE

J. J. Farrell, D. J. Ness and G. M. Teraoka  
TRW Systems Group, Redondo Beach, CA

Survivability evaluation of protective structures under nuclear attack environments is often aided by finite element analyses. Currently, such analyses are limited to two-dimensional (axisymmetric or plain strain) computer calculations. This paper examines several implications of using a zeroth order Fourier expansion of a traveling nuclear airblast loading for calculation of the response of a surface-flush axisymmetric structure.

Various calculational schemes have been used to approximate a nuclear traveling pressure loading in an axisymmetric calculation. The simplest approximation can be made when the airblast is very superseismic with respect to the ground media. In such a case, a uniform (or pancake) load applied simultaneously to all surface nodes would be a reasonable approximation. The time history of this uniform load is usually taken to be the pressure pulse at the structure centerline (axis of symmetry) modified by addition of a rise time sized to minimize spurious oscillations within the grid. A more recent approach has considered computing the average force acting on the structure plan area at any instant of time and then dividing this by the plan area to obtain an "Impulse

"Averaging Load" exhibiting a more realistic rise time and smoothed peak based on the structure transit time. However, it is obvious that such simultaneous loading procedures cannot introduce the effects of uprange loads propagating through the earth media.

Another approximation which has been used is the so called "converging shock" load. In this scheme, the centerline time history pulse is swept across the grid at the proper shock front velocity. This technique does introduce the effects of uprange loads but results in too severe a loading condition as it axisymmetrically models a blast load converging on the structure from all sides.

Fundamentally, an axisymmetric model for a structure-media interaction calculation assumes that the loading and subsequent response is identical for all points lying on a circular ring of radius  $r$  centered upon the symmetry axis of the structure. The method presented in this paper is based on applying, to a given loaded surface node at a radius  $r$  in the 2-dimensional axisymmetric grid, the zeroth order coefficient  $P_0(r, t)$  of a Fourier expansion of the actual traveling nuclear overpressure pulse acting upon the entire circular ring of radius  $r$ .

Qualitatively, the derived pressure time history  $P_0(o, t)$  applied to the surface node on the symmetry axis is identical to the nuclear pressure pulse at that location since this unique node corresponds to a degenerate ring of radius  $r = o$  for which the average pressure is equal to the pressure at that discrete point. For surface nodes off the symmetry axis at a radius  $r$ , a rise time plus a smoothing of the initial shock peak is introduced, both effects increasing monotonically with  $r$ . The arrival time of the applied load pulse at a given node is a monotonically decreasing function of  $r$ , indicating a traveling load traversing the grid toward the structure centerline. Thus, the present method yields a converging type loading which approximates the asymmetry in the actual 3-dimensional nuclear loading.

Relations for  $P_0(r, t)$  have been derived and implemented using the Brode Simple Fit expressions for a nuclear height-of-burst overpressure pulse. This forcing function has then been incorporated into the SAMSON finite element code and check cases run to assess its capability to approximate a 3-dimensional traveling pulse on a 2-dimensional axisymmetric grid.

#### DYNAMIC RESPONSE OF ELECTRICAL CABLES TO SHOCK MOTION

R. W. Doll  
TRW Systems Group, Redondo Beach, CA

The response for flexible cables is derived in terms of the longitudinal, torsional and two-transverse equations of motion. The kinematics of the cable motion are derived in terms of the Frenet-Serret curvature-torsion parameters, and the equations of motion are obtained from Hamilton's Principle. Special attention is given to conditions when the cable's response lies in the plane of excitation or when it is a coupled non-planer response. This investigation shows that only when  $\tau_0$  is equal to zero and either  $\kappa_0$  or  $\kappa_0'$  is equal to zero, or when all three parameters are equal to zero will the response be planer.

An investigation of the cable response is accomplished using a finite element discretization of the equations of motion. In general the development of the curvilinear finite element is based on the assumption that a set of local intrinsic, curvilinear coordinates are specified *a priori* and that the local field can be approximated by cubic Hermite interpolation polynomials in these coordinates resulting in an isoparametric cable element.

The resultant algebraic eigenvalue problem is solved by reducing the problem to tri-diagonal form using a Householders reduction and then using the QR algorithm to solve for the cable eigenvalues and eigenvectors. The results are shown for a quarter circular arc which represented a cable section between an isolated floor and a fixed vertical wall. A qualitative comparison with uninstrumented tests is presented.

#### FAILURE ANALYSIS BY STATISTICAL TECHNIQUES (FAST)

W. H. Rowan  
TRW Systems, Redondo Beach, CA

FAST is a tool developed over the past decade because of the need for evaluating the nuclear survivability of strategic weapons systems. These weapons systems happened to employ many sites built almost identically. This led to early recognition that a statistical approach would be useful—to take into account such random variations as those in soil properties and construction quality.

The FAST methodology has been applied mostly to in-place weapons systems for the purpose of evaluating inherent system hardness or the benefit of hardness improvements. The FAST technique has also been used in safety analysis of ships, and is applicable to earthquake design. In general, it has wide potential applicability to the hardness/survivability evaluation of any military or civilian system.

The hardness evaluation or assessment of a complex system subjected to a hostile environment requires calculation of the probability of response of each component to the hostile environment, determination of the probability of failure of each component for that response, and the combination of the component probabilities to obtain the failure probability of the system. The FAST code has been designed to perform this evaluation in a manner such that parametric sensitivity, trade-off and optimization studies can be readily accomplished.

Typically, all system components are identified and catalogued. In order to more conveniently catalogue the system, its components can be grouped into subsystems. Then the possibility of each component or subsystem directly or indirectly contributing to system failure is ascertained. The individual failure mechanisms and fragilities of the components are determined and related to parameters of the hostile environments.

In the FAST code, each component failure probability is modeled by a fragility curve that defines for each component or subsystem the probability of failure as a function of the local system response to the free field environments. Component probabilities of failure are combined in system network equations to compute system probability of survivability. The system network is a functional description which specifies the series/parallel relationship between components. Components are in series if all

components are required to accomplish an essential system function, and are in parallel if any one could perform the essential function.

An important facet of the FAST methodology is treatment of the underlying uncertainties in predicting system hardness. Of the four system/environment inputs to FAST, the system network is the only one that must be known exactly. The code acknowledges and accommodates finite uncertainty in modeling environments, transfer functions and component fragilities. Uncertainty in environment estimates is often due to the lack of adequate analytic or empirical models for scaling nuclear weapon effects. This is also true of the uncertainties ascribed to transfer functions. Uncertainties in component fragilities are primarily a consequence of insufficient test data on the components at levels near and beyond failure. One of the most valuable features of FAST is that these uncertainties are individually modeled and are properly accounted for in the calculation of system failure probability. Two categories of variations are recognized by the FAST code, namely, random and systematic variations.

The fundamental difference between random and systematic variations is that a systematic variation extends uniformly over a population of facilities whereas random variations extend non-uniformly from one facility to another. Random variations tend to average out over a large population whereas systematic variations do not. It is noted that systematic variations are usually reducible by test and/or analysis programs which improve models of the phenomenology and system behavior. Random variations may also be reduced under some conditions but the value of such improvements is questionable for systems with large populations. The FAST code treats both random and systematic variations of environments, fragilities and transfer functions.

The FAST approach combines separate estimates of the environments, transfer functions, fragilities, corresponding correlation and systematic variability estimates, and a system functional network to provide probabilities of survival of the system, subsystems, and components. Probability of survival is given as a best estimate value along with certainty (or confidence) bands for any pre-selected range from a natural or manmade energy source.

This report contains the following information relative to the FAST techniques:

- A description of the analysis formulation and of the inputs needed to perform system assessment studies
- A description of the computer code and its operation
- Application of the technique to a sample problem which has been designed to address the key aspects of the methodology and its practical aspects.

**DESIGN OF A BLAST LOAD GENERATOR  
FOR  
OVERPRESSURE TESTING**

P. Lieberman  
TRW Systems Group, Redondo Beach, CA

Communication between hardened facilities is commonly performed using long runs of hardened cables that are buried underground. These cables contain splice cases to connect cables from different cable reels. After many years of splice case burial in both dry and wet soil sites, it is important to validate that the hardness requirements are being satisfied for the aged and corroded splice cases. For this reason a blast load generator, for testing exhumed splice cases, was designed and built at Hill AFB, Utah.

The environment experienced by a splice case includes

- Short rise-time to peak pressure which induces acceleration loads
- Peak pressure which could induce brittle material failure
- Total impulse which could induce ductile material failure

The splice cases burial depths are 3 to 4 feet. The surrounding medium could be either water for simulation of a well coupled hydrostatic applied load or soil for simulation of soil-arching after plastic deformation of the case and for simulation of the asymmetric applied load. It was also required that the facility be operated with inert driver gases, and use existing piping available at Hill AFB.

The result of these criteria is a blast load generator with a shock tube driver, vent system, and a test chamber. The shock tube driver is a 1 foot diameter pipe which contains up to 1800 psi with a double-diaphragm activation valve. The vent system dumps the shock tube gases at a rate prescribed by the required total impulse, but the dump is not activated until the entire system is at equilibrium at the peak pressure. The test chamber is 7 feet high and 7 feet in diameter, and proof tested to 1200 psi. The test chamber is filled with soil with water atop the soil.

The peak pressure requirement in the test chamber, free volume above the water surface, and change in water and soil volumes under pressure all determine the pressure and volume of the shock tube driver. This calculation assumes thermodynamic equilibrium.

For a prescribed pressure history in the gas of the small diameter shock tube, the wave reverberations transmitted into the diverging diameter, liquid filled pipes and chambers eventually reflect at the water/soil interface in the test chamber and at the soil/concrete interface at the bottom of the test chamber. The rise to peak pressure at the 3.5 feet depth of soil is markedly different for different shock tube diameters and for different test chamber water and soil depths. This is the main point of the work reported herein. Approaches to achieve rapid rise times are discussed.

There is a marked difference in damage imposed by a soil environment versus a water environment when the imbedded test structure (splice case) deforms plastically. The soil tends to transmit smaller loads to the splice case once it deforms, as compared to water.

# MODAL TEST AND ANALYSIS

---

## DYNAMICAL BEHAVIOUR OF COMPLEX STRUCTURES, USING PART EXPERIMENT PART THEORY

J. C. Cromer and M. Lalanne  
Institut National des Sciences Appliquées, Villeurbanne, France

Dynamic modelling of complex structures is sometimes impossible, even by numerical methods.

In earlier references, other workers have described procedures for the experimental determination and use of modal representation of dynamic characteristics.

In this paper, theoretical procedures are simplified using kinetic and potential energy representation. A general method for calculating complex structures using part experiment, part theory is then exposed using a building block approach [1], [2].

Only the constrained modal method is considered here. The unconstrained modal method has also been studied theoretically.

Practical structures generally possess a very large number of degrees of freedom; in order to reduce this number, the common technique of using the normal modes of the components as generalized coordinates of the system is utilized.

Using this method, we suppose that in order to predict the response of the complete structure in a given frequency range, only a small number of modes need be considered for each component.

The constrained modal method is developed so that the component model is entirely available from experimental data: natural frequencies, modal masses, modal restraining forces at the connection coordinates.

The components whose properties are determined by experiment are then connected with substructures which are modelled by finite element methods. The method is tested on simple examples consisting of cantilever beams. Tests are set up to determine the influence of the number of constrained modes, and the degree of precision required of the experimental data.

- The structure studied here, is a horizontal plate supported at four points analysed by a finite element method on which a vertical cylinder representing a gas diffusion column is fixed. This last component is modelled by its first six experimental constrained modes.
- Experiments have been performed with a new Solartron Analyser System. Modes shapes and natural frequencies of the complete structure have been

obtained using a simultaneous iterative technique. The computer program was written in FORTRAN IV.

- The agreement between calculated and measured modes and frequencies is good over a wide range of frequencies including the first eight natural modes of the complete structure.

In conclusion, we think that this method is suitable for studying the dynamic behaviour of complex systems for which theoretical modelling cannot be performed other advantages of the method are:

- component modelling either by experimental or theoretical data;
- reducing the order of resulting matrices;
- possibility of modifying a component without reevaluating the whole structure;
- component modes influence simulation on the whole structure.

#### REFERENCES

1. A. L. Klosterman, "On the Experimental Determination and Use of Modal Representations of Dynamics Characteristics," Ph. Thesis, 1971
2. A. L. Klosterman and J. R. Lemon, "Dynamic Design Analysis via Building Block Approach," The Shock and Vibration Bulletin 42, Part 1—janv. 1972.

#### THE EXPERIMENTAL DETERMINATION OF VIBRATION PARAMETERS FROM TIME RESPONSES

S. R. Ibrahim  
NASA Langley Research Center, Hampton, Virginia, U.S.A.

and

E. C. Mikulcik  
Department of Mechanical Engineering, The University of Calgary,  
Calgary, Alberta, Canada

This paper describes theoretical aspects of experimental verification of the application of a time domain modal vibration test technique. The theory of the technique is based on a reformulation of the ordinary differential equations of motion of a multi-degree of freedom system with viscous damping. These equations, in state variable form, comprise the mathematical model that is used for identifying a system's vibration parameters. The theory is applicable to both lumped and distributed parameter systems.

Special attention is directed to applying this technique in practice. Several application problems such as exciting the structure, minimizing of measurement data, determining of the order of the mathematical model, minimizing of the amount of instrumentation required and averaging of results are examined and solutions are presented.

The applicability of the technique is verified by two experiments using a cantilever beam and a rectangular plate. The case of the plate involves two close natural frequencies which could not be identified using a frequency sweep test (peak amplitude) because of interference between modes.

The merits of the technique as a practical vibration testing method are the following:

1. No assumptions were made concerning the level of damping or the closeness of natural frequencies in the derivation of the theory of the technique.
2. The free response of the structure under test is used, thus no recording of the initial exciting forces is required.
3. The experimental data required for this technique can be any one of the free acceleration, velocity, displacement or strain responses.
4. The amount of instrumentation required is minimized. A structure, however complex, can be identified in stages by using two stations at a time.

#### IDENTIFICATION OF STRUCTURAL MODAL PARAMETERS BY NODAL DYNAMIC TESTS

N. Miramand, J. F. Billaud, and F. Leleux  
Centre Technique des Industries Mécaniques, Senlis, France

and

J. P. Kernevez  
Université de Technologie de Compiègne, Compiègne, France

Amongst the different experimental techniques used for assessing modal characteristics of a linear structure, methods based on dynamic excitation at a single point of the structure are the easiest to implement. There are several ways to perform excitation: slow or fast frequency sweeping, transient or random excitation. In the latter cases, Fourier analysis of the excitation and of the response of the structure leads to transfer functions which can be assessed directly using a slow sine sweeping excitation.

During these dynamic tests, vibration modes of the structure can be coupled heavily with the nodal excitation and it is necessary to analyse numerically the transfer functions obtained to ascertain with precision the modal parameters of the structure: natural frequencies, generalized masses, stiffnesses and dampings and, in addition, the corresponding modal shapes.

The dynamic identification methods developed in the past can be classified according to the chosen mathematical model describing the structure and the power of identification of vibration modes with nearly coincident frequencies. The damping model might be mainly structural or viscous, and "proportional" or not, according to whether or not the damping matrix incorporated in the mathematical model of the structure can be diagonalised on the base of natural modes of the conservative structure.

The present work deals with identification, after nodal dynamic excitation tests, of modal parameters of a structure with arbitrary viscous damping, and possibly with

practically coincident frequencies of vibration. Damping values are not necessarily low and the restrictive condition that it be possible to diagonalize the damping matrix on the base of the natural modes of the conservative structure is not imposed.

The coefficients of the mobility-displacement functions given by the mathematical model of the structure are calculated by a least squares fit of theoretical values to the experimental results. A variational formulation of the error is established; this leads to the assessment of unknown coefficients by minimising a quadratic functional of the form:  $J(Z) = 1/2(AZ, Z) - (b, Z)$  where  $A$  and  $b$  respectively are a semi-positive definite matrix and a vector function of experimental data;  $Z$  represents the vector of coefficients to be identified.

By decomposition in rational fractions of the so identified transfer functions, the search for poles leads to the complex eigenvalues corresponding to each vibration mode of the structure. The numerators of the rational fractions give the eigenvectors (real or complex) corresponding to these eigenvalues and the modal coefficients which, in the case of proportional damping, are the generalized masses of the structure. This method does not require any preliminary estimation of the results. This is a definite advantage for the analysis of test data.

Several examples of identification are presented to illustrate the performance of this new method in assessing accurate values for modal characteristics of structures in difficult cases. In particular, for structures with practically coincident natural frequencies (comparative frequency difference  $\Delta f/f = 10^{-6}$ ), with low or high damping values, the modes of vibration are defined with precision.

On computer simulated examples, where experimental measurements are supposed to be exact, the relative accuracy obtained on modal characteristics is generally better than  $10^{-3}$ . In addition, the identification method developed does not present undue sensitivity to measurement errors unavoidable when testing structures. The number of modes, real or complex, in the frequency band analysed may be high. It is possible to eliminate the effect of truncation of the modal base, which influences the accuracy of modal characteristics, by searching for more vibration modes than the observed frequency band actually has.

## VISCOUS VS. STRUCTURAL DAMPING IN MODAL ANALYSIS

Mark Richardson and Ron Potter  
Hewlett-Packard Company, Santa Clara, CA

Anyone involved in the study of mechanical vibrations is aware that numerous mechanisms are responsible for the dissipation of energy in a moving structure. We are taught that viscous damping is the easiest and most natural type to model mathematically, but then we learn that structural (hysteretic) and coulomb damping mechanisms actually dominate in the real world. Consequently, various ways have been suggested to incorporate these more realistic damping mechanisms into the system equations.

In this paper, we first review the various damping mechanisms, and introduce a simple way to catalog the various types. Then we show that a viscous damping component

can always be extracted from the actual damping force, and that this viscous damping component accounts for *all* of the energy loss from the system.

As a result of this theory, we find that in order to completely describe the damping characteristics of a *linear* representation of a mechanical structure, only viscous damping need be modeled mathematically, and only the viscous component need be measured. In addition, we show that it is nearly impossible to discriminate between viscous and structural damping without physically altering the structure. This is not to say that damping is independent of displacement amplitude, but that for a given amplitude, there is an equivalent viscous component that describes the energy loss for that amplitude.

This point of view is particularly valuable when we attempt to identify the complex modes of vibration of a mechanical structure using transfer functions measured in the frequency domain. Each vibration mode (at any point on the structure) can be modeled by a simple single degree-of-freedom form, having some effective viscous damping factor, no matter what the actual damping mechanism may be. Any remaining response will represent nonlinear behavior, but does *not* cause any additional energy loss from the structure.

### EXPERIENCES IN USING MODAL SYNTHESIS WITHIN PROJECT REQUIREMENTS

J. A. Garba, B. K. Wada and J. C. Chen  
Structures and Dynamics Section, Jet Propulsion Laboratory, Pasadena, California

Modal synthesis methods have been developed for use by engineers for cost-effective solutions of the lower eigenvectors and eigenvalues of large complex dynamic problems. The number of independent coordinates of the subsystems is reduced by the selection of appropriate displacement functions that represents its contribution to the lower dynamic characteristics of the system. Different forms of displacement functions have been proposed by various investigators as being the "best" or the "most optimum" based upon comparative solutions of relatively simple structures. A limited number of automated modal synthesis programs have been developed during the past few years; however, their success for use by the engineers appear to be limited. A need for a general purpose modal synthesis program using the results of a program such as NASTRAN is being recognized. A question of the selection of the "best" displacement functions for incorporation into a general purpose program will again be reviewed.

The selection of the displacement functions cannot be selected wholly upon theoretical considerations but must include its interaction with the Project and its requirements. The considerations include analysis, hardware interfaces, organizational interfaces, schedules, tests, and resources. Our experiences indicate the selection of the "best" displacement functions are based equally upon Project requirements and theoretical considerations.

The objective of the paper is to describe our experiences in the use of modal synthesis for the Viking Orbiter (VO). The analysis and test plans were initially coordinated with various VO requirements. Good technical results were obtained through the use of an integrated analysis/test modal synthesis effort on both subsystems and systems. The VO required the utilization of many engineers with various experience levels that were

new to JPL and unfamiliar with the JPL computer programs. The overall integration of modal synthesis with various VO requirements are summarized.

Our experience shows the advantages of modal synthesis. The selection and integration of subsystem displacement functions into a system requires a talented engineer with a thorough knowledge of both the analytical and physical aspects of the dynamics of the structure. A general purpose computer program should allow the flexibility for the selection of displacement functions and to provide information whenever inappropriate selections are made. The contents will be of value to engineers contemplating the use of modal synthesis concepts for future projects and the future developers of a general purpose modal synthesis program.

### VIBRATION ANALYSIS OF THE BSE SPACECRAFT USING MODAL SYNTHESIS AND THE DYNAMIC TRANSFORMATION

E. J. Kuhar, Jr.  
General Electric Company, Valley Forge, Pennsylvania

For the Japanese Broadcast Satellite (BSE) Program at the General Electric Space Division, a vibration analysis of the BSE Spacecraft was performed in order to determine flight loads. The basic segments of the satellite included the spacecraft center-body containing communications and housekeeping electronics, a fold-up solar array assembly, a K-Band antenna dish and feed, a secondary propulsion system, and a launch vehicle/spaceship adapter. This three-axis-controlled spacecraft was designed for a stationary equatorial orbit for television rebroadcast after launch on a Thor Delta booster.

The analytical approach to the spacecraft vibration analysis employed a stiffness coupling modal synthesis technique which has been used extensively at the General Electric Space Division. The method uses free-free substructure vibration modes and frequencies. The substructures are coupled together by a stiffness matrix relating the substructures' free attachment coordinates. Since the substructures have no common points (degrees of freedom), design changes were implemented easily at the substructure level without affecting other substructure solutions. A unique computer program called SCAMP (Stiffness Coupling Approach Modal Synthesis Program), was used to obtain a system solution from the substructure modal solutions. Due to the complexity of the BSE spacecraft, a total of 429 modes were available for modal synthesis. Using the Dynamic Transformation [1],[2], SCAMP obtained the first 100 modes for the system solution.

The analytical model for the BSE spacecraft was assembled from six basic substructures: a center-body, an antenna, two solar arrays, and two propulsion tanks. The 2400 degree of freedom center body substructure was modeled using a General Electric finite element program. The finite element model of the launch vehicle/spaceship adapter was used to cantilever the free-free centerbody model at the base of the adapter. A 141 degree of freedom eigenvalue problem was then solved for modes and frequencies to be input into SCAMP. The 1140 degree of freedom antenna model consisted of an antenna dish and feed/support structure. The 78 free-free modes and frequencies were coupled to the centerbody model using the dish support truss stiffness matrix as a coupling "spring." The stowed configuration of the solar arrays each contained 900 degrees of freedom. Included in the 99 degrees of freedom eigenvalue solution for each solar array were seven rigid body modes, six

for the structure and one rotational yoke mode at the shaft/centerbody attachment coordinate. Each solar array was attached to the centerbody using the shaft stiffness interface and at four other locations with vibration isolators. The two propulsion tanks (6 DOF/tank) were treated as rigid lumps. A truss tube support structure was used to couple the tank C.G.'s to the centerbody. Of the 429 available modes, 300 substructure modes were treated by SCAMP, and a system solution of 100 modes and frequencies was obtained for the BSE Spacecraft. Using a 100 Hz cut-off requirement for the highest spacecraft frequency resulted in a 429 degree of freedom, 60 mode spacecraft dynamic model.

The use of SCAMP with the Dynamic Transformation has resulted in an analytical model accurately representing the dynamic characteristics of the BSE Spacecraft even in the higher modes. Modal testing of the BSE Spacecraft dynamic model has confirmed the analytical model computations. These analyses demonstrated how a large complex structure such as the BSE Spacecraft can be handled conveniently and efficiently with great savings in computer costs without modal truncation. Accurate solutions were obtained from small eigenvalue problem solutions due to the unique accuracy of the Dynamic Transformation. The stiffness coupling modal approach used by SCAMP also permits test modes and frequencies to be used as substructure models.

#### REFERENCES

1. Kuhar, E. J., "Selected System Modes Using the Dynamic Transformation with Modal Synthesis," The Shock and Vibration Bulletin, No. 44, Naval Research Laboratory, Washington, D.C., 1974.
2. Kuhar, E. J., Stahle, C. V., "A Dynamic Transformation Method for Modal Synthesis," AIAA Journal, Vol. 12, No. 5, May 1974, pp. 672-678.

#### VIBRATION ANALYSIS OF STRUCTURES USING FIXED-INTERFACE COMPONENT MODES

C. Szu  
TRW Systems, Redondo Beach, CA

This paper describes a modal coupling program (COUPL) which computes vibration modes of a structural system by using fixed-interface component modes. It is based on a model synthesis method developed by Hurty and extended by Craig and Bampton. Using this method, a structural system is considered as an assembly of components. Fixed-interface vibration modes for each component are separately determined and then used to synthesize the system modes. This program can solve problems where the interface are either statically determinate or redundant. It is not necessary to identify statically determinate and redundant interface coordinates. The structural system may have any type of boundary conditions including the free-free type. There is no need to select any specific component as the main one since all components, large or small, are treated alike. There is no constraint on the interconnecting topology of the system of components. Individual components can be modified without affecting the modes of adjacent components, so long as the interface relationships are not changed.

Analyses of a complex structure as a whole may require computer facilities of greater capability than may be available. With the modal coupling program, the computer capacity problem is diminished since, in general, only the lower frequency modes of each component are usually needed. Each component may be modeled in great detail without compromising accuracy. Another advantage is that one component may be changed without remodeling the others. This is particularly useful when components are designed and analyzed by different organizations.

The computer program is divided into one main overlay and four primary overlays. It consists of 43 subroutines having the capability to adjust and determine its field length during execution. There is no limitation on the number of components; however, the total number of system modes is limited to approximately 420. Interface coordinates must be retained as additional degrees of freedom. For structures having a large number of interface connections, the number of component modes used may be limited.

One feature of the program is that it requires fixed-interface vibration modes as well as constraint modes for each component. However, constraint modes are computed directly from the stiffness matrix of the component. A component is considered to be composed of interface and non-interface degrees of freedom. Interface degrees of freedom are those which are common to two or more components. Constraint modes are defined as the deflected shapes of the non-interface degrees of freedom due to successive unit displacement of an interface degree of freedom, all other interface degrees of freedom being totally constrained.

Lagrange equations are used to generate the equations of motion which are expressed in matrix form. For convenience, the method is supported by five appendices. This paper also includes a sample computer run together with an error study.

## SYMMETRIC COMPONENTS IN SYSTEM ANALYSIS

Wayne A. McClelland  
Structural Dynamics Research Corporation, Cincinnati, Ohio

In general, the dynamic analysis of complex mechanical equipment has been an extremely difficult task. However, the emergence of sophisticated finite element techniques and computer interfaced testing equipment has created a new dimension in engineering analysis. One procedure makes use of these combined analytical and experimental techniques to perform a building block analysis of the total system. The technique uses a modified modal synthesis technique to mathematically combine the component or building block data to predict the dynamic behavior of the full system under the prescribed loading conditions. This paper presents a further extension of this building block approach to take advantage of component symmetry (cyclic, reflective, or axisymmetry) in the dynamic simulation of nonsymmetric systems.

### THE BUILDING BLOCK APPROACH

The dynamic analysis of structures by a building block approach provides the dynamicist with a valuable analytical tool for obtaining the dynamic response of extremely

large complex structures. The basic approach is to divide the into a number of smaller inter-connected components, each of which can be analyzed using available digital computer routines or experimental tests. The total system response is then obtained by appropriately coupling the dynamic characteristics for each of the components. This technique is attractive since it parallels the design process where major structural components, or substructures, are often designed by different engineering groups or at different times. It is desirable, therefore, to use a substructure approach so that such designs and modifications may proceed as independently as possible with due consideration being given to the final coupling of substructures to form the complete structure. Groups which design the extremely complex components can rely on experimental test results, while groups designing structurally simpler components can use analytical finite element investigations. The results of the dynamic analysis on each component can then be evaluated by the department with system responsibility to evaluate total system dynamic performance before the system is completely assembled.

#### MODAL PROPERTIES FOR SYMMETRIC COMPONENTS

For quite some time analysts have been predicting the vibration modes of symmetric structures by modeling one region of the structure and specifying boundary conditions to simulate the presence of adjacent regions. For reflective symmetry this is done by applying symmetric or antisymmetric conditions (fixed and free coordinates) along the plane of symmetry. For cyclic or axi-symmetry, the vibration modes become a function of the harmonic coefficient (harmonic order, nodal diameter, Fourier coefficient) and the boundary conditions are related through complex valued trig functions. In the reflective case one set of modes is obtained for each combination of symmetric and antisymmetric boundaries while for rotational symmetry, each harmonic order is associated with a separate set of modes.

The key to the recommended "symmetric component" procedure comes from realizing that given the eigenvectors for the modeled region, the eigenvectors for the entire component can be generated from knowledge of the boundary conditions associated with each mode. Thus for a symmetric component we can derive modal properties (natural frequency, stiffness, mass, and mode shape per vibration mode) for the entire component by calculating modes of the modeled region and then expanding these modes to remaining regions of the component (e.g. full 360° for axisymmetric components).

Once this complete component modal description is obtained, the symmetric component can be coupled with other components, each of which may be symmetric or non-symmetric, via the building block approach to predict the dynamic performance of the total system.

#### EXAMPLE PROBLEM: WHEEL/BEARINGS/BASE SYSTEM

Machine tool applications require vibration-free performance to prevent chatter and insure quality of the machined part. In this application a large horizontal grinding machine (10 feet in diameter) was to be designed with minimum vibration through the tenth harmonic of rotational speed. Complex interaction between the various components (wheel, bearings, drive system, and base) required a detailed system approach. At first glance, the complete system was seen to be non-symmetric, e.g. the base contained vertical ribs and connected to ground at ten angularly spaced locations while the drive

system tied to the base at only three angularly spaced positions. However, certain components did exhibit symmetry; namely wheel axisymmetry and base cyclic-symmetry.

The concept of "symmetric components in system analysis" allowed the wheel to be modeled with very efficient axisymmetric solids of revolution and the 36° base sector to be separately modeled with three dimensional plates and solids. After the wheel and base modes were expanded and combined with the drive system and bearings, the resulting system model was processed to determine the lowest 150 system modes and damped response to harmonic grinding loads.

The computational and modeling efforts for this building block model were compared to estimated costs for a "one-shot" three dimensional plate and solid model of the entire system: even if comparable accuracy could be obtained, the full 3D model would have required five times the man-hours and ten times the computer costs.

#### CONCLUSION

Often non-symmetric structures contain symmetric subsystems or components. In these cases, a building block approach employing modal expansions for symmetric components can greatly simplify and reduce costs in the dynamic simulation of the complete system.

### APPLICATION OF MODAL ANALYSIS SURVEYS IN THE TEST LABORATORY

Henry Caruso  
Westinghouse Electric Corporation, Baltimore, MD

The recent introduction of commercially-available, high-speed digital signal processing equipment has made it practical for any test laboratory to acquire the capability to perform extensive modal analysis surveys. Whereas modal analysis formerly required sophisticated mathematical skills and extensive processing time on limited-access computers, test engineers and technicians with minimal mathematics background can now perform modal surveys of a complexity unattainable a few years before. However, great care must be taken to ensure that the data used is of high quality and that subsequent analyses do not misrepresent this data.

#### AREAS OF CONCERN

Areas of concern for modal surveys generally include main structural elements, interfaces between structural elements, components critical to performance, isolated structures, and structures with critical phase relationships. Sufficient accelerometers must be installed to adequately define the structures of interest and interface behavior. Instrumentation placement must be carefully selected so as to avoid influencing mode shapes with accelerometer mass loading effects.

## TEST SETUP

The manner in which the accelerometer data is acquired will affect the validity of subsequent analyses. If data is to be recorded on magnetic tape, the recording equipment must have recording head alignment sufficiently precise to avoid distorting phase information at high frequencies. A good general practice is to record response and reference (input) data on the same recording head.

The reference and vibration control accelerometers are not necessarily the same nor do they have to be at the same location in the test setup. When the reference signal is based on averaged accelerometer responses, a separate accelerometer on the driving structure should be used as the input reference. Signals from the averaged control accelerometers will be generally unacceptable for this purpose. Likewise, a signal that is the average of more than one accelerometer signal cannot be used as the input reference, since phase information will be distorted by the averaging process.

The test item or fixture should be mounted by means of its normal mounting provisions. Any other significant restraint or damping that would normally be in effect should also be provided. Although it is generally best to excite a structure in a manner similar to that in which it would be loaded in service, the input vibration can be administered at any representative point on the item's primary structure and still produce valid modal data. Since vibration levels for modal analysis surveys can be lower than full test levels, the fixtures used to transmit energy from the exciter to the test item can be relatively light and unsophisticated. Similarly, exciters can be used with lower force-pounds ratings than would be required for an all-up vibration test.

## TEST DESCRIPTION

While the test item is being vibrated, it is important to ensure that no observers touch the test item while data is being recorded. Such external damping, even though seemingly insignificant, can drastically alter mode shapes and lead to erroneous conclusions. Before data is recorded, the test item should be vibrated briefly at low levels to determine whether any loose parts or hardware are audibly apparent. These conditions should be corrected to maintain high accelerometer signal-to-noise ratios. Testing should not be conducted while other significant noise sources are present. Structural or acoustic coupling with such external sources will result in contaminated modal data. Coherence checks while the test is being conducted can be used to verify the quality of data being generated.

## MODAL DISPLAYS

Animated modal displays are valuable analysis tools but must be carefully thought out and constructed. A poorly constructed display will be confusing at best and can lead to inaccurate conclusions. Display generation requires that a real, often complex, physical structure be reduced to a simple, readily interpreted outline drawing. Since, for all practical purposes, the only structural elements that can be represented are those that were instrumented with accelerometers, it is important to think ahead to the final display before the test is run. Accelerometers should be spaced closely enough to detail a structures behavior, since the display will be constructed from straight line segments

between data points. Display proportions can be exaggerated to better highlight structural details and make the display easier to interpret.

### DISPLAY UTILITY

The most frequently used applications of modal analysis in the test laboratory are design analysis and fixture surveys; failure analysis; test setup analysis; and the analysis of field-recorded data.

### DISPLAY LIMITATIONS

There is information that the display will not provide any conclusions that the display alone will not support. These limitations must be recognized by all concerned before the meaning of any display can be completely assessed. It is especially important to explain these limitations to those unfamiliar with modal analysis who nevertheless may be responsible for making decisions based on the analysis results.

Displays depict relative magnitudes of acceleration and therefore accurate numerical values for modal properties cannot be determined from the display. Significant modes may be missing from the mode list and not displayed, depending on the skill and experience of the engineer who performed the data analysis. The display does not show an extended time history of dynamics, but rather imposes a periodicity of motion for ease of visualization. Finally, the spatial relationships between moving structural elements are exaggerated for visualization purposes and may present a misleading picture of actual conditions to the uninitiated.

### MATRIX FORMULATION OF MULTIPLE AND PARTIAL COHERENCE

Ron Potter  
Hewlett-Packard Company, Santa Clara, CA

There are many situations in the field of acoustics and mechanical vibrations where the system under study is best represented as a linear system having multiple inputs and multiple outputs, along with numerous sources of essentially unrelated noise contamination. A typical example is the determination of the various sources of noise generated by a truck engine at some set of distant points, in the presence of contamination from tire and road noises.

The complex representation of multi-I/O (input/output) systems of this type requires a matrix formulation. Most people are familiar with the concept of a transfer matrix in the frequency domain, which describes the output at a particular point that comes (via some path) from a particular input. Many people are familiar with the ordinary coherence concept in single I/O systems, which is a way of characterizing the amount of output power or energy that comes from the input, as opposed to that which comes from some unrelated source.

However, when we study multi-I/O systems, we quickly realize that there may be many interrelations between the various inputs, as well as between the outputs and the contaminating noise. In particular, we may want the output power that originates from a certain group of inputs, with the effects of some other group of inputs removed. We may also want to isolate the contribution of all unrelated noise at the output.

Information of this sort is best described by multiple and/or partial coherence matrices. If there are  $n$  inputs and  $m$  outputs, then we can define  $2^n - 1$  coherence matrices, each of which comprises  $m^2$  real numbers ( $m \times m$  hermitian matrices). All of these numbers have some meaning, depending on the question at hand.

The conventional theory of multiple and partial coherence is essentially a scalar theory, involving only one output, and allowing the removal of only one interfering input signal. In this paper, we derive the general theory of linear multiple input-output systems, in which we define the many possible coherence matrices. We discuss the meaning and interpretation of these matrices and their elements, and we discuss a method of measuring these quantities in a real world environment.

## CLASSIFIED SESSION II SHIPBOARD PROBLEMS AND BLAST EFFECTS

### TRANSIENT WAVEFORM VIBROACOUSTIC DATA ANALYSIS FOR TURBINE VANE AND RAM PUMP LAUNCH SYSTEMS

Ralph C. Leibowitz and J. Lawrence Clatterbuck  
Naval Ship Research and Development Center  
Bethesda, Maryland

This paper quantitatively evaluates and compares the measured torpedo launch waterborne noise sound pressure levels (SPL) produced by the vibroacoustic mechanisms of turbine vane and ram pump launch systems. The basic noise data for the systems were obtained at the Naval Underwater Systems Center's (NUSC) land-based test facility and the data reduction, analysis, evaluation and comparison discussed in more detail below, are being performed at the Naval Ship Research and Development Center (NSRDC). The results of the comparison are considered potentially applicable to the relative quietness of the two ejection systems in an actual submarine.

Because the launch system of a submarine is a complex structure closely coupled to the pressure hull, it is virtually an integral part of the hull. It incorporates complex piping involving various high pressure air subsystems, depth pressure sea water, mechanical interlocks, actuators, a complex of valves, connecting tanks, etc. The torpedo is ejected by the force of the large volume of water that is caused to flow through a slide valve into the torpedo tube during the process of weapon launch. Each of the events, i.e., functions or mechanical actions, such as a firing valve, pump stroke, stop bolt, etc. occurring during the launch cycle may represent, or give rise to, a significant fundamental mechanism or source contributing to the level and character of the noise signal.

The distinctive acoustic transient generated by the torpedo ejection system of a submarine is the earliest signal emitted by the weapon system that is potentially detectable by the enemy's sonar. The detection can be made at great ranges because of the high source level, duration, and low frequency characteristics of the noise signal which consists of both broadband and essentially discrete line spectra. These characteristics of the signal are the major contributors to the total energy in the signal upon which detection depends. Additionally, the distant sonar can also detect the partial energies associated with specific events of the transient launch process. Clearly weapon system effectiveness and submarine survivability requires minimization of the probability of detection and subsequent location and classification by an enemy submarine. Hence, it is imperative to develop and utilize a relatively quiet launch system that will not alert the target.

The Mk 17 Mod 1 Turbine Pump Ejection System (TPES) has been designated for installation on a submarine by NUSC (NP). A multiphased, land-based evaluation program for the TPES is being conducted in the NUSC facility. The first four phases of the evaluation provide vibration and acoustic data, measured at the facility and stored on magnetic tape for both the turbine pump and ram pump torpedo ejection systems. The primary objective of this paper is to compare the relative acoustic performance of these systems

based upon an evaluation at NSRDC of the processed transient acoustic data. The data reduction presently under consideration treats:

- (1) One-third octave band analysis of the transient waveform including:
  - (a) Peaks of short duration potentially identifiable with events in the firing circle
  - (b) Equal half periods of the transient
  - (c) The entire period of the transient
  - (d) Bandwidth limited time history of the transient
  - (e) Repeatability (or reproducibility) of firing cycle data.
- (2) Narrow band analyses of transient waveforms to determine existence of line spectra for fundamental and harmonic frequencies associated with turbine, gears, etc.
- (3) Spectral analysis in time sequence showing change in character of the signal, i.e., three dimensional amplitude, frequency, time, waveform.
- (4) Voiceprint (waveform characteristics) spectrum amplitude recorded as shades from light to dark rather than in terms of absolute magnitude.
- (5) Cumulative broadband response as a function of time.
- (6) Cross correlation and/or cross spectral density of transient waveforms to abstract discrete signals from a broadband noise background and determine the coherence of vibration and acoustic noise signals.
- (7) Ensemble averaging to abstract discrete signals from a broadband vibration and noise background.

A secondary objective is to determine source-transmission paths in the launch systems and the relative contributions of the vibroacoustic sources to the transient acoustic signals being compared.

#### **PROTECTION OF SUBMARINE DECK MOUNTED ELECTRONIC EQUIPMENT FROM SHIPBOARD SHOCK**

Norman M. Nilsen and Richard Bolton  
Strategic Systems Project Office, Washington D.C., and  
Westinghouse Electric Corporation, Sunnyvale, California

Methods of determining electronic equipment foundation, structural and/or isolation system designs for protection against extreme shock loading when mounted on a submarine deck are discussed in detail. Emphasis is placed on a Westinghouse developed dynamic

structural analysis based on finite element theory which was employed to assist in the design of the TRIDENT submarine's SWS electronic equipment foundations.

Recent naval architectural practice in naval submarine design has been to flexibly mount inner secondary decks to the primary hull to reduce hull sound transmissibility and to allow for pressure hull flexibility during deep submergence. Little attention, however, has been given to the shock isolation problems associated with electronics equipment mounting on these low frequency flexible platforms. The electronic components, especially their attachments, are fragile, and subject to failure when exposed to either high accelerations or high stress wave loading. The cabinets which house the electronics are especially susceptible to damage under high displacements. Potential problems span the broad design frequency range from the very low frequencies which produce high displacements, to the very high frequencies associated with stress wave propagations. Deck flexibility may either reinforce or attenuate the input shock motions; therefore the ship design (which is seldom known prior to the equipment design) can significantly affect equipment. Uncertainties are present both in the calculation of the design shock inputs to the ship and its transmissions to the equipment and also in the equipment response and failure limits.

The ramification of these problems on the design of deck mounted electronic equipment and their analysis and proposed verification tests for TRIDENT are discussed in this paper.

#### A FINITE ELEMENT ANALYSIS OF LOW FREQUENCY TRANSDUCERS

C. S. Nichols, Naval Undersea Center  
San Diego, California

This paper presents the results of a finite element analysis of the combined problem of structural vibration and acoustic radiation for several different types of low frequency transducers. The mathematical formulation used to describe the vibratory motion of an elastic body that is immersed in an infinite acoustic medium is discussed. This formulation employs the finite element method to describe the vibratory motion of the transducer. In this formulation, the effect of the acoustic radiation loading on the vibrational motion of the transducer is included by the use of fluid finite elements. The transducer and a sphere of acoustic fluid that surrounds the transducer are modeled with the finite element method. The pressure and normal component of velocity on the sphere are expanded in terms of spherical harmonic basis functions. Because these basis functions are orthogonal with respect to the Helmholtz integral equation, the acoustic impedance can be computed from analytical expressions. At present the use of this formulation has been limited to axisymmetric structures.

The formulation described in the previous paragraph has been used to examine the characteristics of several low frequency transducers. In this paper, a transducer is denoted as low frequency if its primary band of operation is below 500 Hertz.

The first low frequency transducer that will be discussed is the folded horn transducer. This transducer is similar in design to a longitudinal vibrator in that its piezoelectric driver element consists of a stack of longitudinally-poled piezoelectric ceramic

rings. In order to operate efficiently at low frequencies a long effective length is achieved by placing a metal cylinder outside of and concentric to the driver stack. One end of this cylinder is attached to the driver stack and the other end terminates in a circular piston. Instead of attaching a heavy tail mass to the other end of the driver stack, as is done in the longitudinal vibrator, a second metal tube and piston are attached. The transducer is therefore not only axisymmetric but has midplane reflective symmetry. The two radiating pistons are driven with a  $180^\circ$  phase difference. The pistons are air backed and are joined at their perimeters by a rubber seal. The mathematical model is validated by comparing theoretical and experimental plots of source level versus frequency and impedance versus frequency. Various perturbations of material parameters and geometry are examined to determine the effect they have on the response of the transducer in order to gain understanding of how the device operates.

The second low frequency source to be discussed is a membrane enclosed resonant gas cavity that is driven by eight circular pistons. This transducer was developed by Sandia Laboratories. It is shown that the model correctly predicts the experimentally obtained source level at several operational depths. Perturbations of the material parameters of the rubber membrane are examined to determine what characteristics of the membrane material are desirable.

Other low frequency transducers that are discussed are a Helmholtz resonator driven by a piezoelectric disk and a hydroacoustic transducer.

#### **FRAGMENT VELOCITIES FROM BURSTING CYLINDRICAL AND SPHERICAL PRESSURE VESSELS**

R. L. Bessey and J. J. Kulesz  
Southwest Research Institute  
San Antonio, Texas

An analytical method is used to describe bursting gas reservoirs and to predict the maximum fragment velocity attained by pieces from the fragmenting containment vessels. This description applies to processes occurring at a slower rate than HE bomb casing fragmentation such that rupture of the container walls occurs before they have reached a significant portion of the final fragment velocities. The method assumes that the fragments are accelerated while gas escapes through the rupture cracks between the fragments. As internal pressure is reduced by the escaping gas, nearly constant fragment velocities are finally attained (drag forces are not considered). The resultant fragment velocities may be used as initial velocities in trajectory equations for fragment hazard analysis.

A description of this method for a spherical container bursting into  $n$  fragments of circular cross-section was presented in a previous paper.<sup>1</sup> The present paper will consider the cases of a cylindrical container bursting into halves and a cylindrical container bursting into  $n$  axially symmetric fragments. For the latter case, assuming an ideal gas, an adiabatic process, appropriate gas flow equations, and equations of motion for the fragments, we obtain the following non-linear simultaneous differential equations in normalized coordinates.

$$g'' = nP_*[1 - g'^2(P_*)^{\kappa/(K-1)}]^{K/(K-1)}$$

$$g^2 \frac{P_*'}{P_*} = [-\alpha g + \alpha \beta] P_*^{\kappa-1/2K} - 2gg'$$

Where  $g$  is the normalized fragment displacement,  $P_*$  is the normalized pressure of the confined gas  $\alpha$  and  $\beta$  are coefficients (depending on initial conditions and geometry), and  $\kappa$  is the specific heat ratio. These equations are solved numerically and the results compared to the spherical containment vessel case for several values of the geometric parameters and initial state variables.

Results show that the maximum fragment velocities obtained for both cylindrical and spherical containment vessel geometries are nearly independent of the number of fragments chosen,  $n$ , for  $n > 10$ . The predicted fragment velocities are higher for the cylindrical case than the spherical case for equivalent volume and radii. This is probably due to the assumption that no rupture cracks form in the cylinder ends; thus the total crack length per unit surface area for the cylinder is less than for the sphere. The difference between fragment velocities predicted for the spherical and cylindrical cases diminishes with increase in radius and contained gas to containment vessel mass ratio. Fragment velocities for the cylinder are independent of cylinder length for a constant wall thickness.

For the case of a cylindrical vessel bursting into halves, the applicable equations are those of D. B. Taylor and C. F. Price<sup>2</sup> for the spherical vessel, with modifications for the different geometry. These equations are solved numerically. Results for the spherical and cylindrical cases are compared for several values of the geometric parameters and initial state variables.

The results of these analyses are compared to existing data on maximum fragment velocities for bursting pressurized glass vessels of Boyer, et al.<sup>3</sup> The predicted values for the spherical vessels pressurized with air are within 6% of the experimental values. The values for vessels pressurized with Helium are within 17% of the experimental values. A discussion of the application of this analysis to the problem of fragment hazard from exploding liquid propellant tanks will be given.

<sup>1</sup>R. Bessey, Fragment Velocities from Exploding Liquid Propellant Tanks, The Shock and Vibration Bulletin No. 44, Aug. 1974

<sup>2</sup>D. B. Taylor and G. F. Price, "Velocities of Fragments from Bursting Gas Reservoirs," ASME Transactions, Journal of Engineering for Industry, November 1971.

<sup>3</sup>D. W. Boyer, H. L. Brode, I. I. Glass, and J. G. Hall, "Blast from a Pressurized Sphere," UTIA Report No. 48, January 1958

## **STRUCTURES TO SUPPRESS THE EFFECTS OF ACCIDENTAL EXPLOSIONS**

Donald F. Haskell  
Aberdeen Proving Ground, Maryland

This paper presents simplified methods of design for structures to suppress the effects of accidental explosions of high explosive materials. The primary objective is to provide design techniques whereby propagation of explosions or mass detonations will be prevented and protection for personnel and valuable equipment will be provided. The basis for structural design is presented along with the effects of contained and partially contained explosions. Structural response to fragment impact and penetration is treated and the structural response analyses for basic structural components subjected to blast loading is developed.

The structural analysis approach taken here utilizes a semi-inverse energy method of solution. In its development, the blast-deformation damage process is characterized by the law of conservation of energy. Approximate expressions for the work done on the structure by the blast and the structure strain energy are derived. An assumed deformation pattern is used to obtain the final form of the strain energy. The work done on the structure by the blast is found by considering the incident energy flux density of the blast wave. Because of the gross deformation incurred by blast, elastic behavior of the structure material is neglected. The structure is assumed to behave as a rigid-plastic material. This allows the strain energy to be reduced to a simple expression which, when combined with the energy from the blast in the conservation of energy relation, yields an explicit equation for deformation.

Both contained and partially contained explosions are characterized by their blast wave and quasi-static, or static, pressure effects. Work done on the structure is equal to the sum of the blast wave work and the quasi-static pressure work.

The material presented provides a unified method for the preliminary design of structures to suppress the effects of accidental explosions.

## **EXPERIMENTAL DETERMINATION OF THE EFFECTS OF VARIATIONS IN THE EXCITATION PARAMETERS OF BLAST WAVES ON THE HIGH FREQUENCY RESPONSE OF CIRCULAR RINGS**

Paul John Mirabella  
Martin Marietta Corporation, Orlando, Florida

The high frequency response of a circular ring of rectangular cross section interior to a conical shell excited by a blast wave is examined. The ring supports a rigidly attached mass during the excitation. It is hypothesized that the response is a function of the four excitation parameters which characterize the loading. These are: Peak reflected pressure; characteristic time (pulse duration); wave engulfment time; and circumferential distribution. These parameters are varied over a range of interest in an effort to ascertain the structural sensitivity to such perturbations.

A series of tests sponsored by the Department of the Army and the Martin Marietta Corporation was conducted by the Stanford Research Institute on the SPRINT II missile. Data acquired during these tests will be used to verify and support the hypothesis.

The purpose of the test program was to determine the ring response produced by simulated missile entries into blast waves. The various blast entry conditions (altitude, velocity, angle of attack) have associated values of peak reflected pressure, duration, engulfment time and distribution. The objectives of this study are:

- (1) To vary the blast entry parameters independently over a range of interest
- (2) To measure and record the transient response of the ring
- (3) To present the data in a manner facilitating the analysis and indicating the relative magnitude and sense (increasing-decreasing) of a variation
- (4) To assess the sensitivity of the structural response to variations in the blast excitation parameters.

The actual encounter conditions are classified secret and will not be presented or referenced in any part of this document. However, the associated excitation parameters are unclassified when examined independently.

The two circumferential distributions examined are those produced by side-on and head-on missile-blast wave encounters. In former case a planar wave traveling perpendicular to the flight axis is swept across the missile. The resulting forcing function is examined only on the windward half of the ring. Past experience and calibration measurements have shown the pressures on the leeward half of the ring to be negligible by comparison. The function is described by an exponentially decaying, step pressure pulse whose load distribution as a function of  $\theta$  (independent of time) is:

$$P(\theta) = (P_{R_{\max}} - P_{OP}) \cos^2 \theta + P_{OP} \text{ for } -\frac{\pi}{2} \leq \theta \leq \frac{\pi}{2}$$

where  $P_{R_{\max}}$  is the peak reflected pressure measured at the windward ray,  $0^\circ$ , and  $P_{OP}$  is the over-pressure measured at  $90^\circ$ . The head-on encounter is characterized by a uniform load distribution.

The duration of the forcing function is computed by dividing the Impulse,  $I$ , by  $P_{R_{\max}}$ . The Impulse is obtained by integrating the pressure-time history over a time  $T_1$  to  $T_2$  where  $T_1$  corresponds to  $P_{R_{\max}}$  and  $T_2$  corresponds to  $(.1) \times P_{R_{\max}}$ .

The engulfment time is a measure of the velocity with which the blast front traverses the missile at the particular ring station of concern. The range examined varied from  $150 \mu\text{sec}$  to  $450 \mu\text{sec}$ .

On this basis the experimental program was divided into six test series, each examining a specific set of excitation parameters at five different pressures. Table I defines the test matrix.

TABLE I  
TEST MATRIX

Series No.	Pressure Range (psi)	Duration $\mu$ sec	Engulfment $\mu$ sec	Circumferential Distribution
1	50-500	100	350	$\cos^2 \theta$
2	50-500	300	350	$\cos^2 \theta$
3	50-350	100	Instantaneous	Uniform
4	50-350	300	Instantaneous	Uniform
5	50-350	100	150	$\cos^2 \theta$
6	50-350	300	150	$\cos^2 \theta$

The high frequency response of the circular ring considered was found to be dependent on the blast excitation parameters examined. The findings of this paper indicate:

1. The mathematical relationship between peak reflected pressure and transient acceleration is slightly non-linear, however, it may be approximated by a linear curve fit within an acceptable error margin.
2. The structural sensitivity of the ring to variations in pressure and duration was expected to be characterized by linear relationship. Such behavior was verified experimentally.
3. Variations in engulfment time appeared to be of secondary importance in comparison to the response deviations produced by pressure and duration perturbations.
4. Although the response of the ring was shown to be a function of circumferential distribution, the state-of-the-art for explosive testing prohibited a conclusive examination of this parameter.
5. Gross deviations from a  $\cos^2\theta$  distribution to a uniform loading produced an increase in ring acceleration high frequency content. This was attributed to the excitation of the  $n = 0$  or extentional breathing mode.

## MATHEMATICAL MODEL OF A SUBMARINE TEST SECTION SUBJECTED TO UNDERWATER EXPLOSIONS

Robert P. Brooks and Brian C. McNaught  
The M & T Co., Philadelphia, Pennsylvania

### INTRODUCTION

The realistic, full-scale shock testing of equipment is an indispensable part of the Navy "shock hardening" effort. The construction and continuous use of test vehicles such as the floating shock platform (FSP) and the submarine full-scale sections (FSS series) have provided the Navy with reliable, combat-ready equipment.

The authors constructed in 1972 a mathematical model of the standard Navy floating shock platform (Ref. A). This model provided the Navy with a tool for the total simulation of FSP tests. The model was first employed to evaluate the shock vulnerability of submarine-launched cruise missile (SLCM) designs, and currently is being used to qualify the new Mk 14 arresting gear system in lieu of the dynamic design analysis method (DDAM). The worth of the FSP model has been firmly established by the Navy, and its use will become more universal as it becomes more user-oriented.

This paper delineates the completion of a similar "total simulation" model of the full-scale section #8 (FSS-8) test vehicle. Although the model is analogous to the FSP model in intended usage and general format, the dissimilarity of the two vehicles and their intended usage dictated important additions to the modeling philosophy and an efficient utilization of computing.

### THE FSS-8 MATHEMATICAL MODEL

The FSS-8 is a cylindrical structure containing three main chambers: a central test specimen installation space and two adjacent ballast tanks, which are flooded during testing. Smaller trim tanks for achieving the desired stability are mounted to each outermost end bulkhead. The FSS is plated and framed typical of submarine construction.

With the additional complexities presented by circular rather than planar shapes, the basic modeling technique was altered. Accordingly, the FSS shell plating was modeled as a series of flat, rectangular beam "slats" joined along their lengths. A total of 36 "slats" was employed. The mass spacing was chosen such that masses were located at each transverse frame, for a total of 612 masses.

The internal stiffening construction of the ballast tanks was modeled with the same longitudinal spacing as the shell plating but with additional masses provided at each of the stiffener intersections, for a total of 150 masses.

The trim tanks were modeled as simple upright cylinders attached to the end bulkheads of the FSS, for a total of 12 masses.

With six degrees-of-freedom (DOF) per mass, a basic FSS model of 4644 DOF is formed.

## THE UNDERWATER EXPLOSION/HYDRODYNAMIC MODEL

To provide the dynamic input necessary for the response simulation of an FSS test, a semi-empirical model of an underwater explosion and the resulting hydrodynamic forces was constructed. The model includes shock wave, local cavitation, water resistance, and gas globe phenomena. In addition, the concept of air-backed and water-backed plating impingement occurring integrally had to be developed in order to treat the ballast and trim tank's correct response.

## COMPUTING OPTIMIZATION

The complete FSS-8/underwater explosion/hydrodynamic package is a unique "tailor-made" mathematical model. It is written entirely in straightforward FORTRAN. Savings are realized in computing by an efficient finite-difference integration method (Ref. B). For example, a "total" FSS-8 test simulation of the entire 4644 DOF structure, with an integration time step of .0000247 second, to a long-time simulation of 50 milliseconds, costs less than \$200. on a Univac 1108 computer at existing commercial rates.

## CONCLUSIONS

Comparison of the FSS-8 simulation output with available test data has shown good agreement. The low computing costs, coupled with the ability of the model to include practically any structural phenomena for test specimen models, combine to result in a viable tool for the Navy shock hardening program.

## REFERENCES

- a. Brooks, R. P., and McNaught, B. D., "Mathematical Model of a Typical Floating Shock Platform Subjected to Underwater Explosions," *The Shock and Vibration Bulletin*, No. 43, 1973
- b. Brooks, R. P., Goodis, N., and McNaught, B. C., "Mathematical Modeling for the Shock Hardening of Shipboard Weapons," *The International Symposium on Shock Analysis and Testing*, Lyon, France, October 1974